Taylor, Rosalind M. (2011) *The role of the interaction between PiAvr3a and CMPG1 in disease and plant defence.* PhD thesis.

http://theses.gla.ac.uk/2708/

The Role of the Interaction Between PiAvr3a and CMPG1 in Disease and Plant Defence

Thesis submitted for the degree of Doctor of Philosophy

Rosalind M Taylor

Division of Molecular and Cellular Biology,
Faculty of Biochemical and Life Sciences,
The University of Glasgow.

November 2010

Acknowledgments

I would like to acknowledge my supervisors Prof. Paul Birch, Dr Ari Sadanandom and Dr Joel Milner for their continuing support throughout this thesis. Thank you for giving me the opportunity to do this project. A special thank you to Paul for his patience and support during the final stages of this PhD, during my pregnancy and after. I would like to thank my colleagues at The University of Glasgow; Dr lucio Conti, Dr Richard Ewan, Dr Joelle Mesmar, Elizabeth O'Donnell and Craig Carr for their support; social and other wise. Thank you to the Arnott Laboratory and the Bower Building for assisting me through this project. I would also like to thank my colleagues at The Scottish Crop Research Institute for their time and patience; Dr Miles Armstrong, Dr Petra Boevink and Dr Ingo Hein and especially Dr Eleanor Gilroy for her assistance with VIGS, cell death assays and qRT-PCR. Thank you to B-Block and D-Block for allowing me to work there and use their facilities. Many thanks to my friends and family who have supported me emotionally and financially throughout this project. Special thanks to my now husband, Keigh, who has been a huge support and without whom I would have never studied plant science. And finally, to the most significant product of this PhD, my 7 month old son Jaxon, to whom this thesis is dedicated.

Declaration

The work presented in this thesis was completed by the author Rosalind M Taylor unless otherwise stated and has not been submitted for a degree at any other institution.

Abstract

Investigating the individual proteins involved in plant defence and the pathways these proteins are part of is important to gain an understanding of infection and disease resistance processes. It is hoped that this knowledge will help develop solutions to prevent crop infection and increase crop yield. More specifically, CMPG1 was first found to be important in pathogen responses by Kirsch *et al*. (2001) in parsley. It has further been found to have homology to NbACRE74 and AtPUB20 and AtPUB21 implying it is common to many plant species. CMPG1 is an U-Box E3 Ubiquitin ligase and involved in a number of different defence responses (INF1, Cf-9 & Pto/AvrPto). PiAvr3a is an RxLR cytoplasmic effector protein from potato late blight pathogen *Phytophthora infestans*. Its virulence function was shown by its ability to suppress INF1 cell death by Bos *et al*. (2006). This *P. infestans* protein and the plant protein CMPG1 were found to interact in Yeast-two-hybrid studies performed by Dr M Armstrong (Bos *et al*., 2010).

The aims of this project were to determine the nature of this interaction, functionally and biochemically. Does the interaction found in the Yeast-two-hybrid take place in the plant? What are the biological implications of PiAvr3a and CMPG1 interaction? What is the biochemical nature of the interaction? This project used *in planta* studies to investigate the CMPG1-PiAvr3a interaction. The biological reason for why this interaction occurred was studied using virus induced gene silencing (VIGS) and hypersensitive response/cell death suppression assays. The biochemical nature of this interaction was investigated using ubiquitination assays, and purified proteins, *in vitro*. This thesis aimed to provided data to increase the overall understanding of the function of CMPG1 and PiAvr3a during infection.

Firstly, this project found evidence for the stabilisation of StCMPG1 by PiAvr3a as well as possible direct interaction inside plant cells. The stronger interaction with, and stabilisation of StCMPG1 by PiAvr3a[KI], is in accordance with the stronger suppression of INF1 cell death by this form of the effector (Bos *et al*., 2006; 2009). Secondly, evidence for the role of CMPG1 in disease resistance to multiple plant pathogens, including oomycetes, bacteria and fungi was found. PiAvr3a suppresses all of these cell death responses. It is likely that CMPG1 is a target for other effectors from other pathogens. Cell death suppression by PiAvr3a is caused by stabilisation, and thus altered function, of CMPG1. Thirdly, promising and surprising data revealed that PiAvr3a may act as an E2 conjugating enzyme. Moreover, it appeared to act via both lysines 48 and 63, perhaps suggesting that it forms a mixed chain on CMPG1 substrates.

Contents

Figure List

Figure List Continued

Chapter 5   **PiAvr3a Acts as an Ubiquitin Conjugating Enzyme (E2) in the Presence of StCMPG1**

Chapter 6   **Final Discussion**

Appendix

Table List

Abbreviations

Abbreviation	Abbreviated for
Δ	Deletion (Delta)
A	Avirulence
A	Alanine (Ala)
aa	Amino Acid
Acif1	Avr9/Cf9-induced F-box 1
ACRE	Avr9/Cf-9 Rapidly Elicited
Afb	*A. thaliana* Auxin Signaling F Box Protein 2
APC	Anaphase Promoting Complex
Arc1	*Brassica napus* ARM Repeat-Containing 1
ARM	ARMADILLO
AtAtl	*Arabidopsis Toxicos en Levandura*
ATP	Adenosine Triphosphate
AUX	Auxin
Avr	Avirulence
AvrB	Avirulence B
AvrPto	*P. syrinage* pv. Tomato Effector protein
AvrRpm1	*P. syringae* Avirulence RESISTANCE TO P. SYRINGAE PV MACULICOLA 1
AvrRpt2	*P. syringae* Avirulence ROOT PHOTOTROPISM 2
Bak1	*A. thaliana* BRI1 (Brassinosteroid insensitve 1) -associated Receptor Kinase
BiFC	Bimolecular Fluorescence complementation
BSA	Bovine serum albumin
bZIP	Basic region leucine zipper
C	Carboxy-terminal
C	Cystine (Cys)
CBD	Cellulose Binding Domain
CBEL	Cellulose-binding (CB) Elicitor (E) of defense in plants and lectin-like (L)
CC	Coiled Coil
CD	Cell Death
CD Loop	9-residue Ω loop situated between the C and D helices of the protein
CE	Conjugating Enzyme (E2)
Cf	*Cladosporium fulvum*
CFP	Cyan fluorescent protein
cfu	Colony forming units
CHORD	Distinct zinc-binding cysteine and histidine rich domains
CMPG	A protein with a conserved CMPG amino acid motif in its sequence.

Coi1	Coronatine Insensitive 1
Co-IP	Co-immuno precipitation
Cop9	constitutively photomorphogenic 1
CP	Catalytic particle
CSN	COP9 signalosome
cT	Cycle threshold
Cul1	Cullin 1
D	Aspartic Acid (Asp)
DAMP	Damage-associated Molecular pattern
DNA	Deoxyribonucleic acid
dNTP	Deoxynucleotide Triphosphate
dpi	Days post-infiltration
DUB	De-ubiquitinating Enzyme
E	Glutamic Acid (Glu)
E1	Enzyme 1 (Activating)
E2	Enzyme 2 (Conjugating)
E3	Enzyme 3 (Ligase)
E4	Enzyme 4. Ub chain elongation or conjugation factors.
E6-AP	E6-associated protein
Ebf1	Ein3 binding F-box 1
Eds1	Enhanced Disease Susceptibility 1
EER	Avriulence Motif (RXLR-EER)
Efr	*A. thaliana* EF-Tu Receptor
EF-Tu	Elongation Factor Thermo Unstable
ER	Endoplasmic Reticulum
ETI	Effector-triggered Immunity
ETS	Effector-triggered Susceptability
F	Phenylalanine (Phe)
Flg22	*P. syringae* Flagellin 22
Fls2	*A. thaliana* FLAGELLIN SENSITIVE 2
G	Glycine (Gly)
GFP	Green fluorescent protein
Gp42	Glycoprotein 42
H	Histidine (His)
HECT	Homolgy to E6AP C-terminus
hpi	Hours post-infiltration
HR	Hypersensitive Response
Hy5	photomorphogenetic mutant
IAA	Indole-3-acetic acid
ICD	INF1 cell death
IKK	IkB Kinase
INF1	Infestans 1
IPTG	Isopropyl-ß-D-thiogalactopyranoside
ISR	Induced Systemic Resistance
JA	Jasmonatic Acid

K	Lysine (Lys)
LB	Lysogeny broth
LRR	Leucine Rich Repeat
LRR-RK	Leucine Rich Repeat-receptor kinase
MAMP	Microbe-associated Molecular Pattern
MAPK	Mitogen-activated Protein Kinase
MCS	Multiple cloning site
MDM2	Murine Double Minute 2
MLA	Proteins containing a N-terminal CC structure, a central NB site, a LRR region, and a C-terminal non-LRR region
MTI	MAMP-triggered Immunity
N	Amine-terminal; N-terminal
NB	Nucleotide Binding
NBD	Nucleotide Binding Domain
NB-LRR	Nucleotide Binding-Leucine Rich Repeat
NBS	Nucleotide Binding Site
Ndr1	*A. thaliana* NONRACE-SPECIFIC DISEASE RESISTANCE 1
NH2	Amino Functional Group
nim1-1	Noninducible immunity 1-1
NPL	Nep1(Necrosis and Ethylene-inducing Peptide 1)-like Protein
NPR1	NONEXPRESSOR OF PR GENES, also known as NIM1 and SAI1
OD	Optical density
P	Phosphorylated inc. Hyperphosphorylated
PAMP	Pathogen-associated Molecular Pattern
PCD	Programmed Cell Death
PCR	Polymerase Chain Reaction
PexRD	*P. infestans* RxLR Effectors
PhyA	Phytochrome A
PiAvr3a^{EM}	*P. infestans* Avirulence 3a containing amino acids E80 and M103 (mature protein)
PiAvr3a^{KI}	*P. infestans* Avirulence 3a containing amino acids K80 and I103 (mature protein)
PiAvr3a$^{KI/Y147del}$	*P. infestans* Avirulence 3a with the 147th aa deleted
PM	Plasma membrane
PR	Pathogenesis-related
PRR	Protein Recognition Receptor
PtaRME1	Populus tremulax*P. Alba* RING H3 E3 ligase
PTI	PAMP/Pattern-triggered Immunity
Pub17	Plant U-Box 17
PVDF	Polyvinylidene fluoride
PVX	Potato Virus X

R	Resistance
R	Arginine (Arg)
Rar1	*A. thaliana* required for Mla12 resistance
RBS	Ribosomal Binding Site
RBX1	Ruboxistaurin
Rbx1	RING Box
Rcr3	*L. esculentum* Cystine Protease
Rfp1	RING finger protein 1
RFU	Relative fluorescent unit
RIN4	*A. thaliana* RPM1 INTERACTING PROTEIN 4
RING	Really interesting New Gene
RLK	Receptor-like Kinase
RLP	Receptor-like protein
RNA	Ribonucleic acid
ROS	Reactive Oxygen Species
RP	Regulatory particle
Rpm1	*A. thaliana* RESISTANCE TO P. SYRINGAE PV MACULICOLA 1
Rps2	*A. thaliana* RIBOSOMAL PROTEIN 2
RSE	Relative silencing efficiency
RxLR	Avirulence Motif (RxLR-EER)
S	Serine (Ser)
SA	Salicylic Acid
SAR	Systemic Acquired Resistance
SCF	Skp1-Cul1-F-box
SCFTIR	Ubiquitin Ligase; Skp1-Cul1-F-box toll and interleukin-1 receptor
SCRI	Scottish Crop Research Institute
SDS	Sodium dodecyl sulfate
SDS-PAGE	Sodium dodecyl sulfate polyacrylamide gel electrophoresis
Sgt1	*A. thaliana* suppressor of the G2 allele of skp1
Skp1	S-phase kinase-associated protein
Son1	Suppressor of nim1-1
SR	Systemic resistance
SRC	Small Cystine-rich
ß	Beta
SUMO	Small Ubiquitin-like Modifier
sYFP	Split YFP
T3SS	Type Three Secretion System
TBS-T	Tris-buffered Saline-Tween
TIR	Toll and Interleukin-1 receptor
TIR1	Transport inhibitor response 1
TMV	Tobacco Mosaic Virus
TRV	Tomato Rattle Virus

Ub	Ubiquitin
Uba	*A. thaliana* Ubiquitin-like Modifier Activating Enzyme 1&2
UbcH5b	Human Ubquitin Conjugating Enzyme 5b
Ubq11	*A. thaliana* Ubiquitin 11
Ufd2	Ubiquitin Fusion Degradation Protein 2
UPS	Ubiquitin Proteasome System
v/v	Volume by volume
VIGS	Virus Induced Gene Silencing
W	tryptophan (Trp)
w/v	weight by volume
WRKY transcription Factors	Proteins with a Conserved WRKY domain
WT	Wild type
XbAvr/Pth	Xanthomonas bacterium Avirulence Pathogenicity
Y	Tyrosine (Tyr)
Y2H	Yeast Two Hybrid
YC	YFP C-terminal fusion
YFP	Yellow fluorescent protein
YN	YFP N-terminal fusion
Zn+	Zinc Cation
ε	Epsilon
Ω	Omega

Chapter 1. Introduction

1.1 General Introduction

The disruptions of a plant's life cycle by the attack of bacteria, fungi, nematodes, oomycetes or viruses have been studied for decades. Studies of this nature are fuelled by the agricultural industry and the food requirements of the world's population. With the global human population rapidly increasing and crop diseases quickly developing complex methods of attack, it has become necessary to scientifically produce disease resistant crops to cope with this rising threat.

One of the most well known famines to have taken place within Europe due to disease inflicted crop losses was on *Solanum tuberosum* (potato) by the oomycete *Phytophthora infestans* (potato blight) in Ireland between 1845 and 1852. This *"Great Famine"* is an example of the effect *P. infestans* can have on a crop and therefore the human population, and highlights why the interactions between plant proteins and disease resistance proteins are researched. Even today *S. tuberosum* losses due to *P. infestans* infection and the costs of chemical control of this blight exceed £4 billion globally each year (Science Daily press quote from Prof. Paul Birch).

Pathogens infect plants to take advantage of the plant's nutrients and as a platform to complete their life cycle. Pathogens can be divided into 3 main groups; biotrophs, hemibiotrophs and necrotrophs. Biotrophic pathogens obtain nutrients from living plant tissue. They may inhibit plant growth and yield but do not kill the plant. Hemibiotrophic pathogens begin their life cycle using the nutrients from living plant tissue but later kill the plant tissue and live off the detritus. Finally, necrotrophic pathogens benefit from the nutrients provided by dead plant tissue and do not keep the plant alive during infection. *P. infestans* is an example of a hemibiotrophic Oomycete pathogen (Birch and Whisson, 2001). Oomycetes are a group of eukaryotes that are similar but distinctly different from fungi. This group includes not only *P. infestans* but also *Phytophthora sojae* (soy-bean root rot) and *Phytophthora ramorum* (sudden oak death). Introgression of single plant *R* genes from wild relatives is a successful crop protection technique. However the positive results are short lived as new pathogen strains evolve which overcome the resistance. (Qutob et al, 2006)

The *P. infestans* life cycle occurs on host-specific plant tissue and usually reproduces asexually. The life cycle usually begins with airborne sporangia which land on the host tissue and release zoospores (Judelson, 1997). Germination then either occurs indirectly or directly. Indirect germination

occurs when the weather is cool and damp. Direct germination occurs in warmer conditions. Once the host tissue is penetrated nutrients are taken from the host. (Schumann & D'Arcy, 2000). Plants infected with *P. infestans* have small brown or black lesions on the leaves and stems and these lesions kill the plant. The infected plant will also be white on its surface as *P. infestans* sporangia grow in order to complete its life cycle.

The developments made so far in the field of plant disease and defence are summarised in the pages below.

1.2 Plant Infection

Plants have evolved defence mechanisms against invading pathogens. In many cases these defence mechanisms are successful. However, there are some plant species-specific diseases that can have catastrophic effects on the plant's development. The study of plant disease - Plant Pathology - has made immense progress but there are still many discoveries to be made to enable a full understanding of this area, as well as to convert this knowledge into practical solutions.

The method by which *P. infestans* infiltrates the plant's structural defences is very effective at achieving successful infection of *S. tuberosum*. This system is capable of overcoming the sturdy plant cell wall and other layers such as the leaf cuticle. The *P. infestans* secretion system is a mechanism which enables it to secrete and inject pathogenicity proteins into the plant cell cytosol (Hueck, 1998). The pathogen gains access via a number of possibilities. Initially it enters via stomata, wounds or appresorium. It then continues its entry through the plant intercellular spaces such as the apoplast (Jones and Dangl, 2006). As it colonises, it forms haustoria, biotrophic structures in intimate contact with the plant cell membrane. From haustoria, it secretes proteins known as effectors to initiate a chain of events within the plant that results in success for the pathogen (infection) or success for the plant host (no infection; Hueck, 1998 and Whisson *et al.*, 2007). The method by which oomycete eukaryotic microbes like *P. infestans* deliver effectors into the host cell is not yet known. Bacteria are known to use a Type Three Secretion System (T3SS). The structure of the T3SS is shown in **Figure 1.1**.

1.3 Plant Immunity

Plants have an innate immune system which shares similarities to that of animals, but which is not adaptive. When a plant and a pathogen come into contact, the outcome can either be a compatible interaction, in which the plant becomes infected, or an incompatible interaction, where no infection occurs due

Figure 1.1 Diagram of the Type Three Secretion System (T3SS).

The T3SS is the structure by which *Psudomonas syringae*, an example of a gram-negative bacteria, secretes effector proteins into the host cell. The tube like structure, made up of various protein complexes, passes out of the *Psudomonas syringae's* inner and outer membranes and through the plant cuticle, cell wall and to the plasma membrane (PM). The main section of the protein tube is called the pilus. The structure consists of hypersensitive response (HR) and pathogenicity (hrp) proteins. The numerous effector proteins, including Avr proteins, enter the host via the T3SS structure (Collmer *et al*., 2004 and Smith *et al*., 2009).

4
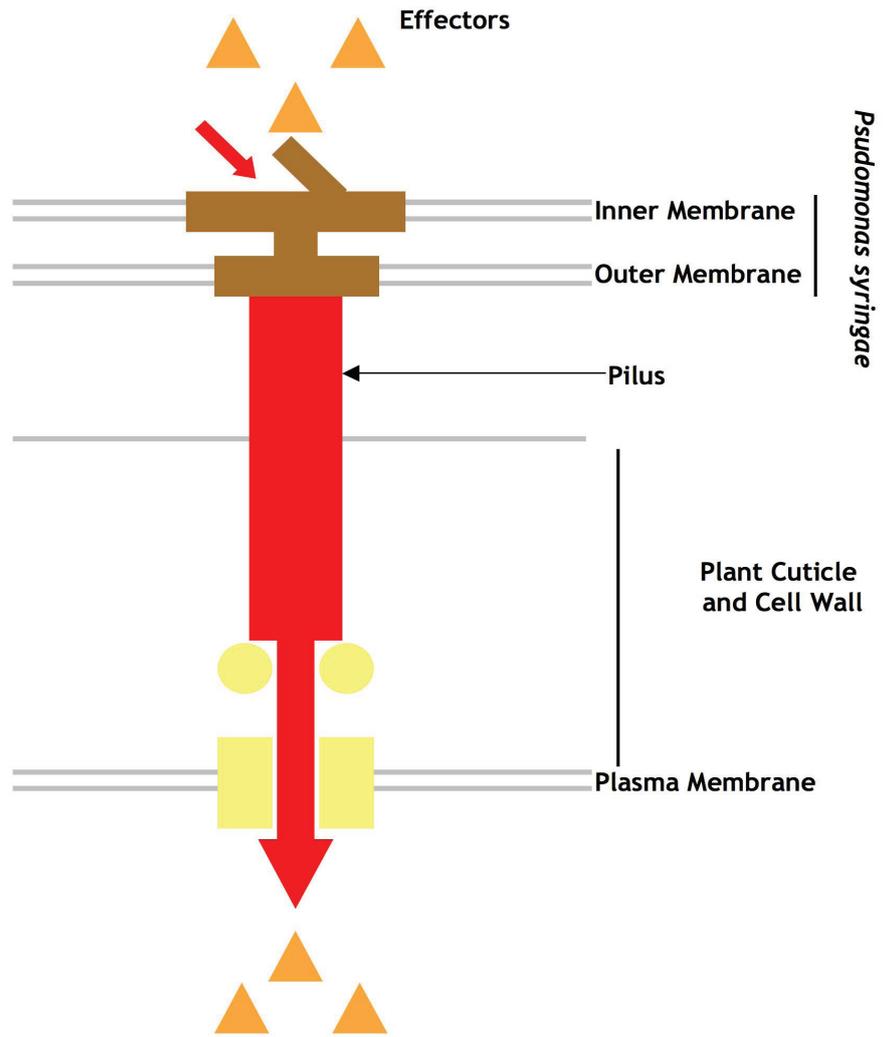
to the plant genetic make-up being unfavourable to the invading pathogen. For example; apple trees are unaffected by the diseases that infect tomato plants as their genetic make-up varies enough to be a "non-host" for tomato pathogens. It is, therefore, likely that plants are exposed to many microbes throughout a life cycle but, as the plant is not a compatible host, there are no visible symptoms (Agrios, 2005).

There are many genes involved in plant defence. These encode proteins that can strengthen host cell walls, act as anti-microbial toxins or enzymes that degrade proteins derived from the pathogen, or simply cause host cells to commit suicide to prevent a biotrophic association with the invading microbe. The more lines of defence a plant has available the more likely the plant has of surviving the attack and continuing a full life cycle with a successful seed yield (Jones and Dangl, 2006 & Chisholme *et al.*, 2006).

The sequence of events from when a pathogen makes contact with the plant surface through to a defence response are described below and shown as a "Zig-zag scheme" in **Figure 1.2**.

1.3.1 MAMP/PAMP-triggered immunity (MTI/PTI)

Microbe/Pathogen Associated Molecular Patterns (MAMPs/PAMPs): *"Surface-exposed, abundant structures that are common to microbial sources, are not found in potential eukaryotic hosts and are indispensable for the microbial lifestyle"* (Medzhitov and Janeway, 1997)

Plants defend themselves against pathogen attack by responding to the secreted molecules, including proteins and effector proteins (Jones and Dangl, 2006 and Hein *et al.*, 2009). The molecules the plant detects at this stage in the infection are called damage- microbe- or pathogen associated molecular patterns (DAMPS/MAMPs/PAMPs) which are secreted and/or present on the invading organism within seconds of making contact (or injury) with the plant surface (Schwessinger and Zipfel, 2008; Hein *et al.*, 2009) and constitutes Phase 1 of **Figure 1.2**. MAMPs/PAMPs include bacterial flagellin, lipopolysaccharides, cold shock proteins, elongation factor TUs (EF-Tu), peptidoglycans, ergosterol, fungal chitin and ß-glucans from bacteria (Yeam *et al.*, 2009). These MAMPs/PAMPs are vital to the pathogen's existence and can include proteins as vital such as cell wall constituents. MAMPs/PAMPs are only found in pathogen species and not the plant host and this makes them useful to the plant to detect invasion (Schwessinger and Zipfel, 2008). There are five individual, well-documented examples of oomycete proteins which are PAMPS or elicitors. These are: the

Figure 1.2 Diagram of the relative relationship between the different stages of early infection to each other and the plant immune system.

In phase 1 pattern/molecular associated molecular patterns (PAMPS/MAMPS) and other elicitors are released from the pathogen and after interacting with protein recognition receptors (PRRs), cause PAMP-triggered immunity (PTI), a defence response that is successful against most invading microbes. Successful pathogens deploy effectors to supress PTI (effector triggered susceptibility; ETS) and the involvement of resistance (R) proteins (Phase 2 and 3). Plants have evolved R proteins to detect effectors. This causes an hypersensitive responce (HR) in the cell as part of effector-triggered immunity (ETI; Phase 3). HR is a strong defence response and is represented by a long, solid arrow on the diagram. Phase four is the reoccurrence of ETS and ETI as part of the effect of different effectors becoming present due to horizontal gene flow. Adapted from Jones and Dangl, (2006) and Hein *et al.*, (2009).
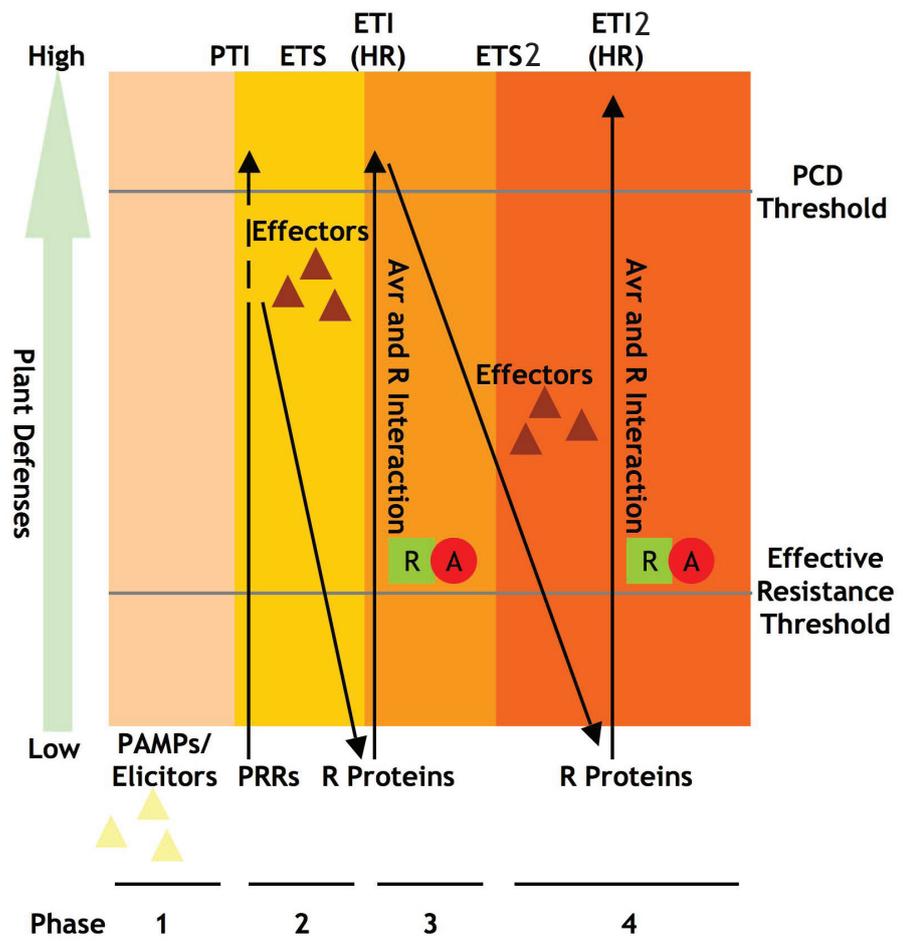
protein Gp42, CBELs, SRC proteins, INF1 and NPLs. They are summarised in **Table 1.1**.

The proteins in the plant that detect MAMPs/PAMPs are pattern-recognition receptors (PRRs) and most are receptor-like kinases (RLKs) or receptor-like proteins (RLPs; Schwessinger and Zipfel, 2008). They are situated on the plasma membrane (PM) and this interaction results in PAMP triggered immunity (PTI; MAMP/PAMP triggered immunity is collectively referred to as PTI). PTI aims to limit microbial growth and prevent the spread of infection (Yeam *et al.*, 2009).

A well-known example of a plant PAMP receptor is FLS2 in *Arabidopsis thaliana* and involves the perception of bacterial flagellin, which all gram-negative and gram-positive bacteria have. The receptor is the PRR FLAGELLIN SENSITIVE 2 (AtFls2) protein, which is a Leucine-Rich Repeat Receptor Kinase (LRR-RK). AtFls2 recognises a 22 amino acid (aa) conserved portion of flagellin, PsFlg22, and the recognition relies on the LRR domain of AtFLS2. PRRs are peptide/molecule-specific. Therefore, if the plant does not have the corresponding PRR for a particular foreign protein, the plant is unable to detect it and is effectively blind to its presence, enabling infection to take place (Gomez-Gomez and Boller, 2000; Boller and He, 2009).

1.3.2 Signalling During PTI

PTI consists of a number of plant responses including the induction of defence genes regulated by WRKY transcription factors (proteins with a conserved WRKY domain) which up-regulate many defence genes (Jones and Dangl, 2006). This type of immunity includes the production of reactive oxygen species (ROS), the initiation of the mitogen-activated protein kinase (MAPK) cascade and changes in ion fluxes (Hein *et al.*, 2009). For a pathogen to successfully overcome PTI it must either evade it with molecules that the plant cannot detect, or have proteins capable of over-riding/switching-off this stage in the plant immune defences. For example after PsFlg22 has been recognised by AtFLS2, AtFLS2 activates defences by transducing signals to the plant nucleus via MAPKs. AtBakI (BRI1-associated receptor kinase; Brassinosteroid insensitve 1) is a protein which acts in conjunction with FLS2 during PTI signalling and this is an example of a protein having multiple roles in the plant as it is involved in brassinosteroid signalling too (Chinchilla *et al*, 2007 & Heese *et al*, 2007). This example is described in more detail in section **1.3.3**.

1.3.3 Effector-triggered Susceptibility (ETS)

When PTI is suppressed by the pathogen's effector proteins, Effector Triggered Susceptibility (ETS) occurs and a compatible interaction is established. This is

Table 1.1 A summary of PAMP and possible PAMP proteins involved in PTI (Adapted from Hein *et al.*, 2009).

Secreted Protein's Name	Species Originated From	Points of Interest	PAMP Activity	Reference
CBEL (Cellulose-binding elicitor lectin)	*Phytopthora infestans, Phytophthora sojae, Phytophthora ramorum & Peronospora parasitica*	Oomycete specific PAMP.	Occurs at the CBEL's two cellulose binding domains (CBDs). It is a cell wall PAMP.	Gaulin *et al.*, 2006; Dumas *et al.*, 2008
GP42 (Transglutaminase; Tgase)	*P. sojae & Phytophthora*	Its activity is calcium-dependent and it is involved in cell differentiation and tissue regeneration.	Occurs at the GP42's 13aa region called Pep-13. Produces PTI responses and is a PAMP.	Nürnberger *et al.*, 1994; Brunner *et al.*, 2002
INF1 (Infestans1)	*P. infestans*	Elicitin	Causes PTI responses and interacts with PAMP receptors. It is a PAMP	Kamoun *et al.*, 2006; Heese *et al.*, 2007
NLPs (PAMP?) (Nep1-like proteins)	Oomycetes, fungi, gram-negative bacteria and gram-positive bacteria.	Two types (I & II). Elicitin/toxin	Cause PAMP associated defence responses in the host. Act outside the cell membrane. No conserved motif is required for PTI.	Fellbrich *et al.*, 2002; Qutob *et al.*, 2006
SCRs (Small cysteine-rich proteins)	Oomycetes: *P. infestans. Phytophthora cactorum*	Undergone diversifying selection and co-evolution	Could be targets for detection by the host. Examples inc. Avr4 and Avr9.	Orsomando *et al.*, 2001; Liu *et al.*, 2005

when the effector proteins prevent PTI and this leads to disease symptoms in the plant (Phase 2 in **Figure 1.2**).

An example of ETS is the protein PsAvrPto delivered into the plant via the T3SS. PsAvrPto has been linked to AtFls2 where PsAvrPto binds to the AtFls2's kinase domain, inhibits the PRRs activity and prevents PTI. PsAvrPto is known to have a similar effect on the AtEfr (EF-Tu Receptor; Elongation Factor Thermo unstable) that binds EF-Tu. PsAvrPto also binds to the AtBak1's kinase domain that in turn prevents the formation of the AtFls2-AtBak1 complex and this prevents effective PTI (Hein *et al.*, 2009).

1.3.4 Effector-Triggered Immunity (ETI)

Effector Triggered Immunity (ETI) is the phase of defence that utilises Resistance (R) proteins to detect effectors, which are then called Avirulence (Avr) proteins. There are 2 main categories of genes that determine whether an interaction is compatible or incompatible. These are resistance genes (*R* genes) that originate in the plant and avirulence genes (*Avr* genes) that originate from the pathogen. Flor put forward a hypothesis in the 1940s involving the interaction of the plant's *R* gene with the invading pathogen's *Avr* gene (Flor, 1942). The presence of both dominant forms of the two genes causes a defence response in the plant and disease does not occur. When an incompatible plant-pathogen interaction occurs defence mechanisms within the plant cell(s) at the point of invasion are activated. This *R* gene mediated resistance occurs within 24 Hours and is collectively known as the hypersensitive response (HR). It results in the death of the invaded cells (cell death; CD) as well as the death of some of the cells surrounding the infection point. This localised programmed CD (PCD) prevents further pathogen invasion occurring and involves the activity of cysteine proteases. The dead cells contain antimicrobial compounds made in response to the pathogen and these reduce the infection spread. Finally, the PCD of the cells prevents the spread of toxins and effector molecules to the rest of the host plant also resulting in reduced infection. If the plant does not have the corresponding dominant *R* gene for the particular pathogen's *Avr* gene, then disease will occur in the plant. This Gene-for-Gene hypothesis is shown diagrammatically in **Figure 1.3a**.

When the two dominant corresponding genes in the pathogen and the plant are present a signal transduction cascade occurs in the plant and this initiates the plant defence responses. There are a number of different R proteins in the plant and they are found in the cytoplasm and nucleus (Burch-Smith *et al.*, 2007 & Gao *et al.*, 2011). All *R* genes share common structural features and can be divided into a number of sub-groups. Over 30 R proteins have a C-terminal

Figure 1.3 Diagram of the Gene-for-Gene Hypothesis and The Guard Theory.
A. The Gene-for-Gene Hypothesis. When both the plant and the pathogen have the corresponding dominant *R* and *Avr* gene alleles disease resistance occurs in the plant. If one or both alleles are not present in the dominant form, disease in the plant occurs. There are several different groups of *R* genes with the main class consisting of the genes coding for proteins with the NBS-LRR regions (nucleotide binding site and leucine rich repeat). These NBS-LRR proteins consist of TIR proteins and Proteins with a leucine zipper in their structure. This class of R proteins is found in the cytoplasm although there are some R proteins that are extracellular. Avr proteins have little structural similarity as it is evolutionary unfavourable to do so.

B. The Guard Theory represented as a diagram using an example of AtRpm1 "guarding" the plant protein RIN4. When *Psudomonas syringae* effector proteins PsAvrRpm1 or/and AvrB enter *A. thaliana's* cytoplasm AtRin4 is hyperphosphorylated (P) and this protein modification activates AtRpm1 mediated disease resistance pathways. AtNdr1 is required for this defence activation to work (Adapted from Day *et al.*, 2006 & Chisholm *et al.*, 2006).

A
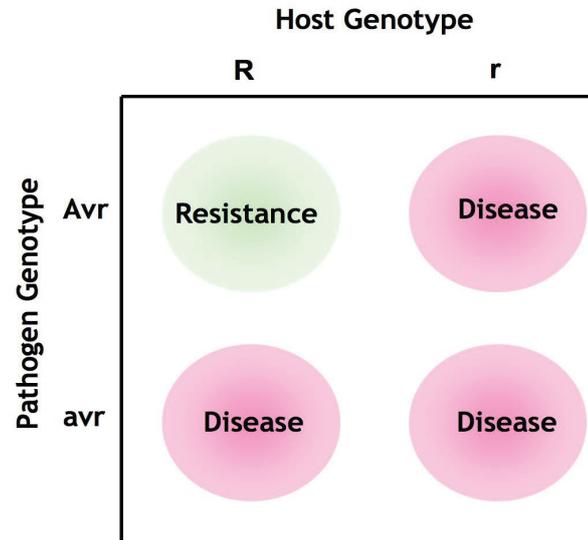
B
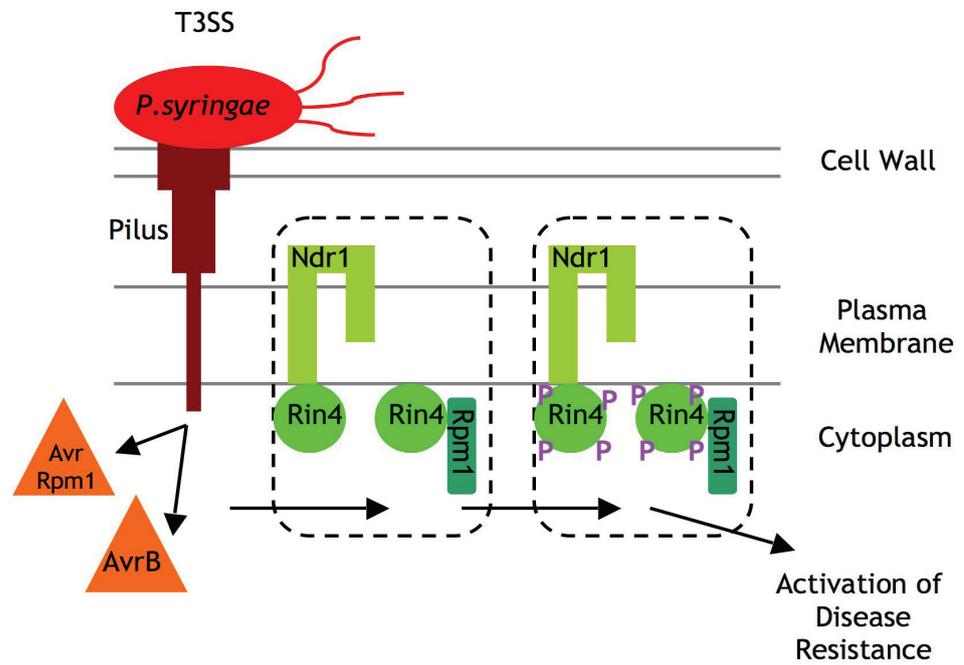
leucine-rich repeat (LRR) that is involved in protein-protein interactions. LRRs have an N-terminal domain, which is usually a coiled coil (CC) or a TIR (Toll/interleukin-1 receptor) protein structure. LRRs have a repeating α-ß protein structure and are involved in protein-protein interactions. Some believe that this protein-protein interaction site is where the Avr protein associates as part of disease resistance. The majority of R proteins found so far have a nucleotide binding domain or site (NBD or NBS). The NBS is vital to an R protein's function because a mutation in the NBS domain results in a loss of function. There are thought to be approximately 150 NB-LRR coding *R* genes in *A. thaliana*. Another, smaller group of R proteins have extracellular LRR domains (e.g. Cf proteins) and another small class encode serine/threonine protein kinases (e.g. Pto; Van Der Biezen and Jones, 1998; Takken and Joosten, 2000; Nimchuk *et al.*, 2003; Belkhadir *et al.*, 2004).

An example of a Gene-for-Gene interaction is the PAMP-PRR interactions in plants of the fungal peptide elicitor CfAvr9 and CfAvr4 from *Cladosporium fulvum* (*Cf*) by the tomato Cf9 and Cf4 receptors respectively in *Solanum lycopersicum*. These *Cf* genes encode a type I trans-membrane glycoprotein with an LRR domain (Thomas *et al.*, 1998). This interaction induces a number of genes known as CfAvr9/LeCf-9 rapidly elicited (ACRE) genes that were identified in tobacco (*Nicotiana tabacum*) which initiates a defence response in the plant (Rowland *et al*, 2005). The Avr-Cf interaction has now been found not to be direct for Cf-2/Avr2, and it is believed that there are intermediate proteins present involved in Avr's perception (Stergiopolis & de Wit, 2009).

The Gene-for-Gene Hypothesis is a simplified version of what is now believed to happen during pathogen invasion and one of its disadvantages, as a hypothesis, is that it implies that the R protein and Avr protein interact directly. However this has been found not to be the case in bacteria. A more recent hypothesis that takes this into account is The Guard Theory (**Figure 1.3b**). This theory involves the indirect association between the R protein and the Avr protein via another plant protein intermediate. It is believed that the Avr protein, to suppress defence, targets this protein intermediate in the plant, which acts as regulator of defence. This results in a structural change in the protein intermediate allowing the R protein to bind to it and this in turn initiates plant defence responses. If the *R* gene is not present, the binding of the Avr protein with the plant protein intermediate prevents the signal transduction cascade in PTI and infection occurs. It is thought that the LRR domain structure provides a ligand-binding domain on which the Avr protein signal can occur (van der Biezen and Jones, 1998; Kaloshian, 2004).

Work done using NBS-LRR proteins supports the Guard Theory and these include RESISTANCE TO *P. SYRINGAE* PV MACULICOLA 1 (AtRpm1) and RPM1 INTERACTING PROTEIN 4 (AtRin4) as shown in **Figure 1.3b**. AtRin4 associates with two different type III effector proteins in the plant and they are PsAvrRpm1 and PsAvrB. It is this association that activates AtRpm1. AtRin4 also associates with PsAvrRpt2, a cysteine protease, which degrades AtRin4 activating the NB-LRR protein AtRps2. AtRin4 also activates NONRACE-SPECIFIC DISEASE RESISTANCE1 (AtNdr1), which is required for the activation of both AtRpm1 and AtRps2 (Mackey *et al.*, 2002; Nimchuk *et al.*, 2003; Belkhadir *et al.*, 2004; Jones and Dangl, 2006).

Another method by which the plant defends itself is via "*The Decoy Theory*". This recent theory involves the pathogen's invading protein binding to the plant proteins, such as kinases, and preventing their function. An example of this is PsAvrPto which binds to kinases to stop their function. If Pto is over expressed there is increased plant defence and it is therefore surmised that Pto is acting as a decoy protein (Kamoun & van der Hoorn, 2009).

Whereas PRRs operate at the PM, R protein interactions occur inside the cell and consist mainly of proteins with NB-LRR domains. Their indirect or direct interactions initiate ETI and result in a strong defence response in the plant called the Hypersensitive Response (HR) at the site of infection. It is not clear how this HR in a particular cell prevents pathogen growth (Jones and Dangl, 2006).

1.3.5 Pathogen Avirulence (Avr) Genes in Detail

An example of an *Avr* gene is CfAvr2 from the fungi *C. fulvum*, which is secreted into the apoplast of tomato plants and localises to the PM. CfAvr2 has an LRR transmembrane domain and its known function is to inhibit plant cysteine proteases (Rooney *et al*, 2005). CfAvr2 also interacts with tomato Rcr3, an apoplastic cyc protease. CfAvr2 is a known virulence factor and inhibits the RCR3 protease released by the plant. Proteases are part of the plant's basal defences and by inhibiting RCR3 CfAvr2 overcome the plant's defences (Krüger *et al.*, 2002; van Esse *et al.*, 2008).

So far there are 11 Avr effector proteins from oomycetes, which have been found to cause HR in hosts expressing the corresponding R protein (Allen *et al.*, 2004; Shan *et al.*, 2004; Armstrong *et al.*, 2005; Rehmany *et al.*, 2005; ; van Poppel *et al.*, 2008; Vleehouwers *et al.*, 2008). These Avr proteins share a common N-terminal 60 aa region which houses a conserved RxLR motif followed by a number of acidic (D/E) aa. These Avr C-terminal regions are responsible for

virulence. The RxLR region has been found to be required for translocation into host cells (Whisson *et al.*, 2007).

PiAvr3a is an RxLR effector protein from *P. infestans* and is the oomycete protein studied in this project. The protein consists of a signal peptide up stream of the RxLR motif for secretion from the pathogen haustorium. This motif is followed by the conserved EER aa sequence at the C-terminus. The RxLR-EER is required for delivery from *P. infestans* into the host cell and is delivered via haustoria into the plant (Whisson *et al.*, 2007). PiAvr3a (K80I103) interacts with the potato R protein R3a and is therefore avirulent (Armstrong *et al.*, 2005). PiAvr3a is thought to be involved in colonisation and the promotion of disease, as it manipulates plant defences by suppressing programmed cell death (PCD; Bos *et al.*, 2006; Birch *et al.*, 2009).

Recent findings have shown that PiAvr3a suppresses CD induced in *Nicotiana benthamiana* by the *P. infestans* PAMP PiInf1 (Infestans 1). The recognition of PiAvr3a by R3a and the suppression of PiInf1 cell death is independent of the RxLR motif and this implies that the aa involved in determining effector function are downstream of the RxLR (Bos *et al.*, 2006). Another critical aa in the PiAvr3a sequence is Y147 at the C-terminal. Mutating Y147 results in no CD suppression and therefore is important for effector function (Bos *et al.*, 2009).

PiAvr3a exists as two different alleles: PiAvr3a^{KI} and PiAvr3a^{EM}. There is a difference of 3 aa between them and only 2 of these are present in the mature protein. PiAvr3a^{EM} (S19, E80, M103) has E and M present in the mature form and PiAvr3a^{KI} (C19, K80, I103) has the K and I in its mature form. As well as aa differences, there are also functional differences. PiAvr3a^{KI} is avirulent and recognised by StR3a. PiAvr3a^{EM} is virulent and not recognised by StR3a (Armstrong *et al.*, 2005). PiAvr3a^{KI} is the form of PiAvr3a which best suppresses PiInf1 cell death whereas PiAvr3a^{EM} does so weakly (Bos *et al.*, 2006, 2009). These functional differences have been accredited to the 2 aa variations, as both proteins are stable and express equally in the cell. Two other *P. infestans* RxLR effectors have been shown to suppress PiInf1 induced cell death called PiPexRD8 and PiPexRD36(45-1). It is becoming apparent that this PiInf1 suppression characteristic is present in only a few RxLR effectors (Bos *et al.*, 2006; Oh *et al.*, 2009).

1.3.6 Signalling During ETI

Effector-triggered susceptibility (ETS) forms the basis for ETI. It is hypothesized that NB-LRR proteins on recognition of Avr effectors are folded into an active signal state by receptor chaperones such as Heat Shock Protein 90 (Hsp90). This

is likely to involve intra- and intermolecular conformational NB-LRR protein changes similar to those already seen in animal systems.

An example of signalling during ETI is the protein AtSgt1 (suppressor of the G2 allele of skp1). AtSgt1 interacts with AtRar1 (required for Mla12 resistance) and both interact with AtHsp90 as part of *R* gene resistance. AtSgt1 is thought to act as a co-chaperone with AtRar1 for AtHsp90 as part of disease resistance and therefore is an example of the signalling that occurs during ETI. AtSgt1 has a role in ubiquitination as a requirement for the function of an SCF (Skp1-Cul1-F-box) E3 ubiquitin ligase (Kadota *et al.*, 2008). This is discussed in more detail below.

Plants do not limit themselves to a single CD response. Defence genes can be activated throughout the plant to employ an all over, systemic defence response. This systemic resistance aims to prevent the spread of disease in other areas of the plant. After an HR has occurred the systemic resistance is activated and this has 2 subgroups: systemic acquired resistance (SAR) resulting from an HR and induced systemic resistance (ISR), activated when the plant is challenged, for example, by bacteria associated with the roots (Smith *et al.*, 2009).

The SAR induced by pathogen uses salicylic acid (SA) as its signal molecule and this type of response can be recognised by the build-up of pathogenesis-related (PR) proteins at the infection point and other locations throughout the plant, especially in areas surrounding the infection point. PR proteins are known to include chitinases and glucanases although the function of many PR proteins is still unknown. ISR is characterised by the involvement of signalling molecules jasmonic acid (JA) and ethylene. ISR does not involve SA. An example of SAR is the response produced in *N. tabacum* when infected with avirulent Tobacco Mosaic Virus (TMV). Infections made elsewhere on the plant after the initial infection produce smaller lesions than on the original site and this is due to SAR (Smith *et al.*, 2009).

1.4 Ubiquitin and Ubiquitination

Ubiquitin (Ub) is a globular, 76 aa protein found in eukaryote cells (Weissman, 2001). The Ub pathway involves more than 6% of the *A. thaliana* proteome which indicates the importance of ubiquitination in plant cellular functions (Downes and Viestra, 2005). Ub exists in the cell as either a monomer or a polymer by forming a poly-ubiquitin chain. Ub plays a major role in the degradation of intracellular proteins and has been linked to plant defence responses. A mono- or poly-Ub chain attaches to a protein and labels it to be

acted on elsewhere in the cell. Ub has been found to act as a label for protein degradation as part of the Ub-Proteasome System (UPS; Pickart and Fushman, 2004).

Ub is a highly conserved protein and there is great similarity between Ubs found in various different species within plants and mammals (Weissman, 2001). Ub has a wide range of functions within the cell and many of these are still not fully understood. The UPS enables the Ub to tag the protein substrate for degradation and this process releases aa from the degraded protein to be recycled and reused within the cell.

1.4.1 The Ubiquitin Cycle

This pathway involves the tagging of cellular proteins via lysine (K) residues in Ub. As will be described further, Ub attaches itself to the protein and to other Ubs using one of its 7 Ks (designated by aa number in the Ub aa sequence; aa: 6, 11, 27, 29, 33, 48 & 63). Ub attaches to itself and other proteins covalently using an iso-peptide bond between the Ub's carboxy-terminal glycine (Gly76) and the protein's ε-amino lysine (Aguilar and Wendland, 2003). The Ub acts as a label and this labelling of the protein substrate enables, for example, the 26S proteasome to detect it and break the substrate into its constituent aa using ATP. There are a number of key stages involved in the binding of Ub to the substrate and its subsequent degradation. The stages involved are described in the following three sections (**1.4.1.1 E1 Activating Enzyme, 1.4.1.2 E2 Conjugating Enzyme, 1.4.1.3 E3 Ligase Enzyme** & **Figure 1.4**).

1.4.1.1 E1 Activating Enzyme

The Ub activating enzyme is known as the E1 and is produced by two genes; *AtUba1* and *AtUba2*. They are two different paralogue isoforms with 81% DNA sequence similarity (Weissman, 2001; Roos-Mattjus and Sistonen, 2004). E1 enables Ub to form an E1-Ub intermediate via an ATP-dependent reaction (Roos-Mattjus and Sistonen, 2004). The bond formed to create this intermediate is a thiol-ester bond which is made at the Ub's carboxy-terminal glycine (Weissman, 2001; Sun and Chen, 2004). This process is the first stage in the UPS pathway and is shown in **Figure 1.4**.

1.4.1.2 E2 Conjugating Enzyme

The Ub-conjugating enzyme, or E2, acts as a carrier for the E1-Ub intermediate. E2 enzymes are usually less than 36 KDa and in the mammalian system there are thought to be approximately 25 Ub-conjugating enzymes. In plants there are 36 identified E2s at this time, however it is believed there are more. These plant E2s have been categorised into 12 different groups based on their properties

19

Figure 1.4 The Ubiquitin-Proteasome System.

Free Ub (represented as blue circles) joins to the plant E1 using ATP and a thiol-ester linkage, which in turn transfers Ub to the corresponding E2. This transfers the Ub to an appropriate E3. The Ub-E3 complex binds to the target protein (represented by an orange cross) by attaching the Ub to one of the protein's lysine residues and forming an isopeptide bond. Poly-ubiquitination occurs by the binding of multiple Ubs to the protein-Ub complex using the lysine on the already protein bound Ub (Vierstra, 2003). If the labelled target protein is tagged for degradation it will travel to the 26S proteasome in the nucleus where DUBs will remove the Ubs and the target protein will be broken into its constituent aa.
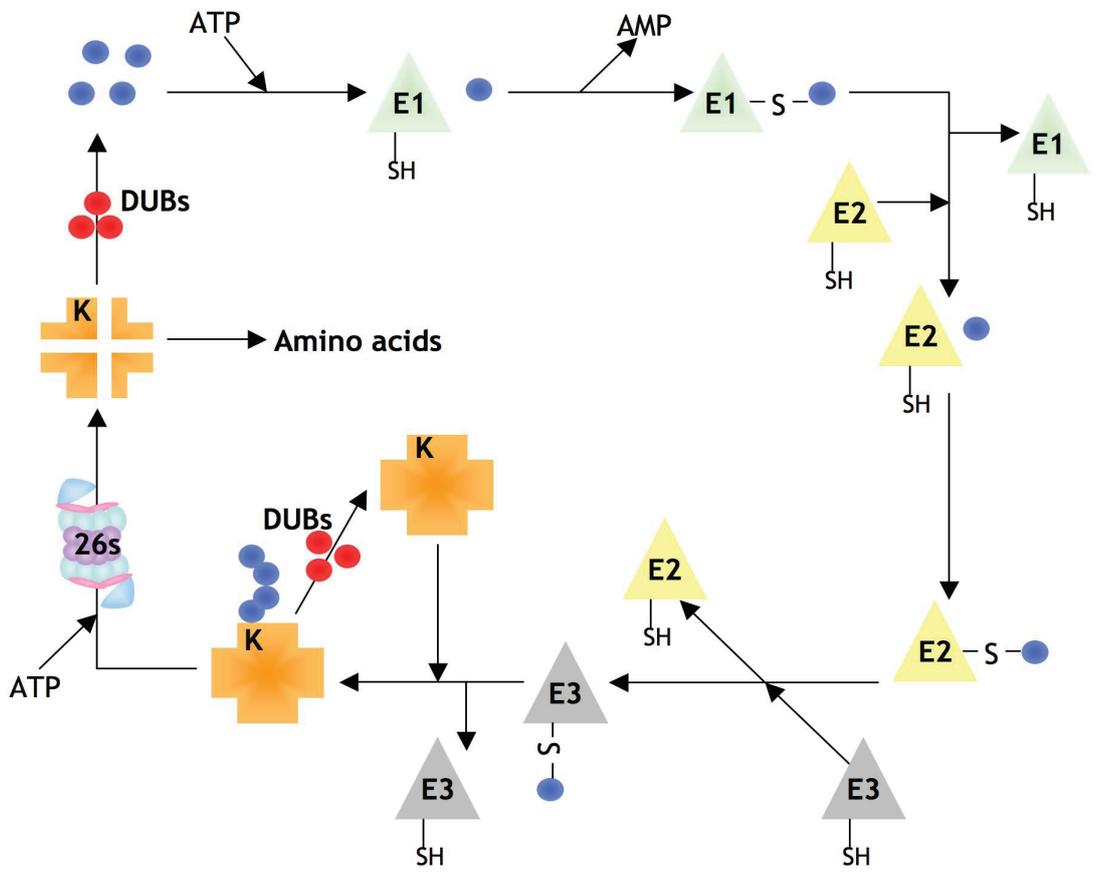
(Callis and Viestra, 2000). The intermediate Ub-E1 is bound to the E2 via a trans-esterification reaction where it joins to a cysteine residue on the E2's active site. E2 carries the intermediate as a thiol-ester to the amino group of the protein and transfers the Ub over to the E2 (Kornitzer and Ciechanover, 2000; Pickart, 2001a; Weissman, 2001). This results in the creation of an Ub-E2 complex.

1.4.1.3 E3 Ligase Enzyme

In the final stage, the E2 binds to an Ub ligase (E3). The binding of the substrate's lysine residue transfers the Ub to the protein resulting in an Ub-substrate complex. The particular E3 involved depends on the protein to be tagged and the specific Ub tag that is required. It is a specific enzyme-substrate interaction. Each E2 is able to interact with more than one E3. Therefore, a specific E2 can be involved in the modification of more than one substrate protein (Roos-Mattjus and Sistonen, 2004; Sun and Chen, 2004). There are a large number of different E3s and they are by far the largest enzyme group out of all the Ub enzymes. It is likely that the full number has not yet been discovered in plants or animals (Roos-Mattjus and Sistonen, 2004).

The UPS, including the three-enzymatic stages: E1, E2 and E3 are summarised in **Figure 1.4**. These enzymatic stages result in conjugation of Ub to the target protein.

There are four different groups of E3s in *A. thaliana* and these are categorised by their structures. They are: HECT (Homologous to E6-AP Carboxyl Terminal), RING/U-Box (Really Interesting New Gene), Cullin-based (also know as SCF) and APC (Anaphase-Promoting complex). Their general structures are shown in **Figure 1.5** and described below.

1.4.1.3a HECT

HECT E3s are enzymes containing a HECT domain, which have a Cys residue. This residue is the aa that the Ub is transferred onto from the E2 during the ubiquitination cycle. HECT E3s are greater than 100 KDa in size and they possess protein-interacting regions such as a coiled-coil (CC). They are categorised by the presence of a 350 aa C-terminal HECT domain which showed homology to an E6-AP C-terminus (Vierstra, 2003). There are a number of HECT E3s and they are differentiated by their different NH_2-terminal domains and this variation allows different HECT E3s to recognise different protein substrates (Glickman and Ciechanover, 2002). The HECT domain has a binding site for an Ub-E2 complex and a conserved cysteine residue that can accept the Ub to form the E3-Ub complex joined by a thiol-ester bond. This binding leads to the final stage where

Figure 1.5 Diagram of the Main Categories of E3 Ligases.
A. RING/U-Box E3 ligases have a common basic structure containing the
structural elements shown. The E2 is represented by C, the position of the
target protein and its Ub are shown on the complex in relation to the RING
domain.

B. HECT E3 ligases have a common basic structure containing the structural
elements shown including a HECT domain.

C. APC E3 ligases have a common basic structure containing the structural
elements shown. The distinction in this group is the presence of the APC2
complex with the CDC20/CDH1 and APC11.

D. SCF Cullin based E3 ligases have a common basic structure containing the
structural elements shown. This E3 ligase group has a target specificity module
as well as a Cullen/RBX1 protein complex (Adapted from Vierstra, 2003).

A Ring/U-box

B HECT

C APC

D Cullen Based/SCF
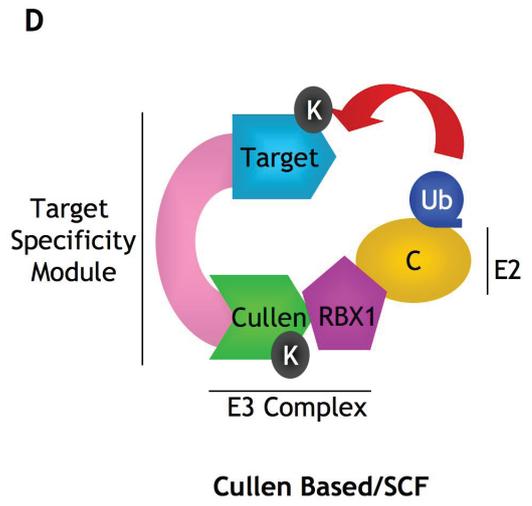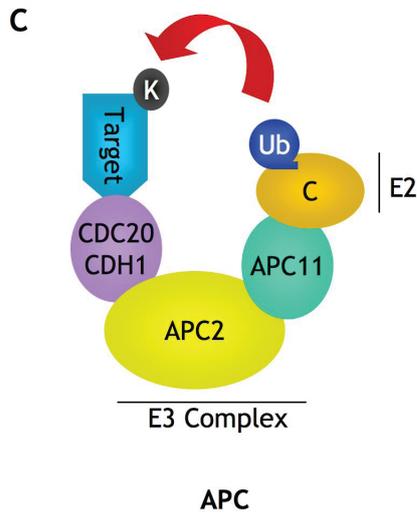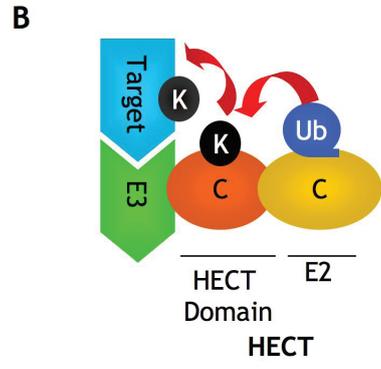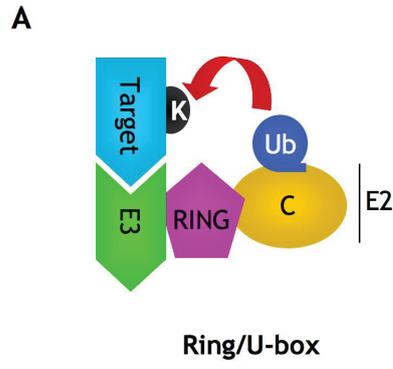
the ubiquitination of the substrate protein takes place. The HECT E3 is thought to identify the protein substrate using its protein interacting motif.

1.4.1.3b RING/U-Box

RING/U-Box E3s (Really Interesting New Gene) all have a RING-finger structure made up of eight Cys and His residues and are thought to bind to two zinc cations. The Zn^+ cations are arranged in an interleaved pattern. RING/U-Box E3s are classified into two groups depending on whether the fifth coordination site is a Cys or a His. They are either RING-HC (fifth coordinate site is a His) or RING-H2 (fifth coordinate is a Cys). The RING/U-Box E3 binds to compatible E2s using peptide bonds between a groove in the RING/U-Box and two loops in the E2. There are two categories of RING/U-Box E3s: single and multi-subunit proteins. About 400 RING/U-Box E3s have now been identified in *A. thaliana*. RING/U-Box E3s are known to have motifs N-terminal to the RING-finger which are involved in target recognition (Glickman and Ciechanover, 2002; Vierstra, 2003; Roos-Mattjus and Sistonen, 2004).

U-Box E3s all have a RING finger called a U-Box. There are approximately 37 U-box E3s in *A. thaliana* and they are thought to use a different method of interaction compared to the zinc chelation used by the RING E3s. RING/U-box E3s are not directly involved in Ub ligation. However, they are a platform for Ub-E2 and the E3 ring finger to interact and enable Ub to label proteins. No Ub-E3 intermediate is formed in this case (Vierstra, 2003).

1.4.1.3c SCF

SCF (Skp1 Cdc53/Cullin F-box receptor; cullin-based) E3s are involved in targeting protein substrates for phosphorylation and were originally found in *Saccharomyces cerevisiae* (budding yeast; Deshales, 1999; Glickman and Ciechanover, 2002). SCF E3s are made up of four polypeptides: SKP1, CDC53 (Cullin), F-box protein and RBX1 (or ROC1 and HRT1). It is the RBX1 that contains a Ring H2-type RING finger that binds E2-Ub. SCF E3s act as a platform for the transfer of Ub from the E2 to the target protein. No Ub-E3 intermediate is formed. It is the F-Box in this group of E3s that results in specificity for particular E2s. Examples include ScCdc43 (ScUbc3) and possibly the HsUbcH5 E2 family. So far 694 F-Boxes have been found in *A. thaliana* and only a small number have had their functions determined (Kornitzer and Ciechanover, 2000; Devoto *et al.*, 2003; Vierstra, 2003).

1.4.1.3d APC

APC (Anaphase Promoting Complex) has 12 or more subunits. The main subunits are Cullin and RING-finger motifs that are involved in ligase activity. It has been

found that one gene encodes the Cullin subunit for APC in plants and therefore it is likely that only one isoform exists. APC is thought to be involved in pathways other then the UPS as well as catalysing the degradation of phosphorylated substrates and mitotic cyclins (Vierstra, 2003; Roos-Mattjus and Sistonen, 2004).

From the information already gathered on E3s it is apparent that the E3 family can label a vast number of different protein substrates for ubiquitination with various fates.

1.4.2 The 26S Proteasome

In the *A. thaliana* genome there are approximately 1300 genes involved in the UPS. This implies that the UPS is a complex system in plants (Vierstra, 2003). The 26S proteasome is the final step in the UPS and is located in the nucleus and cytoplasm of eukaryotic cells. The 26S proteasome recognises Ub chains linked by K48 (Weissman, 2001; Vierstra, 2003; Roos-Mattjus and Sistonen, 2004). The 26S proteasome is large (2.5 MDa) and the structure is shown in **Figure 1.6**.

It can be seen from **Figure 1.6** that the 26S proteasome is made up of two parts: the 20S core protease (or catalytic particle; CP) and the 19S regulatory particle (RP or PA700). The CP is made up of heptameric rings stacked on top of each other with fourteen rings in total made up of seven alpha and seven beta subunits. The alpha rings are located at either end of the stack with beta rings in the centre i.e. a "alpha1-7beta1-7beta1-7alpha1-7" arrangement. The CP requires ATP and Ub to function. This arrangement of the alpha and beta subunits allows only unfolded proteins to enter the chamber. The chamber formed by the rings is situated in the middle of the proteasome and this is where the protease active sites are located. These active sites are where substrate degradation takes place. The selectivity for unfolded proteins is achieved by the alpha subunits forming a narrow gated channel only allowing unfolded proteins to enter (Kornitzer and Ciechanover, 2000; Vierstra, 2003; Roos-Mattjus Sistonen, 2004).

The RP is situated on the top and bottom of the CP. The RP consists of a lid and a base which are each made up of sub-components. The base consists of three non-ATPase subunits and six AAA-ATPases. The AAA-ATPases are arranged in a ring formation. Rpn10 acts as a hinge and is able to interact with the lid and the base of the RP. Rpn10 and the base of the 26S proteasome are believed to be involved in substrate recognition (Nandi *et al.*, 2006).

The lid on the base is made up of 9 Rpn subunits. The lid is hypothesized to be involved in releasing Ub from the protein substrate and moving the protein into

Figure 1.6 The 26S Proteasome

A. The 26S proteasome is made up of a 20S subunit containing alpha and beta rings. The active site for protein degradation is in the centre of the beta rings know as the cleavage site. Two 19S sub-structures are situated at either end of the 20s subunit. The "bases" of the 19S contain nine subunits as well as Rpn10. The base section is made up of six ATPase subunits and Rpn1 and Rpn2. Ubiquitin-labled protein is unfolded and enters at the top for degradation and leaves at the bottom as aa protein constituents. The ubiquitin(s) are removed from the protein substrate before entering the 26S complex by deubiquiting enzymes (DUBS).

B. A cross section of the 26S proteasome showing the cleavage site for protein degradation and the structure inside the cylinder like structure that makes up the body of the 26S proteasome.

A

Release

Ubiquitin Recognition

19S — Lid, Base

20S CP — Alpha, Beta, Beta, Alpha

19S — Base, Lid

Protein Substrate

Amino Acids

B

Unfolding

Opening

Cleavage Site

20S CP
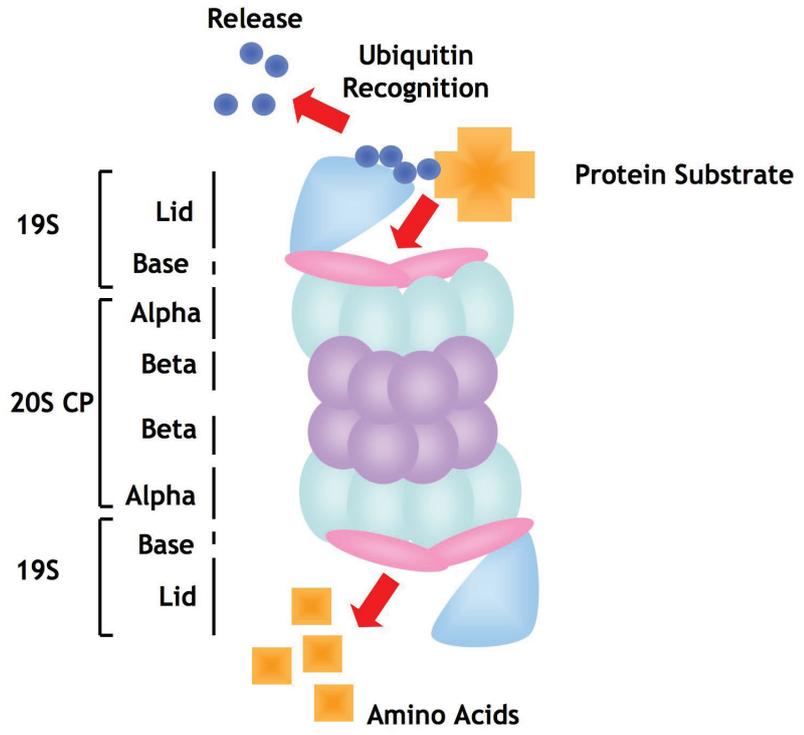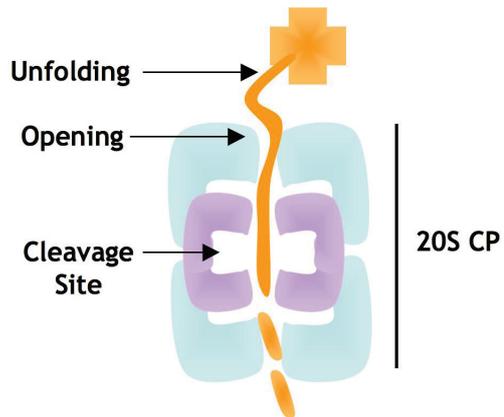
the CP. Rpn11 has been found to be a metalloideubiquitylase which removes the Ub chains from the protein substrate which was shown using mutant Rpn11. The lid's components show homology to CSN (COP9 signalosome) components. CSN is involved in signal transduction in plants as well as in a range of other biological processes. The CSN has been found to compete with the lid for interaction with the rest of the 26S proteasome and can function successfully in the place of the lid. This is supporting evidence as to the roles of the RP lid (Schwechheimer, 2004; Nandi *et al.*, 2006). The exact functions of the RP are not fully understood. However, it is thought that the RP is involved in protein recognition, de-ubiquitination, unfolding of the target protein and the moving of the protein into the active site area of the 26S proteasome (Vierstra, 2003; Roos-Mattjus and Sistonen, 2004).

The Ubs are removed from the target protein before it enters the 26S proteasome by enzymes located at the entrance to the proteasome. There are a number of different forms of these enzymes but collectively they are called de-ubiquitinating enzymes (DUBs) and act to de-attach Ubs and thereby return them to their free state in the cell for reuse.

1.4.3 The Ub Conjugation Cascade

There are more E3s than E2s and more E2s than E1s; therefore the potential number of possible E1-E2-E3 combinations is large. This increasing number of enzymes from E1 to E3 is known as the Ub conjugation cascade. As the UPS progresses from the E1 step to the E3 step the binding specificity of the protein increases. E3 or E3 bound to E2 is the factor that determines the specificity level of substrate recognition (Weissman, 2001). The hierarchical structure of the UPS is shown in **Figure 1.7**.

The UPS cascade has a rhomboid shape as can be seen in **Figure 1.7**. At the top of the cascade is E1 and at the bottom is the 26S proteasome. The largest part of the cascade is where the E2s and E3s interact together. There are many E2s that can interact with E1. There are thousands of E3s that can interact with the hundreds of E2s. More than one E3 can interact with a single E2. This produces the cascade affect and results in a large number of possible E1-E2-E3 combinations providing ubiquitination specificity. This concept of a pyramidal shaped cascade is now thought to be over-simplified and in reality the cascade is a more complex network especially with the possible addition of E4s (Pickart, 2001a; Glickman, 2002).

1.4.4 The Chains of Ubiquitin and Their Fates

This Ub binding cycle can be repeated numerous times to create a poly-ubiquitin

Figure 1.7 The UPS Hierarchy Structure.

The cascade begins with an E1. The E1 reacts with the 100s of possible E2s using ATP. Each E2 can interact with many E3s, which exist in large numbers, possibly thousands. The labelled target protein then enters the 26S proteasome for degradation. This is described as a cascade in that one E1 reacts with many E2s and in turn a single E2 reacts with many different E3s (Glickman and Ciechanover, 2002). The different combination of the 3 enzymes determines the destination of the target protein and the type of ub lysine linkage formed in the Ub chain. Recently the discovery of E4s has led to a debate as to their role either as a subgroup of E3s or as a new class of Ub proteins.
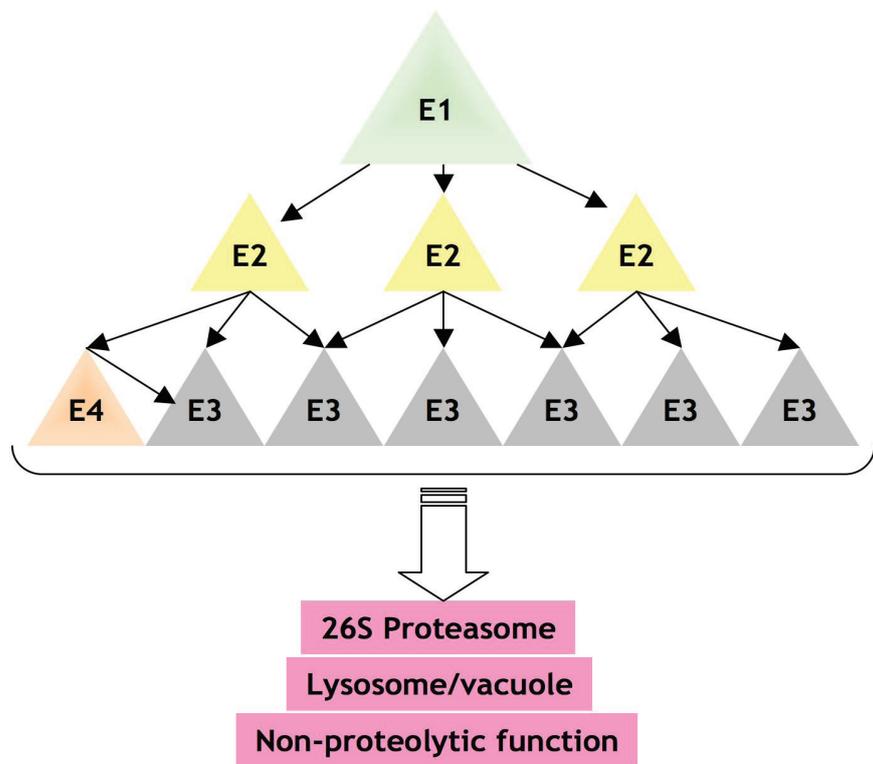
chain on a single substrate protein. The type of chain produced depends on the type of tag required. The poly-ubiquitin chain is formed by Ubs binding to Ubs already attached. The Ubs join at the glycine (Gly76) of the Ubs already attached and its own lysine. Because Ub has seven lysines (K; K6, K11, K27, K29, K33, K48 and K63) this enables a potentially large number of different label combinations. The lysine that is used to form the chain will dictate the final fate of the substrate. For example if the Ub chain formed is at the Ub's lysine 48 (Lys48) the protein will be sent to the 26S proteasome to be degraded (Roos-Mattjus and Sistonen, 2004).

1.5 Ubiquitin has Diverse Biological Roles

In recent years it has become apparent that Ub has a far more diverse role in cells than originally thought. Ub is not only associated with the UPS and is important in many other cell functions in both mammals and plants. In mammals Ub has been found to be involved in DNA repair, protein sorting, virus budding, regulation of cell cycle, IKK (IkB Kinase Complex) activation, immune response, protein misfolding, ER-associated degradation and disease progression (Hicke, 2001; Pickart, 2001b; Roos-Mattjus and Sistonen, 2004; Nandi *et al.*, 2006). The UPS, and hence Ub, has been linked to cancer and cell survival, disease progression, inflammatory responses, immune responses, protein mis-folding and the regulation of the cell cycle in mammals (Nandi *et al.*, 2006). In plants the functions of Ub are not as fully understood but they are known to be involved in circadian rhythms, DNA repair, embryogenesis, endocytosis, floral homeosis, gene expression, hormonal responses, kinase activation, pathogen defence, photomorphogenesis, senescence, silencing, trafficking and trichome differentiation (Vierstra, 2003; Pickart and Fushman, 2004; Sun and Chen, 2004).

It has been found that the poly-Ub chain length decides the type of signal produced by Ub and hence its particular area of involvement. For example, mono- and di-ubiquitination is involved in endocytosis and Ub chains of approximately 4 Ubs are involved in proteasomal degradation. The particular lysine on the Ub used to form the isopeptide bond is also important in Ub's association with different cellular processes. For example, isopeptide bonds formed between Ubs K63 are involved in DNA repair and K48 is a label for protein degradation (Aguilar and Wendland, 2003). It has been realised that Ub and the UPS have a variety of other components involved in the process of Ub labelling and signalling. These intricate networks involving the UPS help to define the meaning of each Ub chain's signal (Vierstra, 2003).

1.5.1 The Pathways Involved in Plant Defence: E3 Ligases

The research into ubiquitination and defence in plants is not as extensive as that in mammals. A summary of the E3 ligases so far found to be involved in plant disease and defence is shown in **Table 1.2** and some of the main discoveries are described below. F-Box proteins have been shown to have a role in plant defence: Coronatine Insensitive 1 (AtCoi1) and Suppressor of nim1-1 (AtSon1). AtCoi1 regulates defence pathways controlled by JA and produces a protein with an F-Box and an LRR domain. AtCoi1 has been found to associate with Skp1, Cul1 and Rbx1 providing strong evidence that the AtCOI1 SCF-complex is involved in the regulation of JA responses as an E3 ligase (Devoto *et al.*, 2003 & Gfeller *et al.*, 2010).

Unlike AtCoi1, AtCPR30 (Constitutive expressor of PR genes 30) is a negative regulator of defense. AtCPR30 is an F-box E3 Ub ligase. It was found to regulate SA-dependent and SA-independent defense signalling. This action is likely to occur through the Ub-proteasome pathway considering the nature of the gene. (Gou *et al.*, 2009).

AtPub17 is a U-box protein and part of the plant specific U-box subgroup that contains an ARMADILLO repeat motif. AtPub17 is an E3 ligase with homology to *N. tabacum* CfAvr9/LeCf9 Rapidly Elicited (NbACRE276) and *Brassica napus* ARM Repeat-Containing 1 (BnArc1). AtPub17 was found to be involved in cell defence signalling and is a positive regulator of CD (Yang *et al.*, 2006). Other possible genes for RING E3 Ub ligases involved in defence include *Arabidopsis Toxicos en Levandura* 2 (AtAtl2) and *Arabidopsis Toxicos en Levandura* 6 (AtATL6), which code for a RING protein and are induced by elicitor treatment. Other possible E3s involved in disease defence include E3s with a U-box, which were also elucidated using elicitor induction. A more recent example of a RING-finger protein's involvement in plant defence is StRfp1 from potato (homologue NtACRE132) that was cloned after potato leaves were infected with *P .infestans*. Over expression line studies showed slower *P. infestans* disease development and it was concluded that StRfp1 is involved in a number of disease responses against *P. infestans* (Ni *et al.*, 2009).

A further E3 involved in disease defence is StCMPG1. StCMPG1 is a U-box ARMADILLO E3 ligase found in potato. It is a protein with a conserved CMPG aa motif in its sequence. It shares homology to genes in *Petroselinum crispum* (PcEli17), *N. tabacum's* Avr9/Cf-9 Rapidly elicited 74 (NtAcre74) and *A. thaliana* Plant U-BOX 20 and 21 (AtPUB20 and AtPUB21). NtAcre74 (NtCMPG1) has been found to be required for R protein-mediated HR and is required for PiInf1 triggered CD (González-Lamothe *et al.*, 2006; Birch *et al.*, 2009). It is not known

Table 1.2 Summary of the Plant E3 Ligases that have a role in plant disease and defence (Durrant *et al.*, 2000; Yin *et al.*, 2000; Kim & Delaney, 2002; Turner *et al.*, 2002; Devoto *et al.*, 2003; Zeng *et al.*, 2004; González-Lamothe et al., 2006; Yang *et al.*, 2006; Dreher & Callis, 2007; Delauré *et al.*, 2008; Trujillo *et al.*, 2008; van der Burg *et al.*, 2008; Bopopi *et al.*, 2010).

Name of Protein(s) including homologues	Protein's involvement in the UPS	Protein's involvement in plant disease and defence	References
AtRar1 & ScSgt1 (Required for Mla12 resistance; suppressor of the G2 allele of Skp1)	Although not directly involved the UPS do interact and regulate SCF E3 ligases.	ScSgt1 regulates and interacts with E3 ligases. ScSgt1 interacts with AtRar1 which is required for gene mediated resistance.	Devoto *et al.*, 2003.
AtEbf1 and AtEbf2 (Ein3 binding F-box; ethylene insensitive 3)	E3 Ligase (SCF)	AtEin3 family of transcription factors regulates defence related genes as part of ethylene and jasmonic acid (JA) pathways. AtEbf1 and AtEbf2 regulate StEin3.	Delauré *et al.*, 2008. Dreher & Callis, 2007
AtCoi1 (Coronatine insensitive 1)	E3 Ligase (SCF F-box)	AtCoi1 is an E3 ligase and is involved in JA signalling and therefore defence responses.	Dreher & Callis, 2007. Turner *et al.*, 2002.
AtSon1 (Suppressor of nim1-1)	E3 Ligase (F-box)	Is a negative defence regulator in SAR-independent resistance.	Kim & Delaney, 2002.
Acif1 (Avr9/Cf9-induced F-box 1; ACRE gene)	E3 Ligase (SCF F-box)	Positive regulator of HR and gene mediated resistance.	van der Berg *et al.*, 2008.
NbACRE132/ AtAlt2 (Arv9/Cf-9 rapidly elicited; *Arabidopsis toxico para levadura*)	E3 Ligase (RING)	Targets defence response related compounds for protolysis. Induced during basel resistance and therefore possibly involved in fungal response pathways.	Durrant *et al.*, 2000. Delauré *et al.*, 2008.
PtaRHE1 (populus tremulaxP. Alba RING H3 E3 ligase). Homologue of AtALT2.	E3 Ligase (RING-H2)	Involved in defence responses as part of Ub mediated regulation.	Bopopi *et al.*, 2010.
AtPub22,23,& 24 (Plant U-box). Closely related to Tobacco CMPG1)	E3 Ligase (U-box)	Negative regulator of PTI and basel resistance.	Trujillo *et al.*, 2008
AtPub17/ NbACRE276	E3 Ligase (U-box)	Positive regulator of ETI and is required for disease resistance.	Yang *et al.*, 2006.
StCMPG1/ NbACRE74	E3 Ligase (U-box)	Positive regulator of ETI and involved in Cf-9 HR.	González-Lamonthe *et al.*, 2006.
Spl1 pv. Oryzae (spotted leaf)	E3 Ligase (U-box)	Negative regulator of basel defence. Spl1 mutants exhibit enhanced defence responces against Rice Blast (*Magnaporthe grisea*)	Yin, 2000. Zeng, 2004.

which E2(s) NtCMPG1 interacts within the plant and whether the E2 involved changes during infection so as to re-determine the labelling of the target protein.

There are a vast number of E3s in the plant and most are uncharacterised. It is therefore likely that there are many additional E3s involved in plant disease and defence and these will become apparent with future research.

1.5.2 The UPS and Altered Disease Resistance Pathways

It has been realised that plants have a complex network of defence pathways and some of the components involved have been identified. Proteins that have been found so far include Non Race-Specific Disease Resistance 1 (AtNdr1), Enhanced Disease Susceptibility 1 (AtEds1) and Required For MLA Resistance 1 (AtRar1) and have been shown to be part of the pathways where resistance is controlled by many different R proteins.

AtRar1 is needed for *R* gene-mediated resistance and has linked E3 Ub ligases with disease resistance in plants. AtRar1 is thought to be in all eukaryotes with the exception of yeast, which has a AtRar1 homologue called Suppressor of the G2 Allele of skp1-4 (ScSgt1). ScSgt1 regulates SCF complex activity via ScSkp1 and has been linked to *R* gene resistance. This was shown using AtSgt1b which is required for SCFTIR1 auxin resistance responses in *A. thaliana*. AtRar1 encodes a protein with two binding domains containing a cysteine and histidine (CHORD) zinc regions and it's homology to ScSgt1 and the ability of ScSgt1 to interact as a AtRar1 protein lead to the conclusion that ubiquitination via SCF complexes are part of *R* gene resistance (Devoto *et al.*, 2003).

Auxin is a component of the hormone responses involved in the plant defence. Auxin is present in the cell as indole-3-acetic acid (IAA) as well as in the form of auxin. Auxin/IAA and three TIR1 F-box proteins, Auxin Signalling F-Box Protein 1 (AtAfb1), Auxin Signalling F-Box Protein 2 (AtAfb2) and Auxin Signalling F-Box Protein 3 (AtAfb3), have been shown to interact. It is thought that AtAfb1, AtAfb2 and AtAfb3 are substrates of particular SCFs and this implies that auxin/IAA is associated with ubiquitination. Other supportive evidence comes from work done with IAA fusion proteins (Dreher and Callis, 2007).

PsAvrPtoB is a T3SS effector protein from *Psudomonas syringae* and has structural similarities in its C-terminus to those found in E3 Ligases. PsAvrPtoB triggers Pto-dependent HR and suppresses the CD triggered by some elicitors. PsAvrPtoB activity in the plant results in UPS-dependent degradation of the host protein Fen kinase. When Fen kinase is present, a plant innate immune response

is activated (Janjusevic *et al.*, 2006; Rosebrock *et al.*, 2007; Birch *et al.*, 2009).

Although much progress has been made in understanding plant disease and resistance there are still many areas left to investigate. Examples of invading pathogen proteins manipulating the plant to evade detection are becoming more common. The role of ubiquitination in this is becoming apparent and is being investigated further.

1.6 Project

1.6.1 Project Background

The published work which provides a background to this project compromises of 3 key papers. These are described in chronological order. Firstly work performed by Kirsch *et al.,* (2001) who studied ELI17 gene expression (later named CMPG1 due to its four conserved aa; Cys, Met, Pro and Gly) in parsley (*P. crispum*). Kirsch *et al.,* (2001) found that ELI17 mRNA level were detected as early as 5 Mins post-elicitor induction. This implied a role for PcCMPG1 as a regulatory protein during host attack and this was supported by its mRNA accumulation at the point of infection. At this time little was known about the CMPG1 protein, however a regulatory role was hypothesised due to the protein's RING finger-like domain and two potential nuclear localisation signals as well as its fast induction during elicitor induction. (Kirsch *et al.,* 2001).

Separately, in 2005, Armstrong *et al.,* (2005) published a paper identifying PiAvr3a (*P. infestans*) and found that the PiAvr3a protein is recognised in the host cytoplasm and then triggers R3a dependent CD. Two alleles were found; S19C, E80K and M103I, where the SEM allele showed virulence and CKI was avirulent. Originally known as Pex147, PiAvr3a was found to be up-regulated before and during potato infection. To confirm PiAvr3a had been identified it was co-expressed with R3a in *N. benthamiana* and no CD occurred. (Armstrong *et al.,* 2005).

At this time CMPG1 and PiAvr3a had both been identified but their function had not been fully investigated.

The work on CMPG1 was updated in 2006 by González-lamonthe *et al.,* (2006). This publication provided evidence that PcCMPG1 was similar to *N. tabacum* ACRE74 (Avr9/Cf-9 rapidly elicited) and *A. thaliana* PUB20/PUB21 (Plant U-box). This homology is shown in **Figure 1.8**. These homologus proteins encoded a U-box protein and therefore suggested a similar role in early defence signalling and protein modification by ubiquitination. CMPG1's aa sequence was found to contain an ARM repeat motif. Experimentally, it was found that CMPG1 has a role in the Cf-9/Avr9-dependent responses in *L. esculentum* and *N. tabacum,* more specifically, the HR response. NtCMPG1 was shown to have *in vitro* ubiquitination activity, acting as an E3 ligase.

The U-box was shown to be vital to the Cf-9/Avr9 induced HR with the use of U-box mutations. NtCMPG1 was shown to be involved in Pto/AvrPto and INF1-mediated CD. González-lamonthe observed that *N. benthamiana* plants silenced

for NbCMPG1 had reduced HR after Avr9/Cf-9 elicitation and the over-expression of NtCMPG1 produced a stronger HR in Cf-9 *N. tabacum* after Avr9 infiltration. Therefore CMPG1 was considered an E3 ligase important in a number of HR responses. (González-Lamothe *et al.*, 2006).

Finally, also in 2006, Bos *et al.*, (2006) published work concerning PiAvr3a. They found PiAvr3a^{KI} was specifically recognised by R3a alone and not its 3 paralogs and both PiAvr3a^{EM} and PiAvr3a^{KI} were stable *in planta*. More notably, PiAvr3a^{KI} suppressed the HR induced by INF1 elicitin, indicating common ground between CMPG1 and PiAvr3a. (Bos *et al.*, 2006).

This summarises the previous published data available at the start of this project. Other data had been collected but not published at the time this project began. For example, the Y2H performed by Dr M Armstrong (SCRI, Dundee, Scotland) which showed the direct interaction of PiAvr3a and StCMPG1 in vivo. (Bos *et al.*, 2010; described in Chapter 3).

1.6.2 Aims
The aims of this project were to determine the nature of this interaction functionally and biochemically:
• Does the interaction found in the Y2H take place in the plant? (Chapter 3)
• What are the biological implications on PiAvr3a and CMPG1 interaction? (Chapter 4)
• What is the biochemical nature of the interaction? (Chapter 5)

This project therefore required *in vivo* work using plants, *in vitro* assays and a combination of plant based techniques. Due to the homolgous nature of CMPG1 in plants it was possible to use model plant system techniques previously developed. The work done to better understand this interaction is detailed in the following chapters.

Figure 1.8 Alignments of the Homologues of CMPG1.
Alignments of the various CMPG1s from Tomato, Potato and Tobacco. Highlighted
in blue is the U-box and in orange is the ARM-like region (Bos et al., 2010).

```
                          10         20         30         40         50         60
dN-StubCMPG1-a ---------- ---------- ---------- PSQFTCPISL DLMKDPVTLS TGITYDRENI
StubCMPG1-b    MIATWRKKRT EKRVTKRGFM K-KTIKELVI PSQFTCPISL DLMKDPVTLS TGITYDRENI
NbCMPG1-a      MISTWRKRRT ERRVAKRGLM EDITSMELVI PRNFTCPISL DLMKDPVTLS TGITYDRENI
NbCMPG1-b      MISTWRKRRT ERRVAKRGLM EDITSMELVI PRNFTCPISL DLMKDPVTLS TGITYDRENI
SlCMPG1        MIATWRKKRT EKRVTKRGFM K-KTNMELVI PSQFTCPISL DLMKDPVTLS TGITYDRENI
```

U-box

```
                          70         80         90        100        110        120
dN-StubCMPG1-a EKWINEGGNQ TCPITNQDLK SYGSGISTID PTLIPNHNIR KMIQQWCVEN KEHGIDRIPT
StubCMPG1-b    EKWINEGGNQ TCPITNQDLK SYGSGISTID PVLIPNHNIR KMIQQWCVEN KEHGIDRIPT
NbCMPG1-a      EKWIEAG-NQ TCPITNQTLR ---------N GEPIPNHSIR KMIQQWCVAN KDHGIERIPT
NbCMPG1-b      EKWIEAG-NQ TCPITNQTLR ---------N GEPIPNHSIR KMIQQWCVEN KDHGIERIQT
SlCMPG1        EKWINEGGNQ TCPITNQELK SYGNGI--VD PVLIPNHNIR KMIQQWCVEN KEHGIDRIPT
```

```
                          130        140        150        160        170        180
dN-StubCMPG1-a PRIPVSSSDV SELLAKITNS SKLEMQDSRL CEELVTRVKN LASESDRNKC CFITNGIGKV
StubCMPG1-b    PRIPISSSDV SELLAKITNS SKLEMQDSRL CEELVTRVKN LASESDRNKC CFVTNGIGKV
NbCMPG1-a      PRIPVTSSEV VELLAKISKG ----MHDSEL CKELVSKVKK LVNESERNKR SFVTNGIAHV
NbCMPG1-b      PRIPVTSSEV VELLAKISKA ----MHDSEL CRELVSKVKK LVNESERNKR CFVTNGTAHV
SlCMPG1        PRIPISSSDV SELLAKITNS SKLEMEKSSS CEELVTSVKN LASESDRNKC CFVTNGIGKV
```

Armadillo-like

```
                          190        200        210        220        230        240
dN-StubCMPG1-a LSSAFLELSK GRNAKNASTE EVILSTLTLF LPLDVKSKTI LGSISSLRCI AWFLKNGSLS
StubCMPG1-b    LSSAFLELSK GKNAKNASTE EVILSTLTLF LPLDVKSKTI LGSISSLRCI AWFLKNGSLS
NbCMPG1-a      LSAAFVAFSK EINMKNASTG EVILSTLTTI LPLDGESKSI LGSISSLRCM VWFLNNGSLS
NbCMPG1-b      LSAAFVAFSE EINMKNASTG ELILSTLTTI LPLDGESKSN LGSISSLGCM VWFLNNGSLS
SlCMPG1        LSSAFLELSK GKNAKNASTE EVILSTLTLF LPLDVKSKTI LGSISSLRSI AWFLKNGSLS
```

```
                          250        260        270        280        290        300
dN-StubCMPG1-a SRRNAVLVLR EIMKLEEKEK VEILLNIEGA LEGLVKLVKE PICPNTTKAS LLTIYHMVIN
StubCMPG1-b    SRRNAVLVLR DIMKMEEQEK VEILLNIEGA LEGLVKLVKE PICPNTTKAS LLTIYHMVIN
NbCMPG1-a      GRRNAVFLLK DILKMEEHDK VEILLGMGGA LEGLVKLVQE PICPTTTKAS LLAIYHMVNP
NbCMPG1-b      SRRNAVFLLK DILKMEEQDK IEILLGMDGA LEGLVKLVKE PICPTTTKAS LLAIYHMVNP
SlCMPG1        SRRNAVVVLR EIMKLEEQEK VEILLNIEGA LEGLVKLVKE PICPNTTKAS LLTIYYMVNN
```

```
                          310        320        330        340        350        360
dN-StubCMPG1-a SSS-----QS LRSRFVDVGL VELLIEILVD CDKSICEKAL GVLDGILSYE EGVKRAYNYA
StubCMPG1-b    SSS-----QS SRSRFVDVGL VELLIELLVD CDKSICEKAL GVLDGILSYE EGVKRAYNYA
NbCMPG1-a      SNSSSFANKK AQSRFADMGL VELLVEMLVD SEKSICEKAL GVLDGICSSV EGRKGVYNYA
NbCMPG1-b      SHSSSFANKK AQSRFADVGL VELLVEMLVD CEKSICEKAL GVLDGICRSI EGRKRAYSYA
SlCMPG1        SSS-----QS SRSRFVDVGL VEMLIEILVN CDKSICEKAL GVLDGILRYE EGVKRASSYA
```

```
                          370        380        390        400        410        420
dN-StubCMPG1-a LSVPVLVKKL LRVSDLATEF SVSILWKI-C KNENNGDCG- VLVEALQVGA FQKLLLMLQV
StubCMPG1-b    LSVPVLVKKL LRVSDLATEF SVSILWKI-C KNENNGDCG- VLVEALQVGA FQKLLLMLQV
NbCMPG1-a      LTVPVLVKKL LRVSDLATEF SVSIIWKI-G KNENRENGGD VLVEALKLGA FQKLLLLLQV
NbCMPG1-b      LTVPVLVKKL LRVSDLATEF SVSIIWKI-G KNENRENGGD VLVEALKLGA FQKLLLLLQV
SlCMPG1        LSVPVLVKKL LRVSDLATEF SVSILWKILC KNENNGDCG- ILVEALQVGA FQKLLVILQV
```

```
                          430        440        450
dN-StubCMPG1-a GCSEITKEKG SELLKLLNVH RDRAECVDSL DFKSLKRTF
StubCMPG1-b    GCSEMTKEKA SELLKLLNVH RDRAECVDSL DFKSLKRTF
NbCMPG1-a      GCSETTKEKA SELLKLMNVH RDRQECVDSL DFKSLKRPF
NbCMPG1-b      GCSDTTKEKA SELLKLLNVH RDRAECVDSL DFKSLKRPF
SlCMPG1        GCSETTKEKA SELLKLLNVH RDRAECVDSL DFKSLKRTF
```

Chapter 2. Materials and Methods

2.1 Materials

2.1.1 Chemicals

The chemicals used in this study were purchased from Sigma-Aldrich (Poole, U.K.), Fisher Scientific U.K. (Southampton, U.K.) or VWR International Ltd (Poole, U.K.), unless otherwise stated:

Product	Company	Catalogue Number
Expand HiFidelity Polymerase	Roche	04738250001
1 Kb DNA Molecular Weight Marker	Promega	G571A
37.5:1 Acrylamide Bis Solution	BioRad Laboratories	161-0158
AMV Reverse Transcriptase	Promega	M510A
Brilliant SYBR Green QPCR Master Mix	Stratagene Ltd	600548
BugBuster Protein Extraction Reagent	Novagen	70584
Chemiluminescent HRP Substrate	Millipore Ltd	WBKLS0500
Complete® Protease Inhibitor Cocktail Tablets	Roche	11836170001
DNA-free DNAse	Ambion	1906
dNTPs	Promega	U1330
His-Bind Affinity Purification Resin	Novagen	69670
Immun-Blot PVDF Membrane	BioRad Laboratories	162-0177
IPTG (Isopropyl-β-D-thiogalactopyranoside)	Calbiochem	na
LR Clonase	Invitrogen Ltd	11791100
Ni-NTA resin	Invitrogen Ltd	R901-01
pENTR D-TOPO Kit	Invitrogen Ltd	K240020
pfu Turbo DNA Polymerase	Stratagene Ltd	09600280
pGEM-T/pGEM-T Easy Systems	Promega	na
Phusion DNA polymerase	Finnzymes	F530S
Power SYBR Green PCR Master Mix	Applied Biosystems	436 7659
Pre-Stain Protein Molecular weight Marker	New England Biolabs	P7708S
QIAprep Spin Miniprep kit	Qiagen Ltd	27104
QIAquick Gel Extraction Kit	Qiagen Ltd	28704
RNAseOut Inhibitor	Invitrogen Ltd	10777019
Semi-Skimmed Dried Milk Powder	Marvel	na
SnakeSkin Pleated Dialysis Tubing	Novagen	68035
SuperscriptII Rnase-1-1 Reverse Transcriptase	Invitrogen Ltd	18064-022
SYBR Safe DNA Gel Stain	Invitrogen Ltd	S33102
T4 DNA Ligase	Promega	M1801

Product	Company	Catalogue Number
Thermopol Taq Polymerase	New England Biolabs	M0267S
TRIzol RNA Extraction	Invitrogen Ltd	15596026
Ubiquitin Assay Kit	Enzo	UW9920
X-Ray Film	Kodak	na

Table 2.1 Chemicals and Reagents Used in the Study

2.1.2 Enzymes

Restriction endonucleases were supplied by Roche and New England Biolabs Ltd. (Hichin, UK).

2.1.3 Bacterial Strains

Unless otherwise stated:

Species	Strain	Supplier
Agrobacterium tumefaciens	GV3101, LBA4404, AGL1 pGRAB	Invitrogen Ltd, SCRI and (Whisson *et al.*, 2007)
Erwinia amylovora	1430	(Gilroy *et al.*, 2007)
Escherichia coli	BL21 (DE3), DH5α	Produced in house
Psudomonas syringae pv. Tomato	DC3000	Norwich, U.K.

Table 2.2 Bacterial Strains Used in the Study

2.1.4 Antibiotics

Antibiotic	Solvent	Stock (mg/mL)	Working (µg/mL)	Manufacture
Ampicillin	H_2O	100	100	Melford
Carbenicillin	H_2O	100	100	Melford
Chloranphenicol	Ethanol	50	50	Duchefa Biochimie
Gentamyocin	H_2O	25	25	Duchefa Biochimie
Hygromycin B	PBS	50	50	Roche
Kanamycin	H_2O	100	100	Melford
Riphampicin	Methanol	10	10	Sigma Aldrich
Spectinomycin	H_2O	50	50	Sigma Aldrich

Table 2.3 Antibiotics Used in this Study

2.1.5 Antibodies

All primary and secondary antibodies used in this study are listed in **Table 2.4.** All dilutions were made in TBS-T (15 mM Tris-HCl pH 7.6, 150 mM NaCl, 0.1% v/v Tween 20) and 5% semi skimmed milk powder.

Primary antibody	Animal Source	Dilution factor	Manufacturer
Anti-FLAG	Mouse Monoclonal	1/1000	Sigma
Anti-GFP	Rabbit Polyclonal	1/1000	Abcam
Anti-HA	Rat Monoclonal	1/2000	Roche
Anti-HIS	Mouse Monoclonal	1/2000	Novagen
Anti-c-MYC	Mouse Monoclonal	1/1000	Abcam
Anti-GST	Mouse Monoclonal	1/1000	Calbiochem

Table 2.4 Primary Antibodies used in this Study

2.2 General Laboratory Procedures

2.2.1 Autoclaving

All sterilisation of equipment and solutions that required heat were carried out in a bench-top (Prestige Medical, Model 220140) or free-standing (Laboratory Thermal Equipment Autoclave 225E) autoclaves.

2.2.2 pH Meter

The pH measurement of solutions was performed using Metler Toledo MP220 pH meter and glass electrode as per the manufacturer's instructions.

2.3 Plant Materials and Growth Conditions

2.3.1 *Nicotiana tabacum* and *Nicotiana benthamiana* Seed Stocks

Transgenic *N. tabacum* seeds carrying the *S. lycopersicum* resistance gene *Cf-9* were kindly provided by Prof. J D Jones (The Sainsbury Laboratory, Norwich, U.K; Hammond-Kosack *et al.*, 1998). Transgenic *N. benthamiana* expressing *R3a* were kindly provided by Dr E van der Vossen (Plant Research International, Wageningen)

2.3.2 *N. tabacum* and *N. benthamiana* on Soil

N. tabacum and *N. benthamiana* seeds were grown as stated in: Ewan, Richard (2008). "*An investigation into the role of deubiquitinating enzymes in plant disease resistance*". PhD thesis, The University of Glasgow. Chapter 2.3.7, Pg.39.

2.4 DNA Methods

2.4.1 Production of Competent DH5α *E. coli* Cells for Transformation

The production of competent DH5α *E. coli* cells for transformation was performed as stated in: Ewan, Richard (2008). "*An investigation into the role of deubiquitinating enzymes in plant disease resistance*". PhD thesis, The University of Glasgow. Chapter 2.4.1, Pg.40.

2.4.2 Heat Shock Transformation of Escherichia coli Cells

Plasmid DNA was transformed into competent *E. coli* cells by defrosting an eppendorf of 50 µL of cells on ice and adding 5 µL of plasmid DNA. After resting on ice for 30 minutes the cells were heat shocked at 42 °C for 30-45 seconds using a water bath (Grant JB2) and placed on ice for 2 minutes. Two hundred micro litres of Lysogeny broth (LB; 1% w/v tryptone, 0.5% w/v yeast extract and 1% w/v NaCl, pH 7.5) media were added and the solution placed on a 37 °C shaking platform (200 rpm) for 90 minutes. The cells were then plated onto a LB media 1% w/v agar plates in a sterile flow cabinet with appropriate antibiotics using a sterile hoop. After drying, the plates were then placed upside down in a 37 °C incubator for ~18 hours.

2.4.3 Electroporation of *E. coli* Cells

The cells were thawed on ice and 5 µL (~200 ng) of plasmid DNA was added. The cells were then transferred into a pre-chilled electroporation cuvette (BioRad) and pulsed with the MicroPulser™ electroporator (BioRad Laboratories). Three hundred micro litres of LB media were added to the cells, which was transferred to an eppendorf tube and incubated in a 28 °C shaking platform (200 rpm) for 90 minutes. Cells were then plated onto LB media 1% agar plates containing the appropriate antibiotics for selection and incubated at 28 °C for 2-3 days until colonies formed.

2.4.4 Isolation of Plasmid DNA

A single colony from a plate or swab from a glycerol stock (300 µL 60% v/v glycerol, 350 µL overnight culture; -80 °C) was taken and used to inoculate 10 mL LB media and placed on a 37 °C shaking-platform (200 rpm) for 18 hours. This culture was then centrifuged at 3000 rpm for 10 minutes. The pellet was then used in the QIAprep® plasmid miniprep kit (Qiagen) as per the manufacturer's instructions. The plasmid DNA was eluted in sterile distilled water and stored at -20 °C.

2.4.5 DNA Quantification

Plasmid DNA concentration was determined using a Nanodrop (NanoDrop Technologies, Inc.) as per the manufacturer's instructions.

2.4.6 DNA Sequencing

DNA sequencing was performed by Dundee Sequencing Service (SCRI, Dundee, Scotland) in accordance with their instructions using a 3730 DNA Analyzer. Sequencing was also carried out by the Sequencing Facility at The University of Glasgow (Glasgow, Scotland) in accordance with their instructions. Sequences were analysed using 4peaks computer software (Mekentosj).

2.4.7 Electrophoresis of DNA and Visualisation

The electrophoresis of DNA and visualisation was performed as stated in:

Ewan, Richard (2008). "*An investigation into the role of deubiquitinating enzymes in plant disease resistance*". PhD thesis, The University of Glasgow. Chapter 2.4.4, Pg.41.

2.4.8 Agarose Gel Extraction of DNA and Purification

The agarose gel extraction and purification of DNA was performed as stated in:

Ewan, Richard (2008). "*An investigation into the role of deubiquitinating enzymes in plant disease resistance*". PhD thesis, The University of Glasgow. Chapter 2.4.5, Pg.41.

2.4.9 DNA Ligation

Extracted DNA was used in a ligation reaction either overnight at 4 ℃ or for 1-6 hours at room temperature. A reaction volume of 10 μL was used consisting of 1 unit of T4 DNA ligase (Promega), 1x ligation buffer (Promega) DNA insert and plasmid. The ratio of DNA:Plasmid was 3:1. Five microlitres of the completed ligation reaction was used to transform competent *E. coli* cells.

2.4.10 Restriction Digest of Plasmid DNA

Plasmid DNA was restriction enzyme digested using one or two enzymes in a total volume of 20 μL or 50 μL (50 μL reaction was used when the digest was to be agarose gel purified; 20 μL for viewing). A reaction consisted of 2 μL (for 20 μL reaction) or 5 μL (for 50 μL reaction) of buffer appropriate to the specific enzymes, 7 μL (for 20 μL reaction) or 25 μL (for 50 μL reaction) plasmid DNA, 0.5-1 μL enzyme(s) and distilled water to the total volume. This was placed in a 37 ℃ incubator for 1-4 hours. Six times loading dye was added to the reaction and viewed using agarose gel electrophoresis and later a Gel Doc (BioRad).

2.4.11 Gateway LR Cloning Reaction

Gateway LR cloning reaction was performed as stated in:

Ewan, Richard (2008). "*An investigation into the role of deubiquitinating enzymes in plant disease resistance*". PhD thesis, The University of Glasgow. Chapter 2.4.11,

Pg.43.

2.4.12 cDNA Synthesis

CDNA synthesis was performed using Superscript® II RT (Invitrogen Ltd) as per the manufacturer's instructions. One micro litre of oligoDT and/or random hexamer primers (10 mM stock solution) was added to 5 μL total RNA and made to a final volume of 10 μL with sterile distilled water. The mixture was heated to 70 °C for 10 minutes, snap-cooled on ice and 5 μL First-Strand buffer, 2 μL 0.1 M DTT (both provided by the kit), 2 μL dNTPs (10 mM each) and 1 μL RNaseOUT (40 units/μL, Invitrogen Ltd) was added. The solution was incubated at 42 °C for 2 minutes and 1 μL SuperscriptTM II RT was added and mixed by pipette. The solution was incubated at 42 °C for 50 minutes then inactivated at 72 °C for 15 minutes. Twenty micro litres of sterile distilled water were added and the cDNA samples stored at -20 °C.

2.5 RNA Methods

2.5.1 Isolation of RNA from Plant Tissue

This method was obtained from Dr H McLellan (Scottish Crop Research Institute; SCRI, Dundee, Scotland). One hundred milligrams of leaf were ground under liquid nitrogen until a pale powder and placed into a cold eppendorf. One millilitre of TRI-reagent was immediately added and the mixture vortexed. The solution was centrifuged at 12,000 g at 4 °C for 10 minutes. The pellet was discarded and 20 μL chloroform was added to the supernatant and vortexed for 15 seconds. This solution was incubated at room temperature for 3 minutes and centrifuged at 10,000 g at 4 °C for 15 minutes. The aqueous phase was transferred into a new eppendorf (~600 μL) and 300 μL isopropanol and 300 μL NaCl/Nacitrate were added and mixed by inversion. This was incubated at room temperature for 10 minutes and centrifuged at 10,000 g at 4 °C for 10 minutes. The supernatant was discarded and the pellet washed with 1 mL 75% ethanol by vortex. This was centrifuged at 10,000 g at 4 °C for 10 minutes and the supernatant discarded. The pellet was briefly dried for 10-15 minutes at room temperature and re-suspended in 50 μL sterile distilled water. The RNA was incubated at 60 °C for 30 minutes. Samples were stored at -80 °C and analysed within one month.

2.5.2 RNA Quantification

RNA quantification was performed as stated in:

Ewan, Richard (2008). "*An investigation into the role of deubiquitinating enzymes in plant disease resistance*". PhD thesis, The University of Glasgow. Chapter 2.4.15, Pg.44.

2.5.3 DNAse Treatment of RNA

To prevent genomic DNA contamination extracted RNA was treated with DNAFree DNAse (Ambion) as per the manufacturer's instructions. The recovered RNA fraction was incubated with 2 units of DNAse I in 1x DNase buffer at 37 °C for 30 minutes. DNAse I was inactivated by the addition of 0.1 volumes DNAse inactivation reagent (mixed for 2 minutes at room temperature prior to use). RNA samples were centrifuged at 10,000 rpm for 1 minute and the supernatant was transferred into a fresh eppendorf.

2.6 Polymerase Chain Reaction (PCR) Methods

2.6.1 Oligonucleotide Primer Design

The primers in this study were designed by the author, and were available in the Sadanandom group (The University of Glasgow, Scotland) oligio stocks or the Birch Group (SCRI, Dundee, Scotland) oligio stocks prior to starting the project. Oligonucleotide primers are 20-25 base paris (bp) in length with a melting temperature of ~60 °C and a GC content of ≥40%. Primers were synthesised by MWG and supplied as 100 μM stocks, which were then diluted to a final concentration of 10 μM in sterile distilled water. Primers used in this study are listed in the Appendix (A1).

2.6.2 Amplification of DNA by PCR

PCR was performed using a MJ Research DNA Engine PTC-200 Peltier Thermal Cycler (Genetic Research Instrumentation, Essex, UK). PCR reactions were usually completed in a final volume of 20 μL. Template DNA (0.2-0.01 ng) was added to 1x Thermopol buffer (NEB) with 0.5 μM of each primer, 250 μM dNTPs and 1 unit of Taq DNA polymerase (NEB). PCR Annealing temperature (TA) was calculated using the following formula: TA = (2 x (A + T) + 4 x (G + C)) – 5. The denaturation step was 2 minutes at 94 °C and the amplification was performed using 28 cycles. A usual cycle consisted of denaturation at 94 °C for 30 seconds, annealing at 55 °C for 30 seconds and extension at 72 °C for 1 minute per Kb of DNA in the target amplicon. This template program was adjusted for the specific requirements of the DNA templates or primers.

2.6.3 Quikchange™ Mutagenesis

Site-directed mutagenesis was performed using the QuikChange™ Site-Directed Mutagenesis Kit (Stratagene, U.S.A.) as per the manufacturer's instructions.

2.6.4 Real Time Quantitative Reverse Transcription PCR (qRTPCR)

qRTPCR was performed using a protocol obtained from Dr E Gilroy (SCRI, Dundee, Scotland). The qRTPCR was carried out on cDNA made from RNA that was extracted from *N. benthamiana*. The primers used in this work can be found in the Appendices (A1) and were designed using http://frodo.wi.mit.edu (Primer3) and the *N. tabacum* ACRE74 mRNA sequence (Rozen, 2000; gi|30013682|gb|AY220485.1|).

Firstly, the primer concentration was optimised using a pool of the cDNA samples with varying primer concentration and ratio. The cDNA concentration was optimised using varying cDNA concentrations with the optimised primers and finally the analytical qRTPCR was performed. The protocol for a standard qRTPCR reaction was as follows: 12.5 μL SYBR Green (Applied Biosystems), 2.0 μL forward primer, 2.0 μL reverse primer, 2.0 μL template and 6.5 μL HPLC water. Total volume was 25 μL. The reactions were carried out on a white 96 well plate in replicates of 3 including "no template" controls. Once all the reactions were added to the plate, the lid was sealed and the plate spun at room temperature at 2000 g for 1 minute. The plate was vortexed and the spin repeated. The plate was inserted into the Chromo4 qRTPCR machine (Bio-Rad). The PCR programme was: 95 °C for 5 seconds, 95 °C for 15 minutes, cycle: 95 °C for 15 seconds, 59 °C for 30 seconds, 72 °C for 30 seconds. The cycle was repeated 40 times. The results were then analysed using Opticon Montior 3 (Bio-Rad) and Microsoft Excel computer software. A melting curve analysis was performed at the end of every run to check that only one PCR product was obtained from primers. Temperature increases by 1 °C from 58 °C to 95 °C scanned each temperature rise as well as the temperature when SYBR green fluorescence is lost was recorded.

2.7 Time Course for Analysing Gene Expression During Infection

N. benthamiana leaves from 20 plants were infiltrated with *E. amylovora* (serially diluted to $2x10^6$ CFU/mL with 10mM $MgCl_2$ & 10mM MES buffer solution) into the abaxial leaf surface with 1 mL syrinage (Gilroy et al., 2007). Five leaves were collected each day through a time course from 0-24 Hrs. Sporangia cDNA from 88069 was prepared as described in Bos *et al*. (2010). Total RNA was extracted from the pooled leaf sample using RNeasy Minikit (Qiagen). *CMPG1* gene expression was normalised with endogenous control gene. NbCMPG1 cT values were normalised with 25S expression and made relative to GFP (for virus induced gene silencing; VIGS) control or day 0 (for expression during infection). As stated in Bos *et al*. (2010).

2.8 *In planta* Protein Expression

2.8.1 Production of *A. tumefaciens* Cells for Electroporation

The production of *A. tumefaciens* cells for electroporation was performed as stated in: Ewan, Richard (2008). "*An investigation into the role of deubiquitinating enzymes in plant disease resistance*". PhD thesis, The University of Glasgow. Chapter 2.6.1, Pg.40.

2.8.2 Electroporation of *A. tumefaciens*

The electroporation of *A. tumefaciens* was performed as stated in:

Ewan, Richard (2008). "*An investigation into the role of deubiquitinating enzymes in plant disease resistance*". PhD thesis, The University of Glasgow. Chapter 2.6.2, Pg.40.

2.8.3 *A. tumefaciens*-mediated Transient Expression of Gene Constructs in *N. tabacum* and *N. benthamiana*

N. benthamiana plants were grown in a greenhouse at 22 °C (day temperature) and 18 °C (night temperature) with a minimum of 16 hours light. *A. tumefaciens* transient expression was performed as described in Latijnhouwers *et al.*, (2005). In brief, overnight *A. tumefaciens* cultures were centrifuged, the pellets resuspended in infiltration buffer (10 mM $MgCl_2$, 10 mM MES pH 5.6) and the concentrations measured at OD_{600}. The bacterial suspension was diluted with the same buffer to adjust the inoculum concentration to final OD_{600} values of between 0.01 and 0.1 depending on the experiment. To the final solution 15 µM [imaging] or 200µM; [expression for western blot] acetosyringone was added and incubated at room temperature for 3-4 Hrs prior to plant inoculation. Infiltrations were performed with a blunt syringe as described in Batoko *et al.* (2000). For experiments requiring co-infiltration of more than one construct, bacterial strains containing the constructs were mixed prior to the leaf infiltration, with the concentration of each strain adjusted to the required final OD_{600}. Infiltrated plants were incubated under normal growth conditions as above for a further 3 days unless otherwise stated.

2.9 Virus Induced Gene Silencing (VIGS)

2.9.1 Preparation of Plasmid Constructs for VIGS

VIGS was performed using vectors originally described in Peart *et al.* (2002), using binary Tobacco Rattle Virus vectors (TRV) in *N. benthamiana*. For *NbCMPG1* silencing, a 250 bp fragment from within the equivalent region used for the *NtCMPG1* RNAi hairpin (González-Lamothe *et al.*, 2006) was cloned in antisense.

A TRV-construct, expressing GFP, was used as a control as described in (Gilroy *et al.*, 2007).

2.9.2 Inoculation of *N. benthamiana* with VIGS Constructs

All *A. tumefaciens* (LBA4404) containing the VIGS constructs for infiltration were maintained on fresh 1% w/v agar LB media plates with antibiotic selection. Ten millilitres of LB media, containing a swab of the agar construct, were grown at 28 °C shaking, (200 rpm; Unitron HT Infors) overnight. Cells were pelleted by centrifugation at 3000 g for 10 minutes (Sorvall Legend RT). Infiltration constituents were mixed: TRV:RNA1 OD_{600} 0.5 and TRV:RNA2 containing *CMPG1* antisense fragments at OD_{600} 0.5 in a 1:1 ratio. OD_{600} was adjusted with infiltration buffer (10 mM $MgCl_2$ and 10 mM MES) to a final OD_{600} of 0.5 (Eppendorf Bio-Photometer on OD_{600} setting) with infiltration buffer. Acetosyringone was added to a final concentration of 200 μM and incubated at room temperature for 3-4 hours prior to plant inoculation. *N. benthamiana* plants were grown until the 4-leaf stage prior to inoculation and the 2 largest leaves were infiltrated using a needle and a blunt 1 mL syringe on the abaxial surface of the leaf. Following culture inoculation *N. benthamiana* plants were grown for a further 3-4 weeks before being analysed by qRT-PCR or used in pathogen experiments (Gilroy *et al.*, 2007).

2.10   Plant Pathology Treatments

2.10.1 Sporation of *P. infestans* in *N. benthamiana*

The stable transformation of *P. infestans* isolate 88069 (homozygous *PiAvr3a^{EM}*) was made using a modified polyethylene glycol (PEG) – $CaCl_2$ – Lipofectin protocol (Judelson, 1991; http://138.23.152.128/protocols/protocols.html). Modifications to this protocol were as described in Grouffaud *et al.* (2008). This transformant was kindly made available to use from Dr S Whisson (SCRI, Dundee, Scotland).

2.10.2 Inoculation of *E. amylovora* in *N. benthamiana*

Inoculation of *E. amylovora* in *N. benthamiana* was performed as stated in Gilroy *et al.* (2007).

2.10.3 HR Assays on *Cf-9* Transgenic *N. tabacum* by Avr9 Elicitor Infiltration

Avr9 peptide (produced by Mr C Carr, The University of Glasgow, Scotland) was infiltrated at a dilution of 1/40 into *Cf-9* transgenic *N. tabacum* 2 days after any initial infiltration. Spot counts were taken 1-2 days post elicitor peptide infiltration.

2.10.4 HR Assays on *N. benthamiana* by *Cf* and *Avr* Constructs

Cf-9, Avr9, Cf-4 and *Avr4* in the pMO'6 bin vector in GV3101 (kindly provided by Prof P de Wit, King Saud University, Netherlands) were freshly streaked on to antibiotic LB 1% w/v agar plates and grown for 2 days at 28 ℃. Overnight cultures were grown from these plates in LB and antibiotic selection. The overnight cultures were pelleted (3000 g, 10 ℃, 10 minutes), re-suspended in infiltration buffer, and made to a final optical density (OD_{600}) of 1.0 (1×10^9 cfu/mL). Acetosyringone was added to a final concentration of 200 μM and incubated at room temperature for 3-4 hours prior to plant inoculation. Plants were infiltrated in a 1:1 ratio (Cf:Avr) into the abaxial side of the leaf. HR was measured after 4-8 days.

2.10.5 Measuring HR Assays on *N. benthamiana* and *N. tabaccum*.

A. tumefaciens cultures prepared as in **2.10.4**. Avr9 peptide infiltrate (or Avr4 peptide infiltrate) was prepared as stated in Hammond-Kossack *et al*. (1998) then infiltrated at a dilution of 1/40 into Cf-9 (or Cf-4) transgenic *N. tabacum* (Rowland *et al*., 2005) 3 days after *Agrobacterium* delivery of pEarley::Pi*Avr3a* constructs or pGWB6:*GFP* as a control. HRs (Avr9/Cf-9, Avr4/Cf-4 and *E. amylovora*) were recorded and photographed between 1-8 days post-infiltration depending on the elicitor. An individual inoculation was counted as positive if >50 % of the inoculated area developed a clear PCD lesion. Data graphs present the mean percentage of total inoculations per plant developing a clear HR with error bars representing +/- standard errors (SE) of combined data from at least 3 biological replicates.

2.10.6 Measuring Mean Lesion Diameter (mm) for *P. infestans*

VIGSed plants were inoculated with *P. infestans*, and lesion sizes were measured using a standard ruler (mm). Concentrated suspension (10 μL) was pipetted on four independent regions of each leaf.

2.10.7 Trypan Blue Staining for *N. benthamiana* Leaves

Staining for dead cells was performed as described in Weigel and Glazebrook (2002). Leaves were boiled in a trypan blue solution (0.25 mg/mL trypan blue –EM Biosciences-, 25% v/v lactic acid, 25% v/v phenol, 25% v/v glycerol, 25% v/v water) for 2 minutes and cooled at room temperature. Leaves were then destained in a 10 g/mL chloral hydrate solution (Sigma) for a few days. After the destaining was complete, the leaves were equilibrated in 70% v/v glycerol for photographing. As stated in Mesmar, Joelle. (2009) "*An Investigation into the Role of Ubiquitination in Plant Immunity*". PhD thesis, The University of Glasgow, Chapter 2 (2.4.1), pg39.

2.11 Confocal Microscopy

2.11.1 Imaging

Imaging was conducted on a Leica TCS-SP2 AOBS (Leica Microsystems Heidelberg GmbH, Germany) using HCX APO L 20x/0.5, 40x/0.8 and 63x/0.9 water dipping lenses. CFP was imaged using 405 nm excitation and its emission was collected from 455–480 nm. The excitation wavelength for YFP was 514 nm and its emission was collected from 525-580 nm when co-expressed with CFP and 530–575 nm when expressed alone or as split-YFP. Co-expressed CFP and YFP were imaged sequentially using a line-by-line mode. The optimal pinhole diameter was maintained at all times. PhotoshopCS software (Adobe Systems Incorporated, USA) was used for post-acquisition image processing. (Bos *et al.*, 2010)

2.11.2 Nuclear Counts

Approximatley 1 cm squares of leaf were exorcised from the *N. benthamiana* plant to be viewed using a razor and the sample was placed on a slide using double sided tape. Samples were viewed as described in **2.11.1 Imaging**, above. Fluorscent cells were counted from one edge of the sample to the other using the confocal microscope. Counts were recorded. Three readings were taken from 3 separate leaf samples per experiment and each experiment was repeated 3 times.

2.11.3 Fluorometer Analysis

Quantification of fluorescence was performed using a SpectraMax M5 fluorometer (Molecular Devices). YFP fluorescence was excited at 514 nm and measured at 580 nm.

2.12 Protein Methods

2.12.1 Protein Extraction from *N. Benthaminana*

Protein extraction was achieved by grinding 1-4 leaves of *N. benthamiana* using a pestle and mortar under liquid nitrogen until a pale green powder was produced. One scoop of PVPP and 250 µL/leaf of IP Buffer (25 mM Tris-HCL pH 7.5, 1 mM EDTA pH 8.0, 150 mM NaCl, 10% v/v glycerol, 0.05% v/v Trition-X 100 , 1x Complete® protease inhibitor cocktail Tablets; 1 per 7 mL IP Buffer) was added and grinding continued until a green paste was formed. The solution was spun at 12,000 rpm at 4°C for 15 minutes and the supernatant saved and the spin repeated on the supernatant. Samples were kept on ice and a Bradford Assay performed on the samples. Once the protein concentration was established the correct loading volume with 1xSDS was heated at 95 °C for 10 minutes. Samples were subsequently run on an SDS-PAGE and analysed using Western Blot.

2.12.2 Bradford Assay Protein Quantification

Two microlitres of protein extract were added to 18 µL sterile distilled water and 780 µL Bradford reagent (made in House). This was inverted and incubated at room temperature for 2 minutes and transferred into a cuvette (FB55147; Fisherbrand). The absorbance of the samples was read at a wavelength of 595 nm against a blank sample (2 µL of the extraction buffer or dialysis solution replacing the protein extract). The concentration of the samples was calculated based on a standard curve obtained by measuring the absorbance of a series of BSA concentration controls (0 ng/µL, 200 ng/µL, 400 ng/µL, 800 ng/µL and 1000 ng/µL).

2.12.3 Protein Precipitation Using Trichloroacetic Acid

Extracted plant protein was concentrated prior to SDS-PAGE separation (if required) using the trichloroacetic acid precipitation method. Using information obtained from the Bradford Assay, the required protein concentration was calculated and the correct volume of extracted protein was mixed in an eppendorf tube with 20 µL of 2% w/v sodium deoxycholate w/v, followed by the addition of 700 µL distilled H_2O and 250 µL of 24% v/v trichloroacetic acid with continued mixing. The solution was incubated on ice for 1 Hour and centrifuged at 12,000 g and 4 °C for 20 minutes. The supernatant was discarded and precipitated protein was re-suspended in 20 µL of 1x SDS-PAGE loading buffer and 2 µL 2 M Tris-HCl.

2.12.4 SDS Polyacrylamide Gel Electrophoresis

Protein samples, mixed with 1x SDS loading buffer (25 mM Tris-HCl pH 6.8, 10% v/v glycerol, 2% w/v SDS, 5% v/v ß-mercaptoethanol, 0.001% bromophenol blue), were boiled at 95 °C for 10 minutes and run on a pre-made SDS-PAGE gel (Sodium Dodecyl Sulfate-Polyacrylamide Gel Electrophoresis). A Pre-stained Protein Marker was used as a size reference. SDS-PAGE gels consisted of 2 parts: an upper stacking gel and lower separating gel. The stacking gel was made of 132 mM Tris-HCl pH 6.8, 4% w/v acrylamide, 0.1% w/v SDS, 0.05% w/v APS, 0.15% v/v TEMED. The 10% SDS-PAGE separating gel was made of 0.38 M Tris-HCl pH 8.8, 10% w/v acrylamide 0.1% w/v SDS, 0.05% w/v APS, 0.07% TEMED. The gels were fitted in a Miniprotean II cassette (BioRad) containing 1x SDS running buffer (25 mM Tris-HCl pH 8.5, 190 mM glycine and 1% w/v SDS). Proteins were electrophoresed at 80 V until they reached the end of the stacking gel, after which the voltage was increased to 130 V until the maker reached the bottom of the gel. Gels were either Coomassie stained or used in a Western Blot.

2.12.5 Coomassie Staining

To visualise all proteins on an SDS-PAGE gel, the gel was immersed in Coomassie stain solution (50% v/v methanol, 13% v/v acetic acid, 0.2% w/v Coomassie

Brilliant Blue R250) for 1 Hour at room temperature with gentle agitation. The Coomassie stain solution was then poured off and the gel was partially de-stained using Coomassie de-stain solution (20% v/v methanol, 5% v/v acetic acid and 75% v/v distilled H$_2$O).

2.12.6 Western Blot

Proteins were transferred to PVDF membrane from the SDS-PAGE using the Mini-PROTEAN Trans-Blot transfer cassette (BioRad) filled with 1x transfer buffer (25 mM Tris-HCl, 190 mM glycine, 20% v/v methanol). The PVDF membrane was activated using methanol prior to use. Electro-transfer was carried out at 100 V for 1 Hour or 30 V overnight at 4 °C.

2.12.7 Staining a Western Blot Membrane

Electro-transferred PVDF membranes were stained in Ponceau Solution (0.1% w/v Ponceau S, 1% v/v acetic acid) for 3-8 minutes and washed in distilled water until bands became clearly visible. The membrane was then air dried at room temperature.

2.12.8 Immunolabelling and Immunodetection of a Western Membrane

The membrane was blocked in 5% w/v semi skimmed low fat milk in TBS-T (15 mM Tris-HCl pH 7.6, 150 mM NaCl, 0.1% v/v Tween 20) with gentle agitation for 1 Hour at room temperature or overnight at 4 °C. The block was poured off and the primary antibody (diluted in TBS-T with 5% semi skimmed low-fat dried milk) was added and incubated with agitation for 2-4 Hours at room temperature or overnight at 4 °C. The dilution factor of the primary antibodies varied depending on the antibody (as per the manufacturer's instructions). The membrane was washed five times with TBS-T for a total of 25 minutes before agitated incubation for 45 minutes at room temperature with the secondary HRP-conjugated antibody. The dilution factor of the primary antibodies varied depending on the antibody (as per the manufacturer's instructions). The membrane was washed five times with TBS-T for a total of 25 minutes at room temperature using agitation. The membrane was visualised using Millipore chemiluminescent substrate in accordance with the manufacturer's instructions and developed using photographic film and a Xograph Imaging System (Compact X4, Automatic X-Ray Film Processor).

2.12.9 Striping a Western Blot Membrane

This method was obtained from Dr L Conti (The University of Glasgow, Scotland). Membranes to be re-probed were stripped using 10 mL of strip buffer (1% w/v SDS, 150 mM ß-mercaptoethanol made to 10 mL with TBS-T) in a container with the membrane for 20 minutes at >100 rpm agitation at room temperature. The strip buffer was discarded and the membrane washed 5 times for a total of 25 minutes

with TBS-T. The membrane was washed with distilled water. The membrane was reactivated with methanol and left to dry at room temperature. The membrane was stored until needed.

2.13 Protein Expression and Purification using *E. coli* (BL21)

2.13.1 Protein Expression
The gene of interest was cloned into an appropriate expression vector. Bl21 (DE3) pLysS *E. coli* cells were transformed with the construct. A single colony was picked and grown overnight at 37 °C with constant shaking (200 rpm) in 10 mL LB media. Five millilitres of this culture were added to 50 mL LB media and grown at 37 °C with shaking (200 rpm) until they reached an OD_{600} of 0.6-0.9. IPTG was added to the culture to a final concentration of 0.5-1.0 mM and grown for 3-4 hours at 37 °C with shaking (200 rpm). One-millilitre aliquots of culture were taken before and after IPTG induction to be later analysed on SDS-PAGE with 1x SDS loading buffer after lysing. Coomassie staining and western blot analysis of the pre-induced and induced samples were used to confirm induction and the solubility of the protein. Cells were pelleted by centrifugation for 15 minutes at 4,500 rpm (GSA rotor, Sorvall) at room temperature and stored at -20 °C until needed.

2.13.2 Protein Purification
GST tagged protein expressed in the soluble fraction was purified using BugBuster Protein Purification Kit (Novagen). GST tagged protein expressed in the insoluble fraction was purified using BugBuster Protein Purification Kit (Novagen), BugBuster Inclusion Body Purification, Protein Refolding kit and GST Protein Purification (all Novagen). HIS tagged protein expressed in the soluble or insoluble fraction was purified using Ni-NTA Purification System for Purification of Polyhistidine-Containing Recombinant Proteins (Invitrogen Ltd). These methods were all carried out as per the manufacturers' instructions. The purified elutions were confirmed using SDS-Page before dialysis was performed.

2.13.3 Protein Dialysis
Proteins were dialysed using 1x Ubiquitination Buffer (40 mM Tris-HCL pH 7.4, 5 mM $MgCl_2$, 50 mM KCl and 10% v/v glycerol; BioMol International) and snakeskin dialysis tubing. The dialysis, carried out at 4 °C, was repeated twice over a period of 24 hours. The purified protein concentration was determined using a Bradford assay and stored in aliquots at -80 °C.

2.14 Co-Immunoprecipitation (Co-IP) in *N. benthamiana*

After protein extraction in *N. benthamiana* was performed, the extract was used in the Miltenyi Biotec (Germany) µMACS Epitope Tag Protein Isolation Kit (Order number: 130 091) as per the manufacturers' instructions. The IP Buffer used in the extraction was used as the Wash Buffer in the IP. Elute and protein extract were analysed using SDS-PAGE western blot.

2.15 Plant Ubiquitination Assay

Ubiquitination assays were performed using an Ubiquitination kit as per the manufacturers' instructions and Yang *et al*. (2006) (Enzo®, formally known as BioMol International).

2.16 Computer Based Methodology-Sequence Analysis and Alignment

Sequence analysis and alignment was performed as stated in:

Ewan, Richard (2008). "*An investigation into the role of deubiquitinating enzymes in plant disease resistance*". PhD thesis, The University of Glasgow. Chapter 2.16.1, Pg.60.

Chapter 3. The Stabilisation of CMPG1 in the Presence of PiAvr3a

3.1 Introduction

It has previously been shown that StCMPG1 is an E3 ligase involved in ubiquitination and required for CD triggered by a range of pathogen elicitors, including the *P. infestans* elicitin, INF1 (González-Lamothe, 2006). PiAvr3a is an RxLR effector protein that has been shown to suppress INF1-triggered CD (ICD; Bos *et al.*, 2006 & Bos *et al.*, 2009). A Yeast Two-Hybrid (Y2H) screen performed by Dr M Armstrong (SCRI, Dundee, Scotland) revealed that StCMPG1a and PiAvr3a interact in the yeast nucleus (**Figure 3.1**). **Figure 3.1** shows that the C-terminal portion of PiAvr3a^{KI}, with or without RxLR-EER-encoding sequences, the PiAvr3a$^{KI/Y147F}$ substitution and PiAvr3a^{EM}, all of which suppress ICD (Bos *et al.*, 2009), interact with StCMPG1a using Y2H, whereas no interaction was observed with either PiAvr3a$^{KI/Y147S}$ or PiAvr3a$^{KI/Y147del}$ forms, which do not suppress ICD (Bos *et al.*, 2009; Bos *et al.*, 2010). An SDS-PAGE western blot confirmed that a lack of interaction with the PiAvr3a$^{KI/Y147del}$ form was not due to protein instability in yeast (Data not shown; Bos *et al.*, 2010). The use of the deletion mutant, as the favoured negative control, stemmed from prior work performed in Bos *et al.* (2006). It is therefore reasonable to hypothesize that StCMPG1 is a potential virulence target for PiAvr3a and that the interaction provides an explanation for how suppression of ICD by PiAvr3a^{KI} occurs. The Y2H screen provides initial evidence to justify experiments to further investigate this protein-protein interaction *in planta*.

3.1.2 Chapter 3 Aims and Objectives

The aims of the work carried out in this chapter were two-fold:

i. Co-express PiAvr3a forms and StCMPG1 *in planta* to confirm their interaction *in vivo* using SDS-PAGE western blots and pull downs (Co-immunoprecipitations; Co-IPs).

ii. Co-express PiAvr3a forms and StCMPG1 *in planta* to visualise their localisation and their interaction using fluorescently labelled forms and confocal microscopy.

Figure 3.1

PiAvr3a^{KI} and PiAvr3a^{EM} with (21-147) and without (60-147) RxLR-EER encoding portions (shown only for PiAvr3a^{KI}) and the PiAvr3a$^{KI/Y147F}$ mutant interact with StCMPG1 in Y2H (LacZ [blue] and –His reporter genes activated). PiAvr3a$^{KI/Y147del}$ (Y147 deletion; Δ) and PiAvr3a$^{KI/Y147S}$ mutants fail to interact with StCMPG1a. Reproduced from Bos *et al*. (2010).

PiAvr3a$^{KI\ 21-147}$

PiAvr3a$^{EM\ 21-147}$

PiAvr3a$^{KI\ 60-147}$

PiAvr3a$^{KI\ 21-S147}$

PiAvr3a$^{KI\ 21-146}$

PiAvr3a$^{KI\ 21-F147}$

LacZ   -His

With RxLR-EER

Without RxLR-EER

147 mutations/deletions
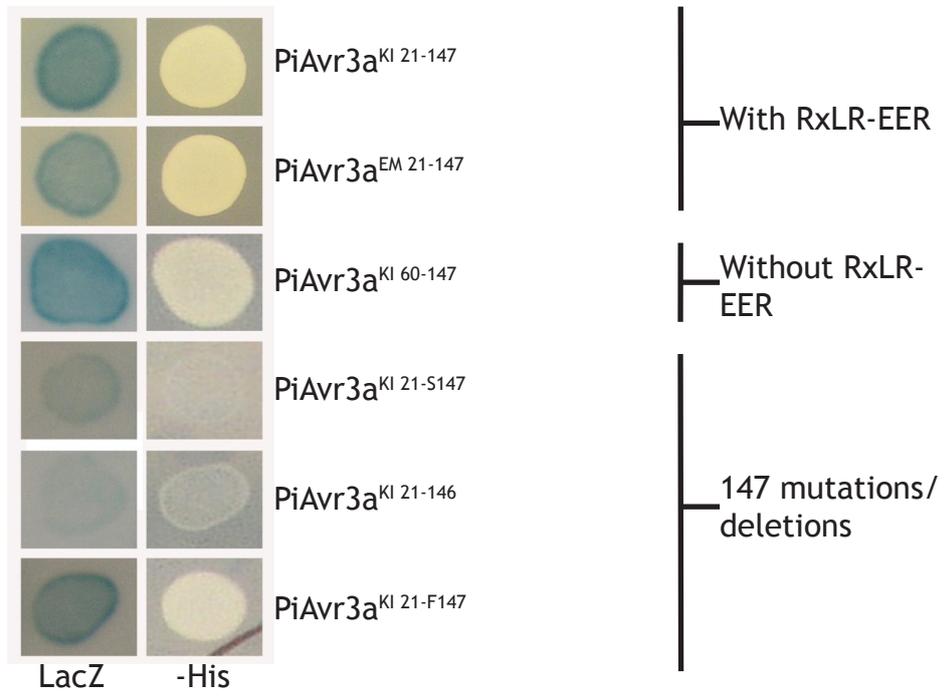
3.2 Results

3.2.1 StCMPG1 is Stabilised *in planta* by the Presence of PiAvr3a[EM] and PiAvr3a[KI].

Figure 3.2A-C shows 3 epitope-tagged constructs used for *in planta* expression, SDS-PAGE western blots and Co-IPs (**Figure 3.2D-E**). FLAG-tagged PiAvr3a[KI] and PiAvr3a[EM] were cloned into the pGR106 expression vector previously (Bos *et al.*, 2006). StCMPG1b (a full length CMPG1 protein from *S. tuberosum* that differs by 11 aa from StCMPG1a; **Figure 1.8**) was cloned into the Gateway expression vector pGWB18 (2.4 DNA Methods). The choice of vectors for cloning was determined by what was available and had been found to be reliable for *in planta* expression in previous work. All vectors contained a *35S* promoter to achieve good protein expression. The vector also had an N-terminal tag. N-terminal FLAG tags for PiAvr3a were used as previous work had found that C-terminal tags abolished both ICD suppression and recognition by R3a (Bos *et al.*, 2006). The tag for the StCMPG1b (4xMYC) was different from the PiAvr3a forms, so as to make it distinguishable on an SDS-PAGE western blot. The PiAvr3a forms were cloned from aa 23 to 147 (or Δ146; tyrosine deletion PiAvr3a[KI] mutant) so they did not contain the signal peptide, which during infection is cleaved during secretion from the pathogen, and is thus not relevant to the interaction with StCMPG1 in the host cell. This made any infiltration expression as realistic as possible at the cellular level.

MYC-StCMPG1b was co-infiltrated with FLAG-PiAvr3a[KI], FLAG-PiAvr3a[EM] or an empty vector control into *Nicotiana benthamiana (*2.8 *In planta* Protein Expression*)*. An initial Reverse Transcription-PCR (RT-PCR) experiment on the RNA extracted from 3 days post infiltration (dpi), transcribed into cDNA, showed expression of all proteins at the RNA level (2.5 RNA Methods & 2.6 PCR Methods; **Figure 3.2G**). More of the same leaf material was processed and run on an SDS-PAGE gel, western blotted and probed with antibodies for the appropriate tags (2.12 Protein Methods). An SDS-PAGE western blot is shown in **Figure 3.2D-F**. The blot shows the accumulation of StCMPG1b protein (approximately 55 KDa) when co-expressed with PiAvr3a[EM] or PiAvr3a[KI] (approximately 17 KDa). However, there was no StCMPG1b protein detected when it was co-infiltrated with an empty vector control.

Combining the information from the RT-PCR and the SDS-PAGE western blot it can be concluded that StCMPG1b requires PiAvr3a to be present to remain as a stable protein. StCMPG1b is expressed at the RNA level but if PiAvr3a is not present the protein produced is not stable and, therefore, possibly degraded. This instability/ stability was seen over experimental replicates and was reproduced by Dr J Bos

Figure 3.2 PiAvr3a^{KI} and PiAvr3a^{EM} Stabilise StCMPG1 *in planta*

A-C. Schematic representations of the constructs used for *in planta* protein expression and western blotting.

A. pGR106::PiAvr3a$^{KI23-147}$. The *35S* promoter and N-terminal FLAG tag are labelled. Made by Dr J Bos.

B. pGR106::PiAvr3a$^{EM23-247}$. The *35S* promoter and N-terminal FLAG tag are labelled. Made by Dr J Bos.

C. pGWB18::StCMPG1b$^{1-1548}$. The *35S* promoter and 4x N-terminal Myc tags are labelled. Made by R Taylor (author).

D-F SDS-PAGE western blot of *in planta* protein expression at 3 dpi. WT *N. benthamiana* plants infiltrated with *A. tumefaciens* (strain GV3101) containing 1:1 ratios of pGWB18::StCMPG1b with the PiAvr3a variants (pGR106::PiAvr3a^{KI} & pGR106::PiAvr3a^{EM}) or an empty vector control. Plants were infiltrated at a final OD$_{600}$ of 0.2 and leaf samples taken at 3 dpi. Total plant protein was extracted from leaf tissue, measured with a Bradford assay and approximately 40 ng of protein from each sample was loaded onto the SDS-PAGE gel. Western blots were probed. Protein size markers are labelled in Kilo Daltons (KDa). This experiment was repeated 3 times with similar results.

D. SDS-PAGE western blot PVDF membrane probed with α:Myc primary antibody to detect StCMPG1b.

E. The same SDS-PAGE Western blot PVDF membrane as in D, stripped and probed with α:FLAG primary antibody to detect PiAvr3a.

F. The PVDF membrane from D & E stained with Ponceau.

G. Electrophoresis DNA agarose gels showing Reverse Transcription-PCR. WT *N.benthamiana* plants infiltrated with *A.tumefaciens* (strain GV3101) containing 1:1 ratios of pGWB18::StCMPG1 with the various PiAvr3a variants (pGR106::PiAvr3a^{KI}, pGR106::PiAvr3a^{EM}, pGWB15::PiAvr3a^{Δ} aka pGWB15::PiAvr3a$^{KI/Y147del}$) or a pGWB6::GFP control (combinations listed across the top of the figure). Plants were infiltrated at a final OD$_{600}$ 0.2 and leaf samples taken 3 dpi. RNA was extracted from leaf tissue, transcribed into DNA and PCR performed. The primer specific reactions were run on an agarose DNA gel under electrophoresis (construct primers listed to the right of the figure; For primer details see the Appendices). DNA fragment size is labelled on the left of the figure in base pairs (bp).
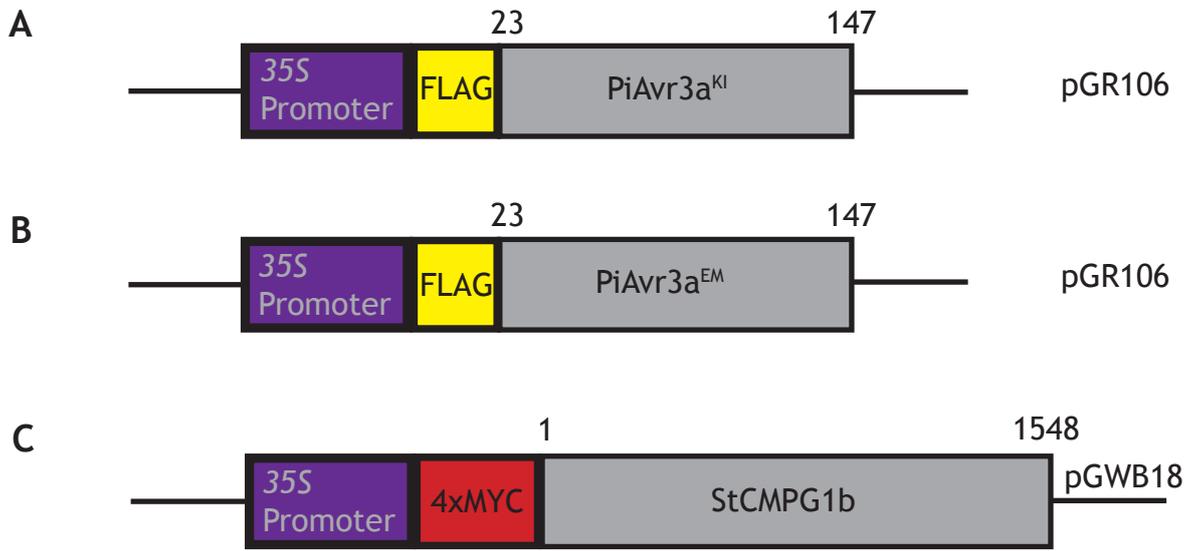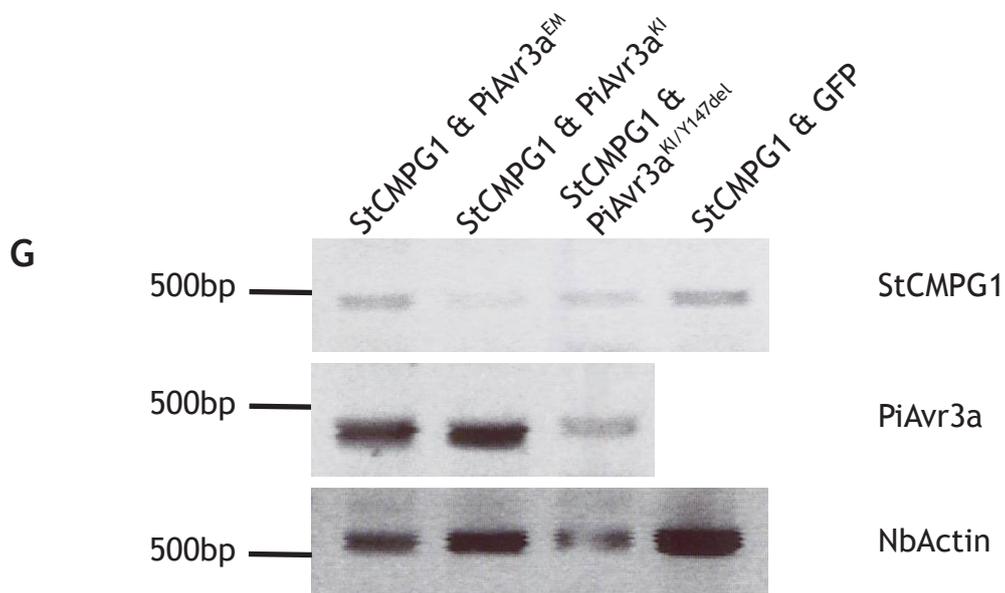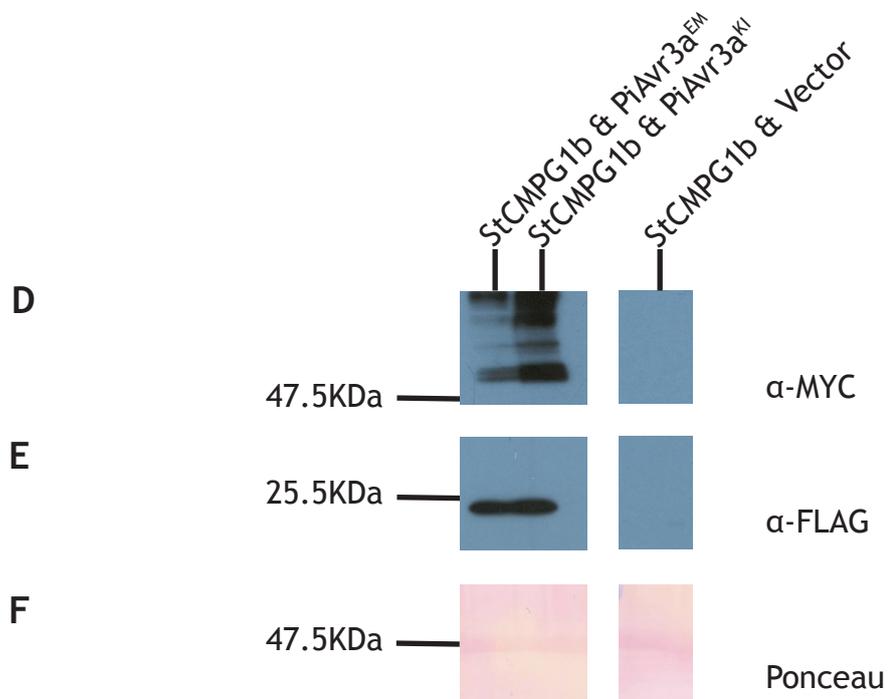
(The Sainsbury Lab, Norwich, U.K). From looking at the SDS-PAGE western blot it appears that StCMPG1b has higher stability with PiAvr3a^{KI} compared to with PiAvr3a^{EM}. Dr J Bos again reproduced this, and in addition she demonstrated that the PiAvr3a$^{KI/Y147del}$ mutant was unable to stabilise StCMPG1 (Bos *et al*. 2010) using western blotting. Nevertheless, although the same amount of total plant protein extract was loaded in all lanes, SDS-PAGE western blots are not quantitative. To investigate if there is a difference in the stability of StCMPG1b with the PiAvr3a^{KI} and PiAvr3a^{EM} forms, and a failure to stabilise CMPG1 by PiAvr3a$^{KI/Y147del}$, split-YFP (BiFC) and co-localisation experiments were employed (see section 3.2.4 and 3.2.5).

The protein expression of StCMPG1b on the SDS-PAGE western blot did not produce a single band when probed but a "laddered" affect with multiple MYC tagged bands above the StCMPG1b, in the presence of PiAvr3a^{EM} and PiAvr3a^{KI}. This could be due to some form of protein processing and/or modification of StCMPG1b. The upper banding is not caused by the PiAvr3a being attached as this would have appeared on the FLAG SDS-PAGE western blot. To investigate this further, a Co-IP would be needed to determine what else was attached to the StCMPG1b, such as ubiquitin or SUMO proteins for example. Dr J Bos also showed modification of StCMPG1b upon its stabilisation by PiAvr3a, although she saw only a single band (Bos *et al.*, 2010).

N. benthamiana Co-IP *in planta* experiments were performed under various conditions with various techniques, including kits (Materials and Methods, 2.14) as well as handmade columns (made with sephadex-G25 [powder] and IP buffer; IP Buffer: 25 mM Tris-HCl pH 7.5, 1 mM EDTA, 150 mM NaCl, 10% glycerol, 0.1-0.05% MP40). Temperature was varied (room temperature or 4 ^{o}C), as were buffer and extraction conditions (variations to the above buffer; extraction with or without the use of PVPP powder and with or without the use of liquid nitrogen). Infiltration OD$_{600}$, plant growth conditions and infiltration times were adapted (OD$_{600}$: 0.1-1.0; young plants through to nearly flowering *N. benthamiana*; Infiltration for a few hours through to 5 days pi). However, despite trying to pull down StCMPG1b, either by its own tag or with the PiAvr3a tag on the constructs, there was no presence of StCMPG1b on SDS-PAGE western blots (data not shown). A number of individuals attempted the *in planta* Co-IP (Dr M Armstrong in SCRI, Dundee and Dr J Bos in The Sainsbury Lab, Norwich). However StCMPG1b could not be detected.

3.2.2 StCMPG1b accumulates in the Nucleus and Cytoplasm when Stabilised by PiAvr3a.

To further investigate the stabilisation of StCMPG1b by PiAvr3a, a construct was made to fuse StCMPG1b to full-length YFP, and MYC-tagged PiAvr3a^{KI}, PiAvr3a^{EM}

and PiAvr3a$^{KI/Y147del}$ constructs were made for co-expression (2.4 DNA Methods; **Figure 3.3A-D**).

The full-length fluorescently tagged construct of StCMPG1b (YFP) was infiltrated, with or without the epitope tagged PiAvr3a (MYC) into *N. benthamiana* leaves and viewed under the Confocal microscope at 60 hours post-infiltration (hpi; 2.11 Confocal Microscopy). Representatives of the images taken are shown in **Figure 3.3E** and **Figure 3.3F,** and quantified (by counting fluorescent nuclei) in **Figure 3.3G**. The images show that when StCMPG1b-YFP is infiltrated on its own there is no detectable fluorescence, implying a lack of protein stability. When StCMPG1b-YFP is co-infiltrated with either MYC-PiAvr3a^{EM} or MYC-PiAvr3a^{KI}, which were not fluorescently tagged, there is YFP fluorescence in the cell appearing in the cytoplasm and the nucleus. These images provide further evidence that StCMPG1b is stabilised by the presence of PiAvr3a^{KI} and PiAvr3a^{EM} and also reveal that, upon stabilisation, StCMPG1b is detectable in the nucleus. In some cases nuclear bodies could be seen in the nucleus containing YFP. The reason for these bodies could not be determined, as they did not appear consistently in the experimental replications. The localisation of StCMPG1b in the nucleus was not expected, as it is too large (55 KDa), even without the addition of YFP, to passively enter it.

The YFP fluorescence in **Figures 3.3D-G** show a varying amount of fluorescence between StCMPG1b infiltrated with PiAvr3a^{EM} and StCMPG1b infiltrated with PiAvr3a^{KI}. More fluorescent nuclei were detected with PiAvr3a^{KI} compared to PiAvr3a^{EM}, which supports the previous results seen with the SDS-PAGE western blot (**Figure 3.2**) that this form of PiAvr3a more strongly stabilises StCMPG1b.

3.2.3 PiAvr3a$^{KI/Y147del}$ does not Stabilise StCMPG1b

In the previous sections, PiAvr3a^{KI} and PiAvr3a^{EM} were shown to stabilise StCMPG1b *in planta*. Y2H results suggested that PiAvr3a$^{KI/Y147del}$ does not interact with StCMPG1b. Therefore it was investigated whether this mutant form of PiAvr3a was able to stabilise StCMPG1b. For this, additional constructs were made, cloning into the pB7WGC2 vector, to fuse CFP to the N-terminus of PiAvr3a^{KI}, PiAvr3a^{EM} and PiAvr3a$^{KI/Y147del}$ (2.4 DNA Methods; **Figure 3.4A-C**). To investigate whether these were themselves stable and active *in planta*, each was expressed in *N. benthamiana* leaves and protein extracted, SDS-PAGE western blotted and probed with GFP antibody. In each case, a band of expected size (44 KDa) from CFP-PiAvr3a fusions was observed (2.12 Protein Methods; **Figure 3.4D**). To investigate whether these remained active, each was co-expressed with R3a. As expected, a strong HR was observed when co-expressing R3a with PiAvr3a^{KI} or PiAvr3a$^{KI/Y147del}$, whereas no such HR was observed following co-expression with PiAvr3a^{EM} (2.12 Protein Methods; **Figure 3.4E**).

Figure 3.3 StCMPG1b Accumulates in the Cytoplasm and Nucleus upon Stabilisation with PiAvr3a

A-D Schematic representations of the constructs used for *in planta* protein expression and confocal microscope experiments.

A. pEarley203::PiAvr3a$^{EM23-147}$. The *35S* promoter and the N-terminal MYC tag are labelled. Made by R Taylor (author).

B. pEarley203::PiAvr3a$^{KI23-147}$. The *35S* promoter and N-terminal MYC tag are labelled. Made by R Taylor (author).

C. pEarley203::PiAvr3a$^{KI23-146}$. The *35S* promoter and N-terminal MYC tag are labelled. The neagative control Y147 deletion mutant. Made by R Taylor (author).

D. pB7YWG2::StCMPG1b$^{1-1548}$. The *35S* promoter and C-terminal YFP tag are labelled. Made by Dr P Boevink.

E and F. Confocal microscope images visualising StCMPG1b-YFP fluorescence. pB7YWG2::StCMPG1b was infiltrated alone or with a PiAvr3a construct as indicated at a final OD$_{600}$ 0.01. Images represent what was seen over 3 repetitions at 60 hpi. **E.** A leaf at 20x magnification for each sample, showing a number of cells. Scale bar represents 50µm.

F. A leaf at 40x magnification for each sample, showing a closer view of individual leaf cells. Scale bar represents 10µm

Gi. A bar graphs showing fluorescent nuclear counts for the infiltrated constructs. This trend was seen over 3 replicate experiments as shown.

Gii. Confocal microscope images visualising StCMPG1b-YFP fluorescence. pB7YWG2::StCMPG1b was infiltrated alone or with a PiAvr3a construct as indicated. Images represent what was seen over 3 repetitions. The magnification and scale bars are shown. Scale bars represent 50µm.

Ai

```
35S          4xMYC    23        PiAvr3a^KI    147
Promoter                                              pEarley203
```

B

```
35S          4xMYC    23        PiAvr3a^EM    147
Promoter                                              pEarley203
```

C

```
35S          4xMYC    23     PiAvr3a^KI/Y147del  147
Promoter                                              pEarley203
```

D

```
35S          1        StCMPG1b        1548   YFP
Promoter                                              pB7YWG2
```
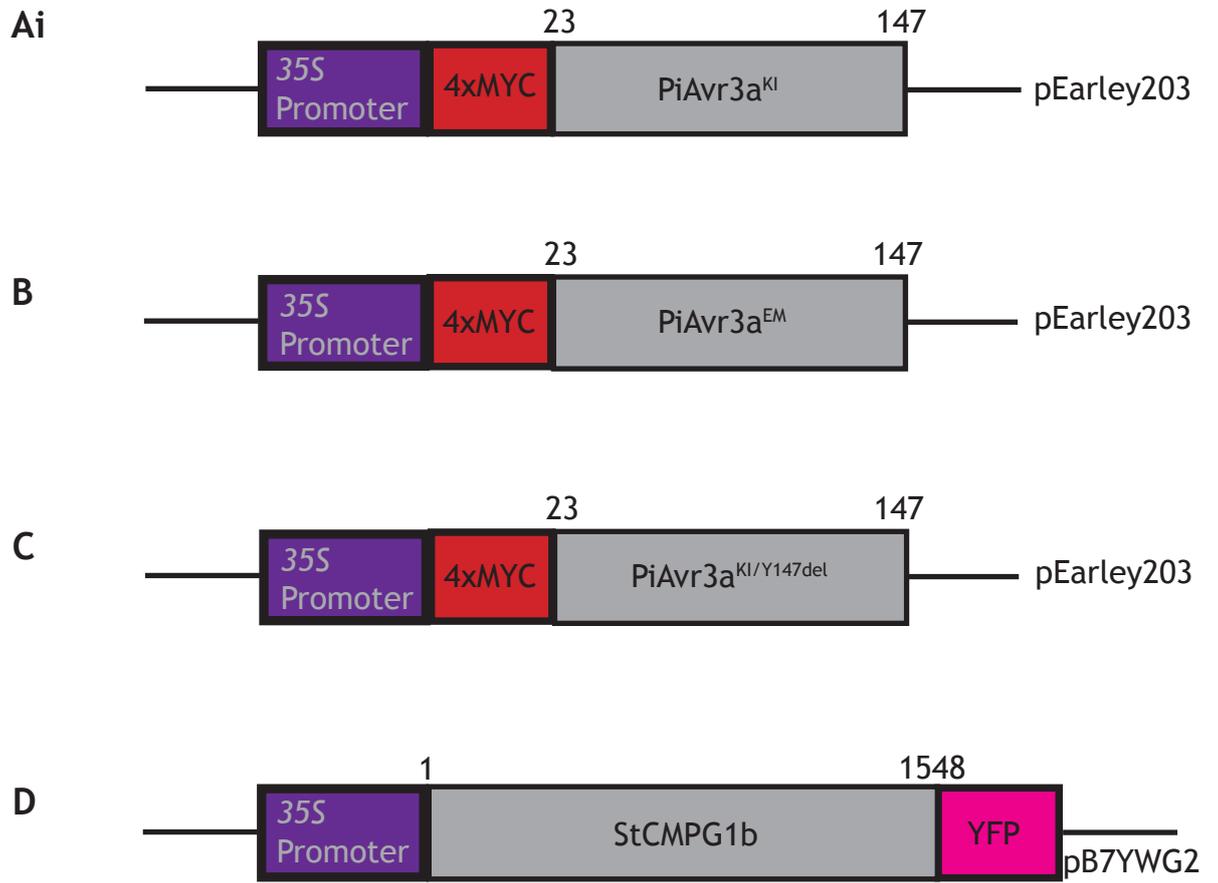
| StCMPG1b-YFP | StCMPG1b-YFP and PiAvr3a^KI | StCMPG1b-YFP and PiAvr3a^EM |

E

F

Gi

Rep 1

Rep 2

Rep 3

- StCMPG1-YFP & PiAvr3aKI
- StCMPG1-YFP & PiAvr3aEM
- StCMPG1-YFP & PiAvr3aKI/Y147del
- StCMPG1-YFP

Gii

StCMPG1b-YFP and PiAvr3a^{KI}

StCMPG1b-YFP and PiAvr3a^{EM}

StCMPG1b-YFP and PiAvr3a$^{KI/Y147del}$
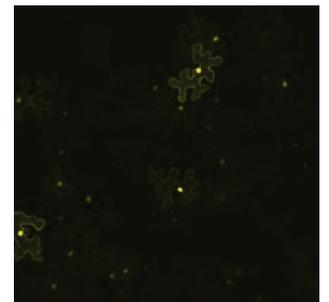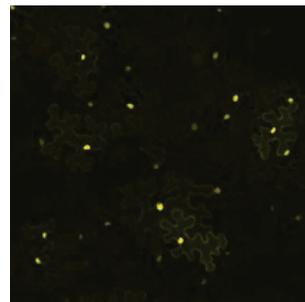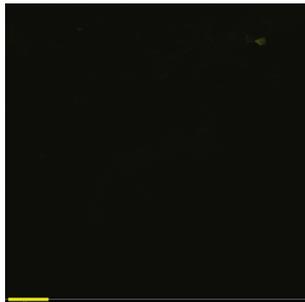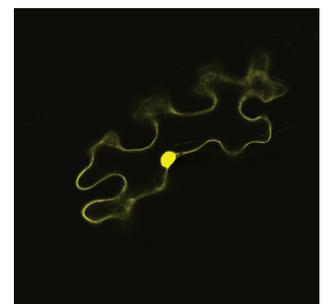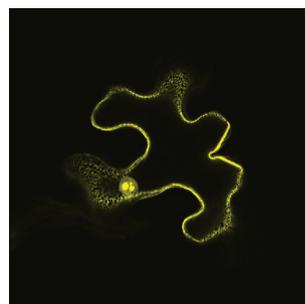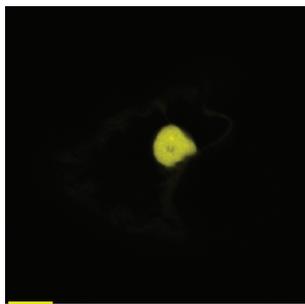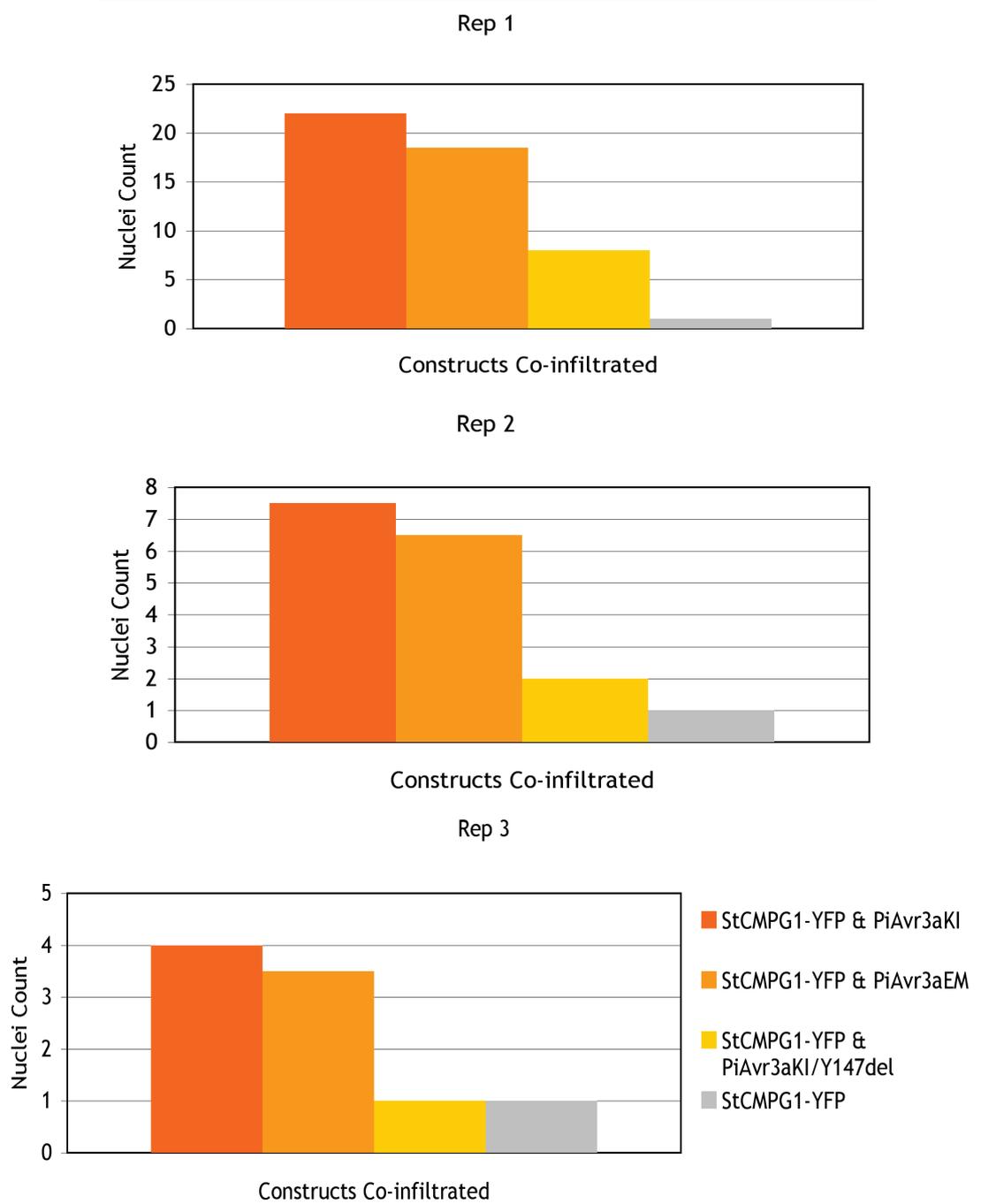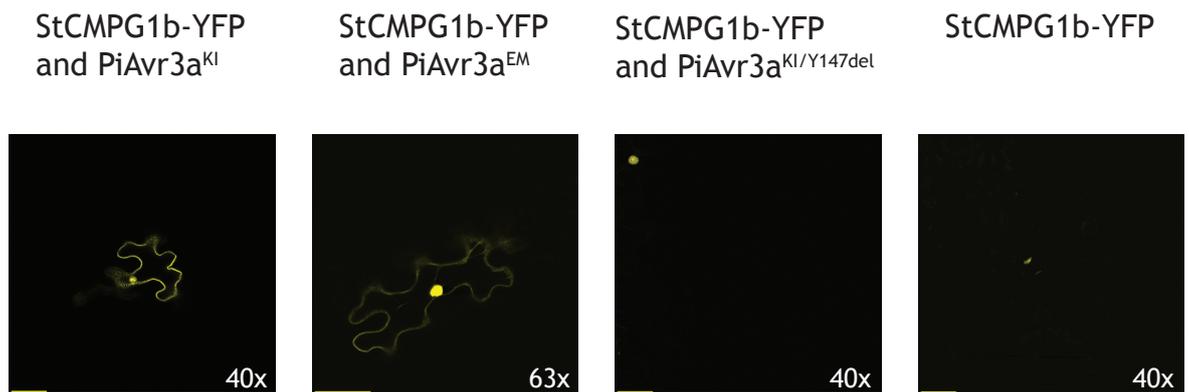
StCMPG1b-YFP

Figure 3.4 PiAvr3a^{KI/Y147del} Mutant does not Stabilise StCMPG1b

A-C. Schematic representations of the constructs used for *in planta* protein expression and confocal microscope experiments. Made by Dr P Boevink.

A. pB7WGC2::PiAvr3a$^{KI23-147}$, showing *35S* promoter and the N-terminal CFP.

B. pB7WGC2::PiAvr3a$^{EM23-147}$, showing *35S* promoter and the N-terminal CFP.

C. B7WGC2::PiAvr3a$^{KI/Y147del23-146}$, showing *35S* promoter and the N-terminal CFP.

D. SDS-PAGE western blot probed with α:GFP antibody following expression in *N. benthamiana* of CFP-PiAvr3a^{KI} (1), CFP-PiAvr3a^{EM} (2), CFP-PiAvr3a$^{KI/Y147del}$ (Δ; 3). Protein from uninfiltrated leaf is shown in (4). Protein loading is indicated by Ponceau staining (PS). All three constructs generated intact CFP fusions *in planta*.

E. Expression of *R3a* alone, and co-expression of CFP-PiAvr3a^{KI} (KI), CFP-PiAvr3a^{EM} (EM) and CFP-PiAvr3a$^{KI/Y147del}$ (Δ147) with R3a in *N. benthamiana*. As expected, both CFP-PiAvr3a^{KI} and CFP-PiAvr3a$^{KI/Y147del}$, triggered R3a-mediated CD.

F. Co-expression of CFP-PiAvr3a^{KI} (KI), CFP-PiAvr3a^{EM} (EM) and CFPPiAvr3a$^{KI/Y147del}$ (Δ147) with full-length StCMPG1b-YFP visualised at 3 dpi using confocal microscopy. Upper panels show CFP fluorescence, lower panels show YFP. Whereas CFP fluorescence was similar in each experiment, indicating similar levels of CFP-PiAvr3a^{KI}, CFP-PiAvr3a^{EM} and CFP-PiAvr3a$^{KI/Y147del}$ (KIΔ147) proteins, StCMPG1b-YFP fluorescence was significantly stronger following co-expression with CFP::PiAvr3a^{KI} than with CFP::PiAvr3a^{EM}, and barely detectable with CFP::PiAvr3a$^{KI/Y147del}$, further indicating that PiAvr3a^{KI} more strongly stabilises StCMPG1b. The scale bar is 200 μm.

A

B

C

D

E

F
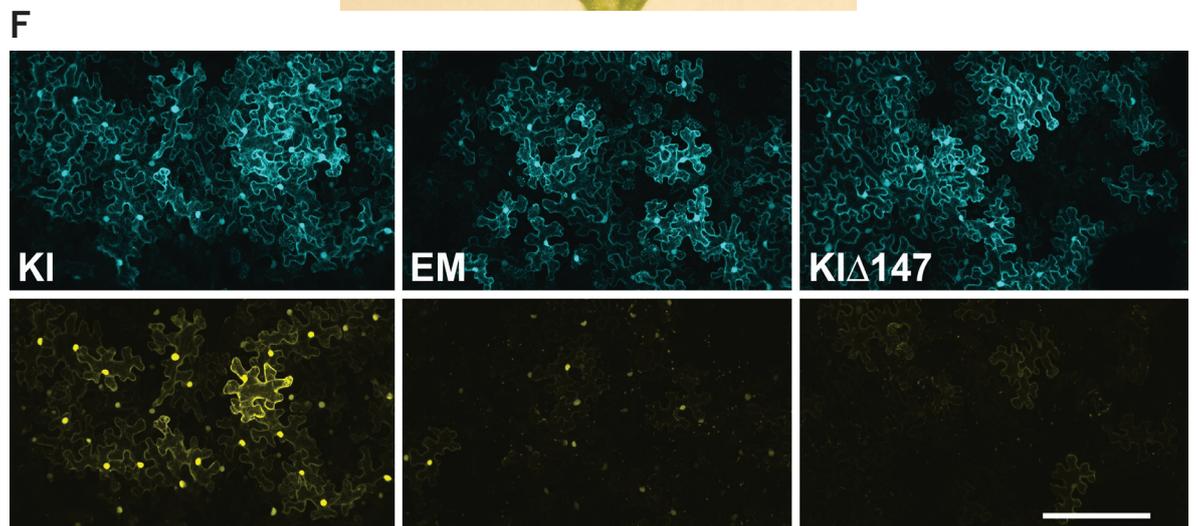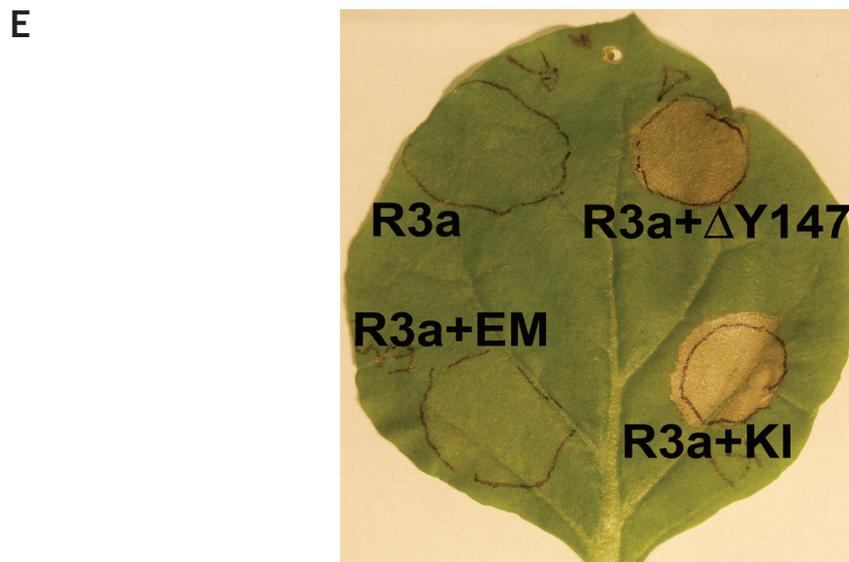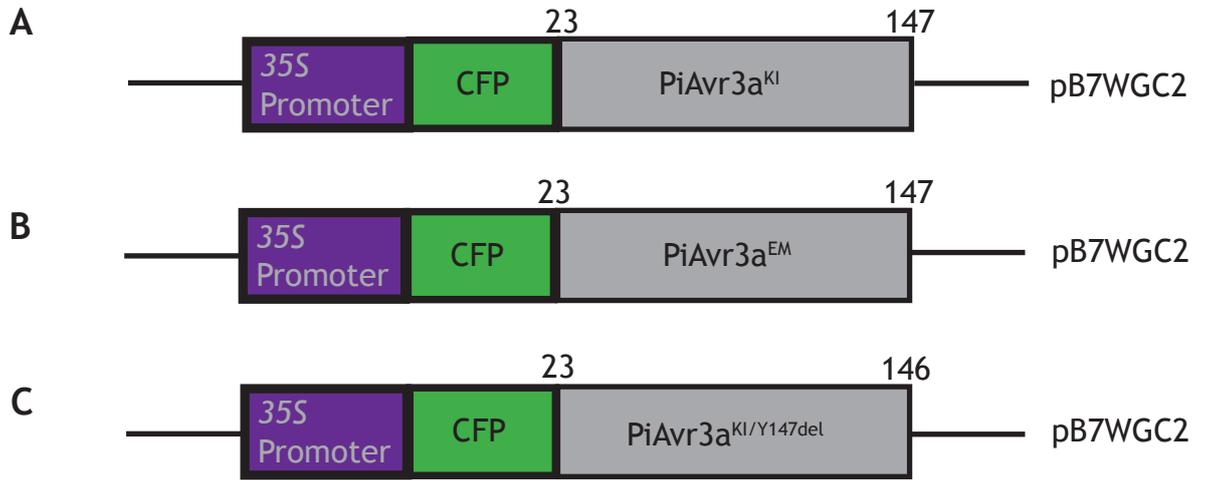
The StCMPG1b-YFP construct was co-expressed with each of the CFP-PiAvr3a constructs and confocal images were generated at 3 dpi (2.11 Confocal Microscopy & 2.12 Protein Methods; **Figure 3.4F**). Similar levels of CFP fluorescence were observed in each experiment, indicating the presence of the CFP-PiAvr3a fusions. As shown previously, both CFP-PiAvr3a^{KI} (strongly) and CFP-PiAvr3a^{EM} (weakly) stabilised StCMPG1b-YFP. However, StCMPG1b-YFP fluorescence was barely detectable with CFP-PiAvr3a$^{KI/Y147del}$, indicating that this mutant form does not stabilise StCMPG1b (**Figure 3.4F**). This is in agreement with a failure to interact with StCMPG1b in Y2H (**Figure 3.1**).

3.2.4 StCMPG1b Interacts with PiAvr3a in the Plant Cell.

To observe if StCMPG1b and PiAvr3a do interact *in planta,* Split-YFP constructs were generated (2.4 DNA Methods; **Figure 3.5A-F**). **Figure 3.5G** shows 4 images of split-YFP for the StCMPG1b-YC construct co-infiltrated with the various YN-PiAvr3a constructs and a vector-YN control (2.8 *In planta* Protein Expression; generating free YN). It can be seen that there is more fluorescence with the YN-PiAvr3a^{KI} form compared to the other 3 (YN-PiAvr3^{EM}, YN-PiAvr3a$^{KI/Y147del}$ and Vector-YN; **Fig 3.5G**). This implies that PiAvr3a^{KI} interacts with StCMPG1b more strongly than PiAvr3a^{EM}. There is more fluorescence seen with the YN-PiAvr3a^{EM} form compared to the YN-PiAvr3a$^{KI/Y147del}$ and the Vector-YN. The low level of YFP fluorescence between StCMPG1b-YC and YN-PiAvr3a$^{KI/Y147del}$ is in agreement with the failure of this mutant PiAvr3a form to interact with StCMPG1b in Y2H, or to stabilise StCMPG1b *in planta*. To confirm a lack of stability due to a lack of interaction, free PiAvr3a^{KI} was co-expressed with StCMPG1b-YC and YN-PiAvr3a$^{KI/Y147del}$ and showed no increased fluorescence (data not shown; Bos *et al.,* 2010).

3.2.5 Quantitative Fluorometer Readings Confirm Strong Stabilisation of StCMPG1b in the Presence on PiAvr3a^{KI}, weak in the Presence of PiAvr3a^{EM}, and Barely Detectable in the Presence of PiAvr3a$^{KI/Y147del}$.

To quantify fluorescence generated in the split-YFP experiments in **3.2.4**, a fluorometer was used and constructs as in **Figure 3.5** with exchanged tags (i.e. YN was fused to CMPG1 and YC to the PiAvr3a constructs). *N. benthaminana* leaf samples were processed and the level of fluorescence measured (2.8 *In Planta* Protein Methods). The results of the experiments performed as the means over multiple replicates are shown in **Figure 3.5H**. The graph shows the amount of fluorescence (Relative Fluorescence Units; RFU) for the various samples, including Standard Error (SE) bars. A GFP control (Transgenic *N. benthaminana* expressing free full-length GFP) shows an RFU value of 123.15 RFU. StCMPG1b-YN & YC-PiAvr3a^{KI} has the second highest value for the samples of 110.57 RFU. StCMPG1b-YN and YC-PiAvr3a^{EM} produced 53.34 RFU and StCMPG1b-YN & YC-PiAvr3a$^{KI/Y147del}$ generated

Figure 3.5 PiAvr3a interacts with StCMPG1b *in planta*

A-F. Schematic representations of the constructs used, each showing *35S* promoter and fluorescent tags, for *in planta* protein expression and confocal microscope experiments.

A. Free pBatTL-B-sYFPC. Made by Dr P Boevink.

B. pBatTL-B-sYFPN ::StCMPG1b$^{1-1548}$. Made by Dr P Boevink.

C. pBatTL-B-sYFPC ::StCMPG1b$^{1-1548}$. Made by Dr P Boevink.

D. pCL112::PiAvr3a$^{KI23-147}$. Made by R Taylor (author).

E. pCL112::PiAvr3a$^{EM23-147}$. Made by R Taylor (author).

F. pCL112::PiAvr3a$^{KI/Y147del23-146}$ (Δ). Made by R Taylor (author).

G. Confocal images showing sYFP and the interaction of StCMPG1b with PiAvr3a^{KI} and PiAvr3a^{EM} but not with PiAvr3a$^{KI/Y147del}$. The confocal microscopy images were taken following co-expression in *N. benthamiana* of split YFP constructs StCMPG1b-YC with a vector expressing Free-YN, and StCMPG1b-YC with N-YFP::PiAvr3a^{KI}, N-YFP::PiAvr3a^{EM}, NYFP::PiAvr3a$^{KI/Y147del}$ (Δ) constructs as indicated in the images. The scale bar is 200 μm.

H. Fluorometer measurements (in Relative Fluorescence Units; RFU) following co-expression in *N. benthamiana* of the split YFP constructs StCMPG1b::N-YFP (YN), StCMPG1b::C-YFP (YC), N-YFP::PiAvr3a^{KI}, N-YFP::PiAvr3a^{EM}, NYFP::PiAvr3a$^{KI/Y147del}$ as indicated. Error bars (+/-) were calculated using Standard Deviation divided by the square route of the population (n).

A 35S Promoter | Free | sYFP — pBatTL-B-sYFPC

B 35S Promoter | StCMPG1b (1–1548) | sYFP — pBatTL-B-sYFPC

C 35S Promoter | sYFP | StCMPG1b (1–1548) — pBatTL-B-sYFPN

D 35S Promoter | sYFP | PiAvr3a^{KI} (23–147) — pCL112

E 35S Promoter | sYFP | PiAvr3a^{EM} (23–147) — pCL112

F 35S Promoter | sYFP | PiAvr3a$^{KI/Y147del}$ (23–146) — pCL112

G

CMPG1-YC+free YN

CMPG1-YC+Avr3aKI-YN

CMPG1-YC+Avr3aEM-YN

CMPG1-YC+Avr3aKIΔY147-YN

H

Legend:
- Uninfiltrated
- GFP
- StCMPG1b-YC and StCMPG1b-YN
- StCMPG1b-YC and PiAvr3aKI-YN
- StCMPG1b-YC and PiAvr3aEM-YN
- StCMPG1-YC and PiAvr3aKI/Y147del-YN

Y-axis: RFU (0.00–140.00)
X-axis: Constructs

41.44 RFU, which is much less compared to co-expression of StCMPG1b-YN with YC-PiAvr3a^{KI}. Co-expression of StCMPG1b-YN with YC-PiAvr3a^{EM} generated more fluorescence than StCMPG1b-YN with YC-PiAvr3a$^{KI/Y147del}$, implying that aa Y147 is important in the function of PiAvr3a, in addition to the two naturally occurring aa differences (EM & KI). The fluorescence for the negative controls (Un-infiltrated leaf and StCMPG1b-YN co-expressed with StCMPG1b-YC) was less than the positive control (Transgenic *N. benthaminana* GFP) and the 3 PiAvr3a co-infiltrated samples (**Figure 3.5**). These results indicate that, in addition to stabilising StCMPG1b, PiAvr3a^{KI} and, to a lesser extent PiAvr3a^{EM}, both directly interact with, or are in close proximity to, StCMPG1b *in planta*. There is little evidence for interaction between PiAvr3a$^{KI/Y147del}$ and StCMPG1b in these experiments, in agreement with Y2H experiments.

3.3 Discussion

PTI and ETI are two forms of plant defence that help the plant evade pathogen infection in its early stages. Pathogens suppress PTI using effector proteins that may be delivered inside the host cell. Some effector proteins are recognised by plant R proteins, resulting in ETI. This prevents the pathogen from infecting by triggering PCD as part of the HR. Pathogen effectors are known to block PCD, as part of PTI or ETI (Chisholm *et al*, 2006; Grant *et al*, 2006; Jones and Dangl, 2006; Block *et al*, 2008).

Previous work has established that PiAvr3a^{KI} activates R3a to trigger ETI in potato, whereas PiAvr3a^{EM} does not (Armstrong *et al.*, 2005). In addition, PiAvr3a^{KI} strongly suppresses PCD triggered by the secreted PAMP, INF1, whereas PiAvr3a^{EM} only weakly suppresses it (Bos *et al.*, 2006; 2009). ICD has been shown previously to require the host ubiquitin E3 ligase CMPG1 (González-Lamothe *et al.*, 2006). The interaction, in Y2H, between PiAvr3a^{KI} and PiAvr3a^{EM} with StCMPG1a, suggests that this host protein may be a virulence target of *P. infestans*, and the means by which the effector PiAvr3a suppresses ICD.

3.3.1 StCMPG1b is Stabilised by PiAvr3a to Prevent its Normal Function.
The expression of StCMPG1b alone *in planta* could not be detected on an SDS-PAGE western blot, which suggests that the protein is quickly degraded upon formation in the cell. However, when expressed in conjunction with PiAvr3a^{KI} or PiAvr3a^{EM}, StCMPG1b could be detected. This shows that PiAvr3a stabilises StCMPG1b in the cell and from this observation implies StCMPG1b is normally expressed in the cell but degraded very quickly and therefore its presence cannot be detected.

SDS-PAGE westerns probed for MYC-StCMPG1b also revealed upper banding in the StCMPG1b and PiAvr3a co-expressed samples. This upper banding would indicate some form of StCMPG1b protein modification, which could include ubiquitination or SUMOylation (SUMO; Small ubiquitin-like modifier). Considering that StCMPG1b is a known ubiquitin E3 ligase it is possible that the modification is ubquitination. However, this can only be surmised, as Co-IPs did not prove successful. If StCMPG1b could have been pulled-down, mass-spectrometry may have revealed the nature of the StCMPG1b modification.

The hypothesis that StCMPG1b could be modified, as part of ubiquitination, was investigated by Dr J Bos. Data collected showed that when StCMPG1b was expressed alone, following treatment with the 26S proteasome inhibitors MG132 and epoxomicin, there was an increase in the amount of StCMPG1b detected (Bos *et al.*, 2010). This result provides evidence for the involvement of the 26S proteasome, and therefore potentially ubiquitination, in the processing of StCMPG1b. Moreover, Dr J Bos showed that C37A and W64A mutated forms of StCMPG1b, which disable the U-box and thus prevent E3 ligase activity, were stable when expressed in *N. benthamiana*. This indicates that instability (26S proteasome-dependent degradation) of StCMPG1b is dependent on its own activity.

In conjunction with the results presented in this chapter other data collected by Dr J Bos showed, using western blot hybridisation, that PiAvr3a^{KI} and PiAvr3a^{EM}, but not the PiAvr3a$^{KI/Y147del}$ form, stabilised StCMPG1b. *N. benthamiana* CMPG1 full-length proteins encoded by two different *NbCMPG1* genes and CMPG1 full-length protein from *S. lycopersicum* were all also stabilised by PiAvr3a^{KI} and PiAvr3a^{EM} but not PiAvr3a$^{KI/Y147del}$. *N. benthamiana* and *S. lycopersicum* are both hosts for *P. infestans*. With the stabilisation of StCMPG1 by PiAvr3a occurring across multiple species it would appear this is a conserved role for PiAvr3a in *P. infestans* host-interactions and, therefore, likely to be an important mechanism. It should be noted that, in stabilising StCMPG1, PiAvr3a prevents its normal function (which includes self-mediated degradation, and thus presumably degradation of its targets in the host cell), and this may thus be the means by which PiAvr3a prevents ICD.

3.3.2 Upon Stabilisation, StCMPG1b Accumulates in the Nucleus and the Cytoplasm.

StCMPG1b was visualised under the Confocal microscope using fluorescently tagged constructs. Images showed that for the fluorescently tagged StCMPG1b alone there was little or no fluorescence and, therefore, no detectable protein. However, when co-infiltrated with epitope-tagged or CFP-fused PiAv3a^{KI} or PiAvr3a^{EM}, there was fluorescence and, therefore, stabilisation of StCMPG1b. The images showed that, upon stabilisation, StCMPG1b was evident in the nucleus and the cytoplasm.

StCMPG1b is too large to passively enter the nucleus, and it will require further work to investigate the significance of this localisation. EDS1 (Enhanced Disease Susceptibility 1) is an example of a protein with a role in the activation of defence related genes found to accumulate in the cytoplasm and nucleus and promote a defence responce in the plant. This involves access to the nucleus via nuclear porins. StCMPG1b could have a similar mode of action with the association of PiAvr3a. (Garcia *et al.*, 2010)

3.3.3 There is Variation in Stabilisation of StCMPG1b by the two Naturally Occurring Forms of PiAvr3a (PiAvr3a^EM and PiAvr3a^KI)

Two main approaches were taken to see if a difference in the stabilisation of StCMPG1b by the two naturally occurring forms of PiAvr3a (PiAvr3a^EM and PiAvr3a^KI) existed. These were nuclear counts and fluorometer readings. Nuclear counts were initially used as an indication as to any difference between the two forms of PiAvr3a. This method proved reliable in terms of relative difference within a set of counts for a particular set of infiltrated leaves but proved unreliable in terms of comparison to other replicate experiments, as the actual numbers varied substantially, making Standard Deviations and Standard Errors ambiguous and inconclusive. **Figure 3.3F** shows a set of counts, which reveal the relationship between the infiltrated construct combinations for a particular experimental replication. The second method used a fluorescence reader, which produced a relative fluorescent value for the amount of fluorescence in a crushed leaf sample. This method proved more quantitative and more consistently reliable between experimental replicates (for the split-YFP experiment). The results from both show that PiAvr3a^KI generates more StCMPG1b stability when compared to PiAvr3a^EM and that the Y147 aa is required for this stabilisation and localisation.

3.3.4 Does StCMPG1b Interact Directly with PiAvr3a?

Whether StCMPG1b interacts directly with PiAvr3a or not, has not been fully resolved. There is supporting data for the direct interaction, such as the Y2H, and an indication in split-YFP experiments that stabilisation may require interaction, or close proximity to reconstitute full YFP fluorescence. However, many failed attempts at co-immunoprecipitation indicated that the interaction was not easy to verify *in planta* with this technique. However, it should be noted that also pull-down experiments are not a conclusive demonstration of direct binary interaction, as the pull-down could still be mediated through a third protein intermediate.

The Y2H showed equal interaction between StCMPG1a and PiAvr3a^KI and StCMPG1a and PiAvr3a^EM. The split-YFP and *in planta* co-expression results presented throughout the chapter, indicated that PiAvr3a^KI more strongly interacts with and stabilises StCMPG1b than does PiAvr3a^EM. These *in planta* results, although

differing from the Y2H, nevertheless support the relative abilities of PiAvr3a^{KI} and PiAvr3a^{EM} to suppress ICD.

3.3.5 PiAvr3a CD Suppression and Recognition by R3a are Independent Activities

The expression of *R3a* alone, co-expression of PiAvr3a^{KI}, PiAvr3a^{EM} and PiAvr3a$^{KI/Y147del}$ with *R3a* in *N. benthamiana* showed both PiAvr3a^{KI} and PiAvr3a$^{KI/Y147del}$ triggered R3a-mediated CD, whereas PiAvr3a^{EM} did not (**Figure 3.4**). This not only demonstrates that this activity was retained by the N-terminal CFP fusions but also that, because the mutant PiAvr3a$^{KI/Y147del}$ does not interact or stabilise StCMPG1b, that StCMPG1b is not involved in R3a-mediated CD.

This Chapter describes evidence for the stabilisation of StCMPG1b by PiAvr3a as well as possible direct interaction. The stronger interaction with, and stabilisation of StCMPG1b by PiAvr3a^{KI}, is in accordance with the stronger suppression of ICD by this form of the effector (Bos *et al.*, 2006; 2009).

Chapter 4. The Role of CMPG1 During Infection

4.1 Introduction

From Chapter 3 it is evident that the interaction, whether direct or indirect, between StCMPG1 and PiAvr3a is active and results in the stabilisation of StCMPG1. The reason for this stabilisation is not clear although, in stabilising StCMPG1, PiAvr3a is preventing or altering its normal activity. This may include the degradation of itself and presumably, therefore, its substrates in the host cell, via the 26S proteasome (Bos *et al.*, 2010). The stabilisation occurs strongly with PiAvr3a^{KI} and less strongly with PiAvr3a^{EM}, which reflects the relative abilities of these effector forms to suppress INF1-triggered host CD (ICD; Bos *et al.*, 2006; 2009). The mutant PiAvr3a$^{KI/Y147del}$ form, which is unable to suppress ICD, does not interact with or stabilise StCMPG1 (Chapter 3; Bos *et al.*, 2010).

In addition to ICD, CD following the interaction between the Cf-9 resistance protein and *C. fulvum* Avr9 protein requires CMPG1 (González-Lamothe *et al.*, 2006). To gain confidence that the CD suppression of ICD by PiAvr3a was due to its stabilisation of CMPG1, it was important to investigate additional defence-associated CD recognition events, to see if they were CMPG1-dependent and suppressed by PiAvr3a. Moreover, it was important to determine the role that CMPG1 plays in the interaction between *P. infestans* and its host plants.

4.1.1 Chapter 4 Aims and Objectives

The objective for the work performed in this chapter was to build on the conclusions from Chapter 3. The aims were two-fold:

i. Attempt to relate the interaction of StCMPG1 and PiAvr3a with a variety of host-disease resistance mechanisms.

ii. Investigate if StCMPG1 is a target for *P. infestans* during infection and observe the effect the absence of CMPG1 has on infection.

4.2 Results

4.2.1 The Use of VIGS and *N. benthamiana* to Determine the Role of CMPG1 in Defence.

Much of the work undergone in Chapter 4 involved the use of VIGS. This gene silencing technique is used throughout plant science to investigate plant gene function. VIGS was used over other gene silencing techniques because it is rapid and transient, requiring no plant transformation and avoiding the problems of lethality due to knock down of essential genes. Many years have been spent refining the experimental protocol, especially for functional analyses within the *Solanaceae*, where there are a lack of gene knock-out approaches (Lu *et al.*, 2003; Burch-Smith *et al.*, 2004). It was therefore a logical option for the gene function investigations in this Chapter.

N. benthamiana was chosen for this project as it grows quickly, has a short life cycle, and is a host plant for important *Solanaceous* pathogens such as *P. infestans*. *N. benthamiana* has been shown to be viable for VIGS and has more pronounced symptoms compared to other species when used in conjunction with VIGS (Lu *et al.* 2003; Burch-Smith *et al.*, 2004).

4.2.2 Constructs

Prior to experiments being performed, *Tobacco Rattle Virus* (TRV) constructs were made for VIGS of NbCMPG1 to investigate the objectives for Chapter 4 (**Figure 4.1**; 2.9 VIGS).

Figure 4.1A is a diagrammatical representation of the pYL192 RNA1 vector that is a component of the bipartite TRV vector (RNA1: RNA2 infiltrated at 1:1 ratio) used for VIGS in *N. benthamiana*. **Figure 4.1B** is a diagram of the RNA2 vector pYL156. This vector contains the Multiple Cloning Site (MCS) for the fragment of the gene to be silenced (Gilroy *et al.*, 2007). In this case, the gene of interest was *NbCMPG1* and *GFP* was used as a control. Two constructs for *NbCMPG1* were made using different fragments of the gene to ensure only the gene of interest was silenced effectively. **Figure 4.1C** is a diagram of *CMPG1* showing the relative position of the U-box-encoding region, as well as the regions cloned in anti-sense to create the silencing vector constructs (labelled "*CMPG1I*" & "*CMPG1II*"). Above these are indicated the original regions used to create an RNAi tobacco line by González-Lamothe *et al.*, (2006). Arrows show the region of CMPG1 where qRT-PCR primers were made to confirm gene silencing in VIGSed *N. benthamiana* (See Appendix A1 for details).

4.2.3 Primers and Optimisation

Figure 4.1 Schematic Representations of the Constructs used for VIGS in *N. benthamiana*.

A. RNA1 vector pYL192 used as part of VIGS in a 1:1 ratio (OD_{600} 1.0 with a final of 0.5; RNA1:RNA2) where RNA2 contains the anti-sense silencing construct fragment of interest. The 2x*35S* promoter is shown. (Gilroy *et al*., 2007).

B. RNA2 vector pYL156 used as part of VIGS in a 1:1 ratio RNA1:RNA2 where RNA2 contains the anti-sense silencing construct fragment of interest. The fragment used originated from the gene *NbCMPG1*. The vector contains a 2x *35S* promoter region. (Gilroy *et al*., 2007)

C. Diagrammatical representation of *NbCMPG1* showing the relative locations of the primers (arrows labelled 1-4 representing RTS1, RTS2, RTS3 and RTS4 respectively; See Appendix for details) used to confirm gene silencing (shown using arrows) and the fragment used to construct the RNAi transgenic *N. tobacum* (line labelled "NtRNAi"; González-Lamothe *et al*, 2006). The region used to achieve VIGS is also labelled "*CMPG1I*" and "*CMPG1II*" (Bos *et al*., 2010).

A

pYL192
19370 bp

RB

2X35S promoter

134K

194K

MP

16K

Rz

NOS terminator

LB

B

pYL156
9663 bp

LB

2X35S

CP

MCS

*Eco*RI (2417)

*Xba*I (2423)

*Stu*I (2431)

*Nco*I (2435)

*Bam*HI (2441)

*Kpn*I (2451)

*Sac*I (2457)

*Mlu*I (2459)

*Xho*I (2465)

*Sma*I (2474)

Rz

NOS terminator

RB

C

NtRNAi

183   631

1 89   350   603

NbCMPG1

CMPG1I   CMPG1II

1   2   3   4
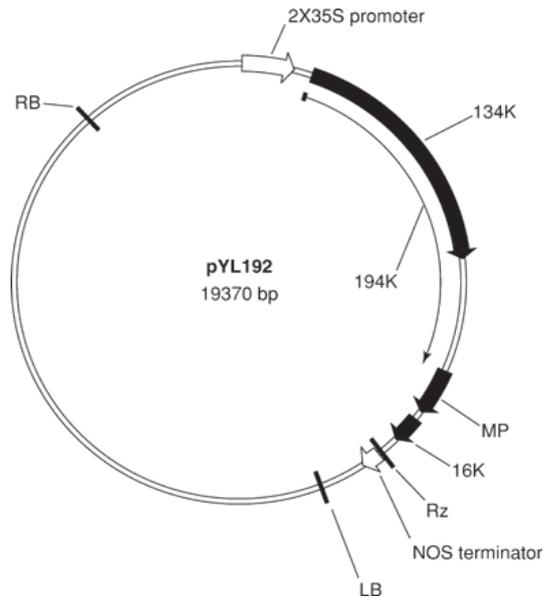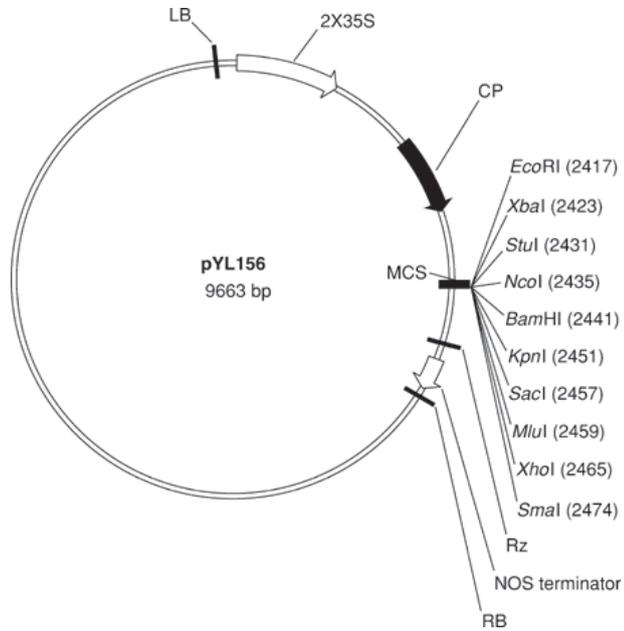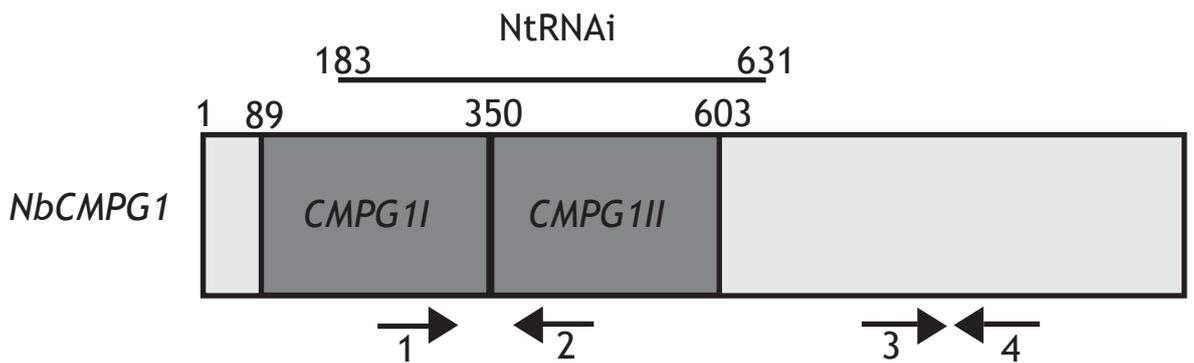
To confirm that gene silencing was occurring in the VIGSed *N. benthamiana* plants, a melting curve analysis was performed on qRT-PCR primer pairs RTS1/RTS2 and RTS3/RTS4 to ascertain the most reliable and consistent pair to use (**Figure 4.2A&B**; RTS1/RTS2 and RTS3/RTS4 respectively; 2.9 VIGS). From the graphs it can be seen that there is more than one peak for RTS3/RTS4. This means the primers are not specific for the region originally designed to anneal to and, therefore, are unsuitable due to a lack of specificity. RTS1/RTS2 have one peak and, therefore, one product. RTS1/RTS2 are only attaching to a product of expected size and were thus used in this study.

Figure 4.2C summarises the mean C(t) value and standard deviation for different dilutions of cDNA. The most suitable concentration of *N. benthamiana* cDNA to use is that with the lowest C(t) value and lowest standard deviation. In this case, it was a 1/10 dilution. This was used to analyse leaf samples for their silencing efficiency.

4.2.4 Assessment of the levels of silencing of *NbCMPG1* in VIGSed *N. benthamiana*

The efficiency of silencing for both vectors, TRV::*NbCMPG1 I* and TRV::*NbCMPG1 II* was assessed 4-5 weeks after their inoculation into *N. benthamiana*, and compared to levels after inoculation of the TRV::*GFP* control using qRT-PCR primers RTS1/RTS2 (**Figure 4.3**). TRV::*GFP* was used as a control to confirm the vector and the infiltration technique was not causing a silencing effect on the gene in question . TRV::*GFP* provided qRT-PCR data for comparison to the *NbCMPG1*-silenced plants. TRV::*GFP* was used to compare any physical growth differences in the various silenced plants. Of which there were none. *GFP* is a gene not present in plants naturally and has been used previously as a silencing control (Gilroy *et al.*, 2007). It was therefore a good control candidate for this work. It can be seen that in the VIGSed plants there is reduced *NbCMPG1* expression compared to the TRV::*GFP* control. Error bars for the replicate values show an overlap for silencing with TRV::*NbCMPG1I* and the GFP control. This could be due to the very low (uninduced) levels of *NbCMPG1* in the plant naturally, generating considerable variation in the *GFP* control plants. Nevertheless, it would still appear that *NbCMPG1* is silenced by both constructs. Having two independent VIGS *NbCMPG1* silencing constructs helps to eradicate any anomalous results.

4.2.5 There is Less Avr9/Cf-9 HR in *N. benthamiana NbCMPG1* Silenced Plants

To confirm the previous observation that CMPG1 is required for PCD triggered by the interaction between tomato Cf-9 R protein and Avr9 from *C. fulvum* (González-Lamothe *et al.*, 2006), *N. benthamiana NbCMPG1* silenced plants were infiltrated with a 1:1 ratio of *Avr9:Cf-9 (*2.8 *In Planta* Protein Expression & 2.10

Figure 4.2 A summary of the qRT-PCR cDNA primer optimisation for the primers RTS1/RTS2 and RTS3/RTS4 (See Appendix). And cDNA for N. benthamiana VIGS silencing conformation.

A. Graph obtained from the melting curve analysis for qRT-PCR primer optimisation for primers RTS1/RTS2 showing the fluorescence peak produced during the qRT-PCR run.

B. Graph obtained from the melting curve analysis for qRT-PCR primer optimisation for primers RTS3/RTS4 showing the fluorescence peaks produced during the qRT-PCR run.

C. Table shows the cDNA dilution, concentration (ng), Mean C(t) value and standard deviation for the cDNA obtained from RNA from VIGS inoculated *N. benthamiana*. Highlighted in grey is the cDNA concentration (µg/µL) with the lowest C(t) and the lowest standard deviation. This dilution was used to confirm silencing with qRT-PCR for *NbCMPG1* VIGS.

A

RTS1/RTS2

B

RTS3/RTS4
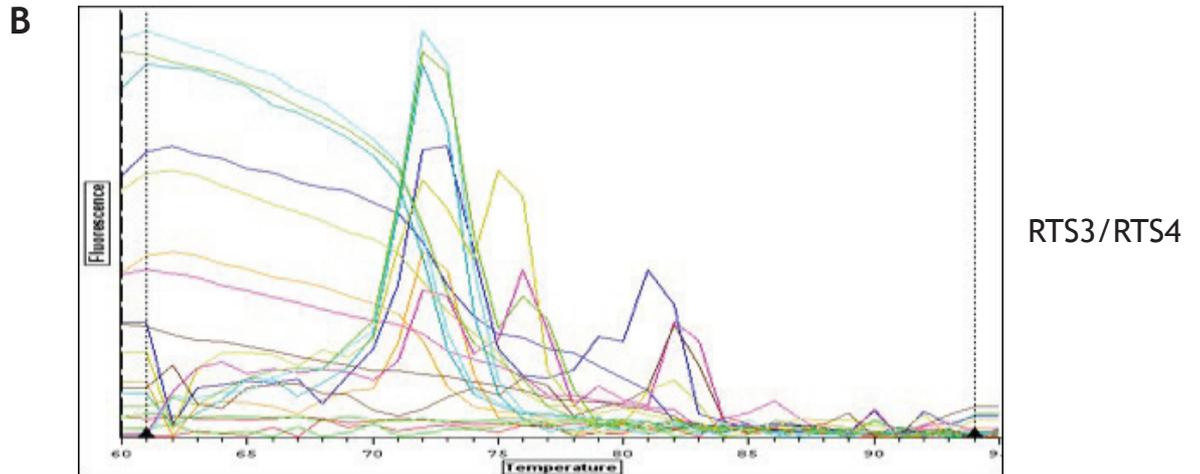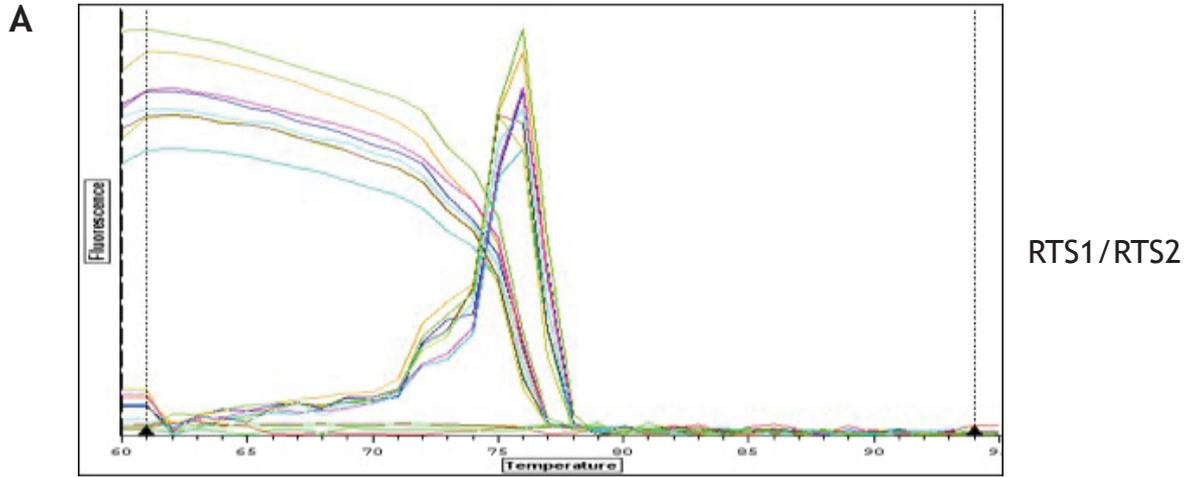
C

cDNA Dilution	cDNA (ng)	Average Ct	StDev
1/5	1.000	28.51	0.64
1/7.5	0.667	28.98	0.18
1/10	0.500	28.84	0.43
1/15	0.333	29.37	0.93
1/20	0.250	30.46	0.57
1/30	0.167	30.24	0.14
1/40	0.125	31.15	0.75

Figure 4.3 Bar graph depicting the relative silencing efficiency of the pYL156::NbCMPG1 I and pYL156::NbCMPG1 II VIGS constructs relative to the pYL156::GFP control.

Error bars are shown for each VIGS construct. RNA was extracted from VIGS infiltrated *N. benthamiana* 4-5 weeks post-infiltration. cDNA was made from the RNA and used in qRT-PCR. Primers used for the qRT-PCR were RTS1/RTS2. The values represent the average of 3 independent leaf replicates and the qRT-PCR control gene used as a comparison was 25S and random hexamer primers (Gilroy *et al.*, 2007). Error bars (+/-) were calculated using Standard Deviation divided by the square route of the population (n).
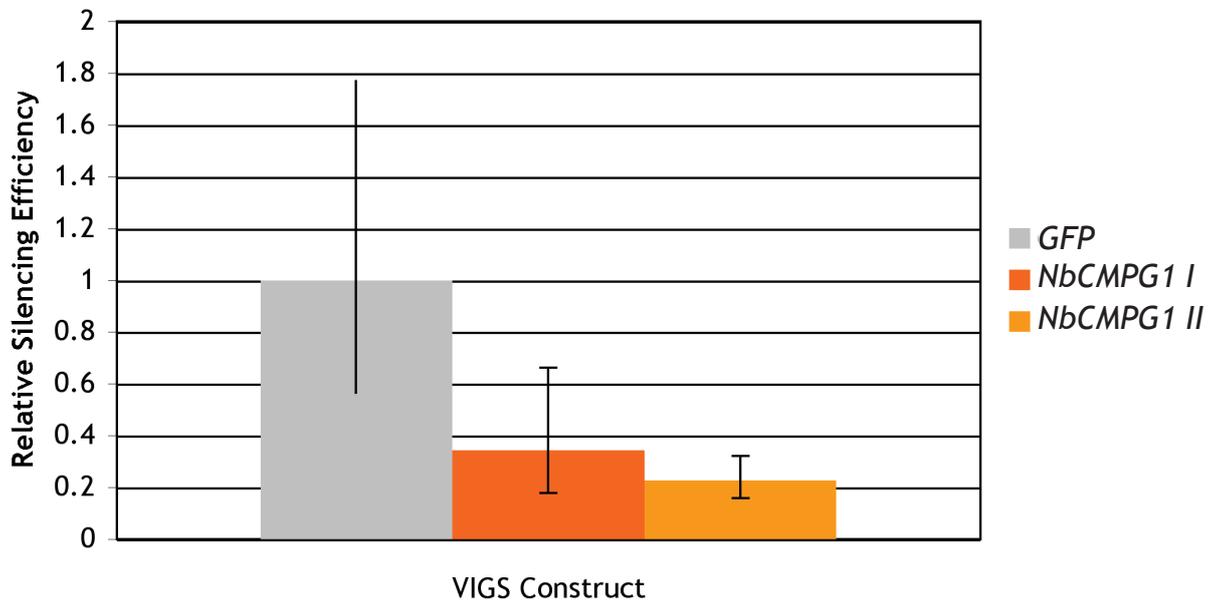
Plant Pathology Treatments). Representative images from the experiments are shown in **Figure 4.4A**. From the GFP control, it can be seen there is Avr9/Cf-9-induced HR throughout the infiltrated site. For both *NbCMPG1* VIGSed plants there is significantly reduced Avr9/Cf-9 HR. To confirm this observation percentage HR was recorded and the means for three replicate experiments, with standard errors, are shown in the bar graph in **Figure 4.4B**. The levels of Avr9/Cf-9 HR were similar between *NbCMPG1* silenced plants and significantly reduced when compared to the *GFP* control (**Figure 4.4B**).

Figure 4.4 provides evidence that CMPG1 is required for Cf9/Avr9-mediated HR. However, it was still unknown whether PiAvr3a could suppress this CD.

4.2.6 There is a Decrease in Avr9/Cf-9 HR in the Presence of PiAvr3a in *Cf-9* Transgenic *N. tabacum*

To investigate whether PiAvr3a can suppress the Avr9/Cf-9 HR, Cf-9 transgenic *N. tabacum* was infiltrated with pEarley203::*PiAvr3a^{KI}*, pEarley203::*PiAvr3a^{EM}*, pEarley203::*PiAvr3a$^{KI/Y147del}$* and pGWB6::*GFP* (infiltration control; 2.8 *In Planta* Protein Expression & 2.10 Plant Pathology Treatments) at an OD$_{600}$ of 0.2. After 3 days post-inoculation, a 1/40 dilution of Avr9 peptide was spot infiltrated and after 2-3 days the HR spots were counted and recorded for each construct (**Figure 4.5A&B**).

Figure 4.5A shows images taken for one of the 3 replicate experiments and shows what was seen consistently over the replicates. It can be seen that there are little Avr9/Cf-9 induced HRs for the leaves infiltrated with *PiAvr3a^{KI}* and *PiAvr3a^{EM}*. For leaves infiltrated with *PiAvr3a$^{KI/Y147del}$* and the *GFP* control there are Avr9/Cf-9 HRs throughout the infiltrated zones. The Avr9/Cf-9 HR spots were counted (**Figure 4.5B**). The mean percentage Avr9/Cf-9 HRs for 3 replicated experiments show there are less Avr9/Cf-9 induced HRs for the leaves infiltrated with PiAvr3a^{KI} and PiAvr3a^{EM} (6% and 26% of infiltration zones, respectively). For leaves infiltrated with PiAvr3a$^{KI/Y147del}$ and the GFP control there were similar high levels of Avr9/Cf-9 HRs (77% and 79%, respectively). Error bars for PiAvr3a^{EM} and PiAvr3a^{KI} show no overlap and, therefore, there are differences between the amounts of HRs seen for these constructs, which are significantly less than the PiAvr3a$^{KI/Y147del}$ and GFP controls. The error bars for PiAvr3a$^{KI/Y147del}$ and GFP control overlapped showing no difference between the amounts of Avr9/Cf-9 HR seen for either (**Figure 4.5B**). These results showed a similar pattern to that observed for suppression of ICD by PiAvr3a forms (Bos *et al.*, 2009).

4.2.7 *N. benthamiana* NbCMPG1-Silenced Plants have Reduced Avr4/Cf-4 HR
To observe if the results in 4.2.5 were also true to another Cf-resistance response,

Figure 4.4 The effect on Avr9/Cf-9 HR by VIGS *pYL156::NbCMPG1 I* and *pYL156::NbCMPG1 II* compared to a VIGS *pYL156::GFP* control.
A. Photographs of the Avr9/Cf-9 HR on the *N. benthamiana* leaf surface for the 2 VIGSed constructs and a GFP control. Photographs represent what was consistently seen over 3 experimental replicates and white dashed circles show the areas infiltrated. (Gilroy *et al.*, 2011)

B. Bar graph of mean percentage Avr9/Cf-9 HR counted on the 2 VIGSed constructs and a *GFP* control. The mean represents 3 experimental replicates and error bars are shown for the Avr9/Cf-9 HR with each construct. Error bars (+/-) were calculated using Standard Deviation divided by the square route of the population (n). (Gilroy *et al.*, 2011)

A

GFP   *NbCMPG1 I*   *NbCMPG1 II*
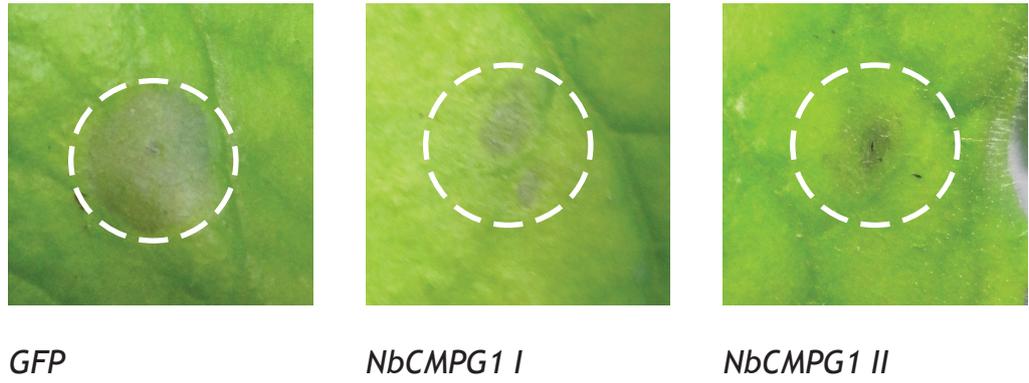
B
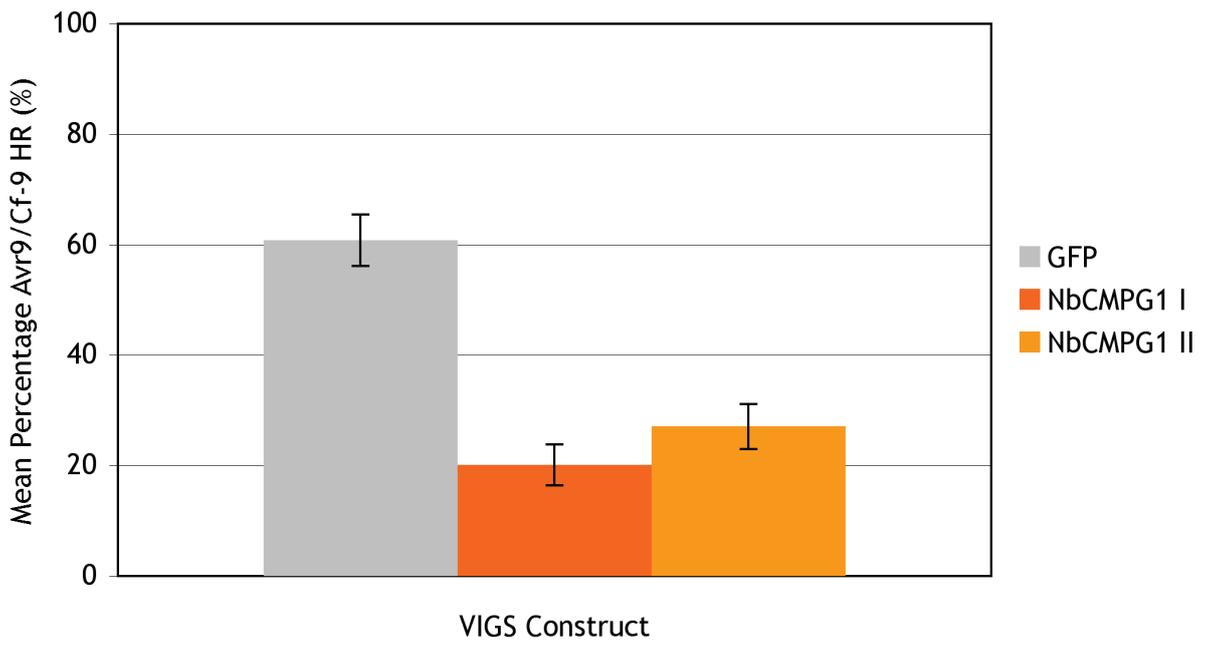
Figure 4.5 Effect of PiAvr3a on the HR produced by Avr9 peptide on *Cf-9* transgenic *N. tabacum* compared to *pGWB6::GFP* control.

A. Photographs of *Cf-9* transgenic *N. tabacum* infiltrated with *Agrobacterium* strains delivering pEarley203::*PiAvr3a^{KI}*, pEarley203::*PiAvr3a^{EM}*, pEarley203::*PiAvr3a$^{KI/Y147del}$* and pGWB6::*GFP* individually at OD$_{600}$ 0.2 and 3 days later infiltrated with Avr9 peptide (1/40 dilution). Avr9/Cf-9 HR was visible between 48-36 Hours post-peptide infiltration. The photographs represent what was seen over 3 experimental replications. (Gilroy *et al.*, 2011)

B. Bar graph of mean percentage HR of Avr9 peptide for each of the expression constructs infiltrated into *Cf-9* transgenic *N. tabacum*. The mean was made from 3 biological experimental replications and error bars (+/- SE) for each construct's Avr9 peptides HR are shown. Error bars (+/-) were calculated using Standard Deviation divided by the square route of the population (n). (Gilroy *et al.*, 2011)

A

PiAvr3a^{KI} PiAvr3a^{EM} PiAvr3a$^{KI/Y147del}$ GFP
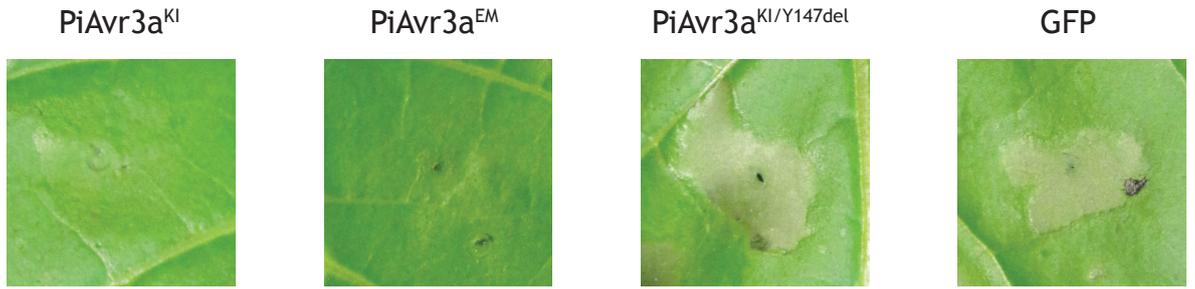
B
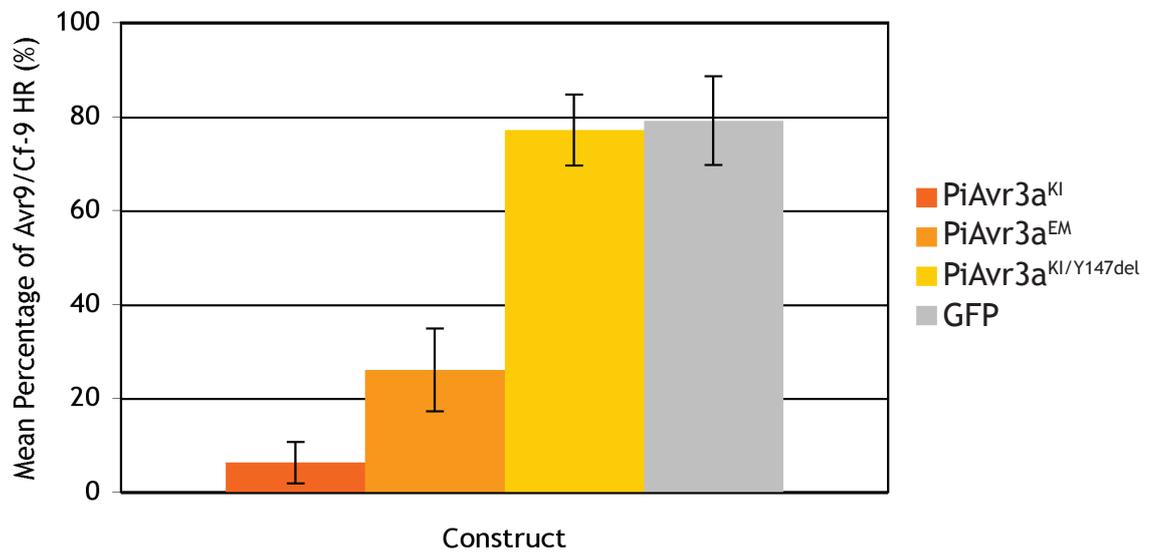
N. benthamiana NbCMPG1 silenced plants were infiltrated with a 1:1 ratio of Avr4:Cf-4 (2.8 *In planta* Protein Expression & 2.10 Plant Pathology Treatments). Representative images for one experimental replicate are shown in **Figure 4.6A**. For the *GFP* control there is Avr4/Cf-4 induced HR throughout the infiltrated site. In comparison, for the *NbCMPG1* VIGSed plants there is reduced Avr4/Cf-4 HR. To confirm this, percentage Avr4/Cf-4 HR was recorded and a mean for three replicate experiments are shown in the bar graph in **Figure 4.6B**. There is similar, significantly reduced Avr4/Cf-4 HR in *NbCMPG1* VIGSed plants compared to the *GFP* control.

This result provides evidence that CMPG1 is required for the Avr4/Cf-4 HR in addition to the Avr9/Cf-9 HR. Future work for this was to investigate whether PiAvr3a forms are able to suppress Cf-4-mediated HR. This work was completed by Dr E Gilroy (SCRI, Dundee, U.K) after I had left the laboratory and found, as predicted, PiAvr3a^{KI} and PiAvr3a^{EM}, but not the PiAvr3a$^{KI/Y147del}$ mutant, were able to suppress Cf-4-mediated CD (see Final Discussion).

4.2.8 *NbCMPG1* is Up-regulated During *Erwinia amylovora* Non-host HR

Having established that CMPG1 is involved in Cf-mediated HR the investigation was extended to a non-host resistance response, the HR triggered in *N. benthamiana* by *Erwinia amylovora* (Eam; Gilroy *et al.*, 2007; Oh *et al.*, 2007). The expression of *NbCMPG1* during *E. amylovora* infection was investigated across a time-course, following *N. benthamiana* infiltratration with *E. amylovora*, up to and including 24 Hours, the point at which a visible, confluent HR can be detected (Gilroy *et al.*, 2007; 2.8 *In planta* Protein Expression, 2.9 VIGS & 2.10 Plant Pathology Treatments). QRT-PCR was performed using primers RTS1 and RTS2. The graph in **Figure 4.7A** shows normalised values obtained relative to 0 hpi. Two distinct peaks of *NbCMPG1* up-regulation were seen, a 100-fold increase after 1 hpi and a 225-fold increase at 24 hpi, at the onset of the HR. Little *NbCMPG1* expression was detected at other time points. The graph implies that NbCMPG1 is required not only during the initial stages of the plant response but also in the later stages. This experiment was only attempted once. Nevertheless, the two distinct peaks of up-regulation were dramatic and thus likely to be reproducible.

4.2.9 *N. benthamiana NbCMPG1* Silenced Plants Show Reduced *E. amylovora* HR

N. benthamiana plants expressing TRV::*GFP* control, or TRV::*NbCMPG1 I* and *II* constructs, were infiltrated with *E. amylovora (*2.8 *In planta* Protein Expression, 2.9 VIGS & 2.10 Plant Pathology Treatments. **Figure 4.7B** shows images of the *E. amylovora* infiltration zones 48 hpi of control and VIGSed *N. benthamiana* plants. It can be seen that there is more *E. amylovora* HR with the TRV::*GFP* control

Figure 4.6 The effect on Avr4/Cf-4 HR by VIGS *pYL156::NbCMPG1 I* and *pYL156::NbCMPG1 II* compared to a VIGS *pYL156::GFP* control.
A. Photographs of the Avr4/Cf-4 HR on the *N. benthamiana* leaf surface for the 2 VIGSed constructs and GFP control. Photographs represent what was consistently seen over 3 experimental replicates. (Gilroy *et al.*, 2011)

B. Bar graph of mean percentage Avr4/Cf-4 HR counted on the 2 VIGSed constructs and a GFP control. The mean represents 3 experimental replicates and error bars are shown for each construct's Avr4/Cf-4 HR. Error bars (+/-) were calculated using Standard Deviation divided by the square route of the population (n). (Gilroy *et al.*, 2011)

A

GFP　　　　　*NbCMPG1 I*　　　　　*NbCMPG1 II*
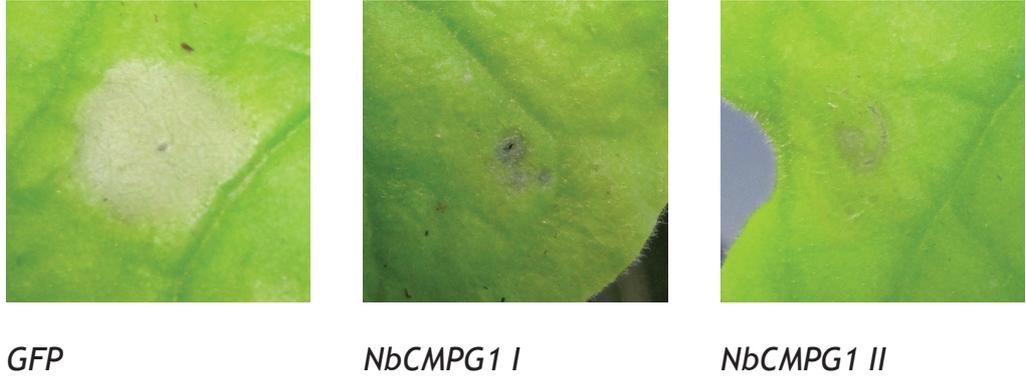
B
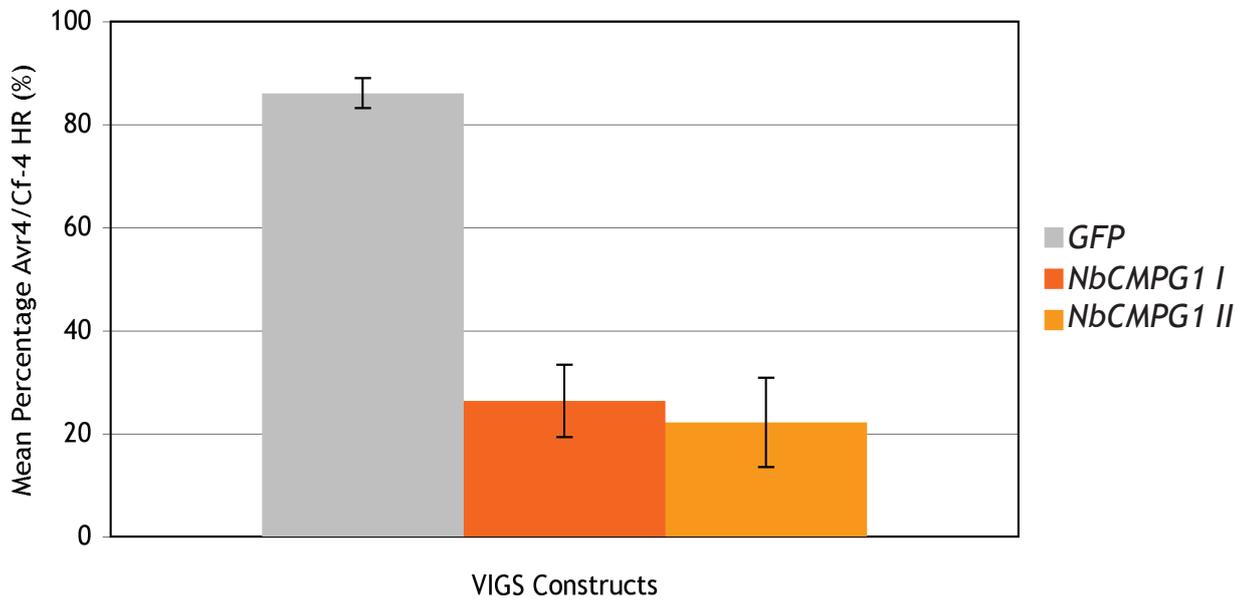
Figure 4.7 The effect on *E*. *amylovora* HR by VIGS using *pYL156::NbCMPG1 I* and *pYL156::NbCMPG1 II* compared to a VIGS *pYL156::GFP* control.
A. Bar graph of a time course obtained over 24 Hours using qRT-PCR. Error bars for each time point are shown. RNA was obtained from VIGS pYL156::*GFP N. benthamiana* infected with *E. amylovora* and cDNA obtained from the RNA for qRT-PCR analysis. The Y-axis is relative to 0 Hours *NbCMPG1* expression and was obtained using primers RTS1 and RTS2. The graph shows one experimental replicate (with 3 technical replicates to remove experimental error). Error bars (+/-) were calculated using Standard Deviation divided by the square route of the population (n).

B. Photographs of the *E. amylovora* HR on the *N. benthamiana* leaf surface for the 2 VIGSed constructs and a *GFP* control. Photographs represent what was consistently seen over 3 experimental replications.

C. Bar graph of mean percentage *E. amylovora* HR counted on the 2 VIGSed constructs and *GFP* control. The mean represents 3 experimental replicates and error bars are shown for each VIGSed construct's *E. amylovora* HR and *GFP* control. Error bars (+/-) were calculated using Standard Deviation divided by the square route of the population (n).

A

TRV::*GFP*

B

GFP   *NbCMPG1 I*   *NbCMPG1 II*

C
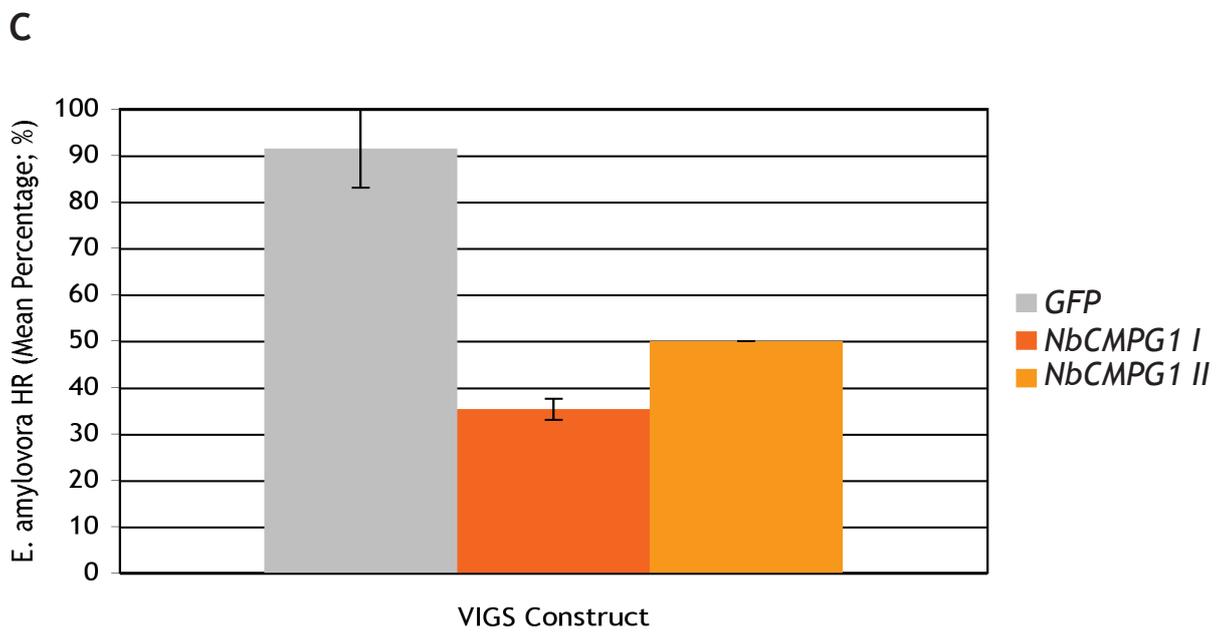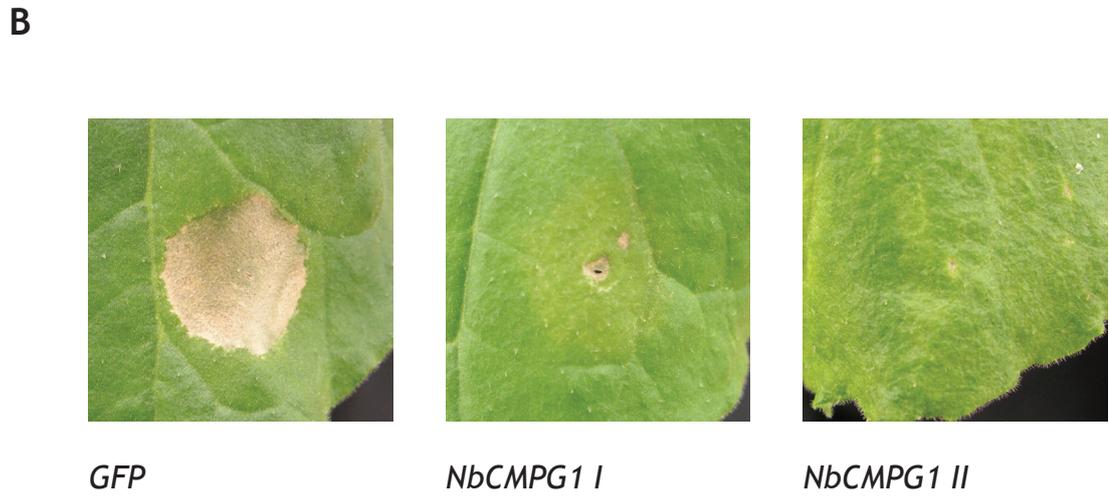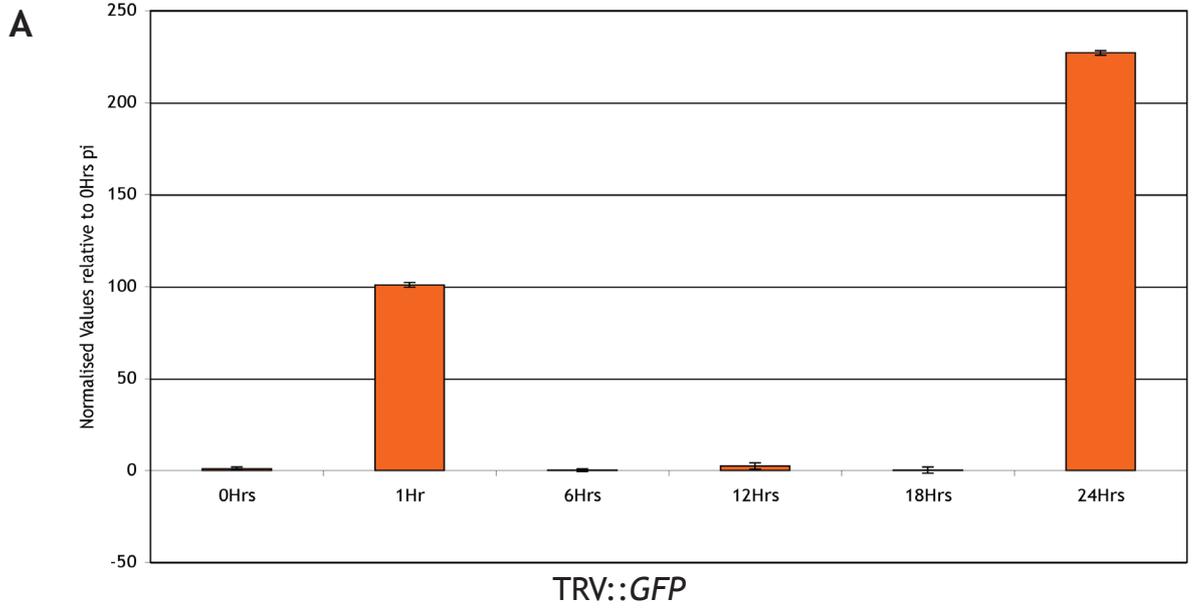
compared to TRV::*NbCMPG1 I* and TRV::*NbCMPG1 II* plants. This visual result was quantified over 3 replicate experiments, counting infiltration zones showing confluent HR. The Mean Percentage (%) *E. amylovora* HRs for the different plants over 3 replicate experiments are shown in **Figure 4.7C**. From this experiment, it is apparent that *N. benthamiana* requires NbCMPG1 to mount an HR when infiltrated by *E. amylovora*.

4.2.10 In *N. benthamiana* there is a Decrease in *E. amylovora* Induced HR in the Presence of PiAvr3a

To see if PiAvr3a was able to suppress *E. amylovora* HR, *N. benthamiana* was infiltrated with *Agrobacterium* delivering pEarley203::*PiAvr3a^{KI}*, pEarley203::*PiAvr3a^{EM}*, pEarley203::*PiAvr3a^{KI/Y147del}* and pGWB6::*GFP* (infiltration control) at an OD$_{600}$ of 0.2 (2.8 *In planta* Protein Expression & 2.10 Plant Pathology Treatments). After 3 days post-inoculation, *E. amylovora* was infiltrated over these zones. Zones showing HR were counted and recorded for each construct. The results for this work are shown in **Figure 4.8A&B**.

Images shown in **Figure 4.8A** are a representation of the plant responses seen in all 3 replicate experiments. The *E. amylovora* HR zones were counted and represented in a graph (**Figure 4.9B**). There were few *E. amylovora*-induced HRs on leaves expressing with *PiAvr3a^{KI}* or *PiAvr3a^{EM}*. However, in the case of leaves expressing *PiAvr3a^{KI/Y147del}* or the *GFP* control, *E. amylovora* HRs were seen in the majority of cases. These results are similar to those for ICD suppression (Bos *et al.*, 2009) and Avr9/Cf-9 HR suppression (above), and indicate a further CMPG1-dependent CD that is suppressed strongly by PiAvr3a^{KI}, weakly by PiAvr3a^{EM}, and not at all by the PiAvr3a^{KI/Y147del} mutant form.

4.2.11 There is Reduced *P. infestans* Sporulation and Growth During the Necrotropic Phase of Infection on *N. benthamiana NbCMPG1*-Silenced Plants

In addition to assessing the role of CMPG1 in defence responses leading to CD, it was important also to investigate the roles CMPG1 and PiAvr3a may play during a compatible *P. infestans*-host interaction. *N. benthamiana* plants silenced with the two TRV::*NbCMPG1* VIGS constructs were inoculated with *P. infestans* and lesion size and sporulation were monitored throughout the infections cycle (**Figure 4.9A-D;** 2.8 *In planta* Protein Expression, 2.9 VIGS & 2.10 Plant Pathology Treatments). **Figure 4.9A** shows a qRT-PCR analysis of NbCMPG1 expression across a time course from 1–5 days post-infiltration (dpi), relative to day 0. *NbCMPG1* transcripts accumulated to a level 9-fold higher at 3 dpi than at time 0, before decreasing at 4–5 dpi. This indicates a tightly regulated peak of induction at 3 dpi and provides evidence that CMPG1 is potentially involved in PTI during biotrophy and PCD, the necrotrophic phase of infection (Bos *et al.*, 2010). **Figure 4.9B** shows

Figure 4.8 Effect of PiAvr3a on the HR produced on *N. tabacum* by *E. amylovora* compared to *pGWB6*::*GFP* control.

A. Photographs of *N. tabacum* infiltrated with pEarley203::*PiAvr3a^{KI}*, pEarley203::*PiAvr3a^{EM}*, pEarley203::*PiAvr3a$^{KI/Y147del}$* and pGWB6::*GFP* individually at OD_{600} 0.2 and after 3 days, infiltrated with *E. amylovora* (OD_{600} 0.01). HR was visible between 48-36 hpi with *E. amylovora*. Photographs represent what was seen for 3 experimental replicates.

B. Bar graph of mean percentage HR of *E. amylovora* for each of the plant expression constructs infiltrated. The mean consists of 3 experimental replicates and error bars for the construct's *E. amylovora* HR are shown. Error bars (+/-) were calculated using Standard Deviation divided by the square route of the population (n).

A

| PiAvr3a^{KI} | PiAvr3a^{EM} | PiAvr3a$^{KI/Y147del}$ | GFP |

B
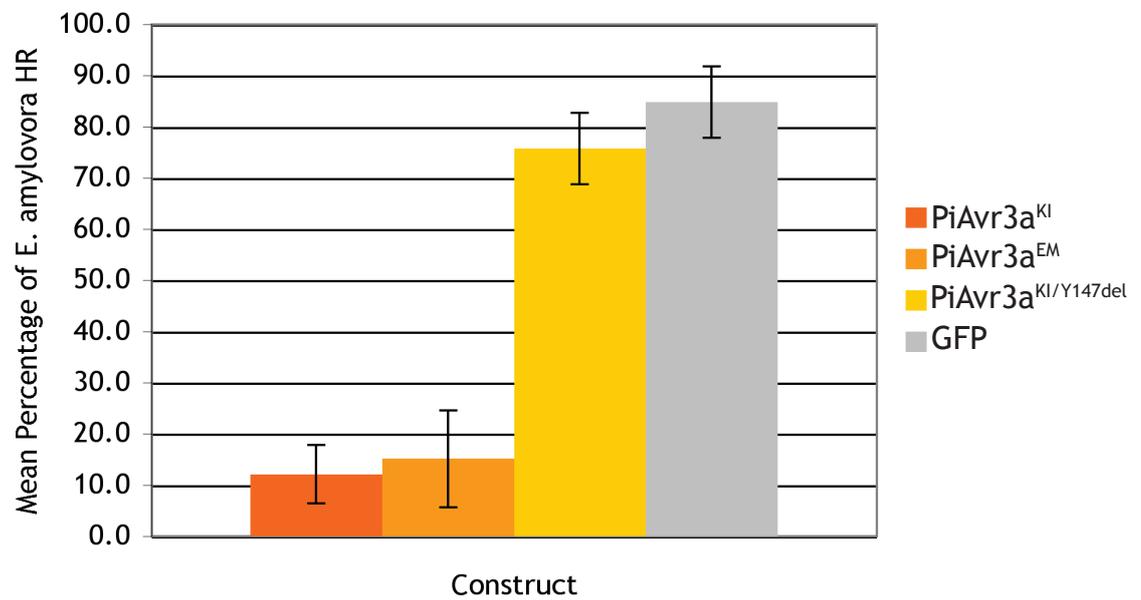
Figure 4.9 The effect on *P. infestans* (strain 88069; PiAvr3a^{EM} homozygote) sporalation HR by VIGS *pYL156::NbCMPG1 I* and *pYL156::NbCMPG1 II* compared to VIGS *pYL156::GFP* control.

Three replicate experiments were performed.

A. Real-time RT-PCR analysis of NbCMPG1 expression across a time course from 1–5 dpi, relative to day 0 (sampled 5 Minutes after inoculation of *P. infestans* sporangia/zoospores), which was given a value of 1. NbCMPG1 transcripts accumulated to a level 9-fold higher at 3 dpi than at time 0, before decreasing at 4–5 dpi, indicating a tightly regulated peak of induction at 3 dpi. Error bars (+/-) were calculated using Standard Deviation divided by the square route of the population (n). (Bos *et al.*, 2010).

B. Photographs of *P. infestans* sporulation on the *N. benthaminana* leaf surface for the 2 VIGSed constructs and a *GFP* control, including trypan blue staining (below) 5-7 dpi. (Bos *et al.*, 2010)
Bi Photographs of leaf images.
Bii Photographs of the corresponding leaf after trypan blue staining to visualise the HR.

C. Bar graph of mean percentage *P. infestans* HR counted on the 2 VIGSed constructs and a *GFP* control. Error bars are shown for each construct's *E. amylovora* HR. Error bars (+/-) were calculated using Standard Deviation divided by the square route of the population (n).

D. Bar graph of a sporulation pattern diameter (mm) for the infection. Error bars for each constructs sporulation diameter are shown. Error bars (+/-) were calculated using Standard Deviation divided by the square route of the population (n).

A

Bi GFP   NbCMPG1 I   NbCMPG1 II

ii

C

D
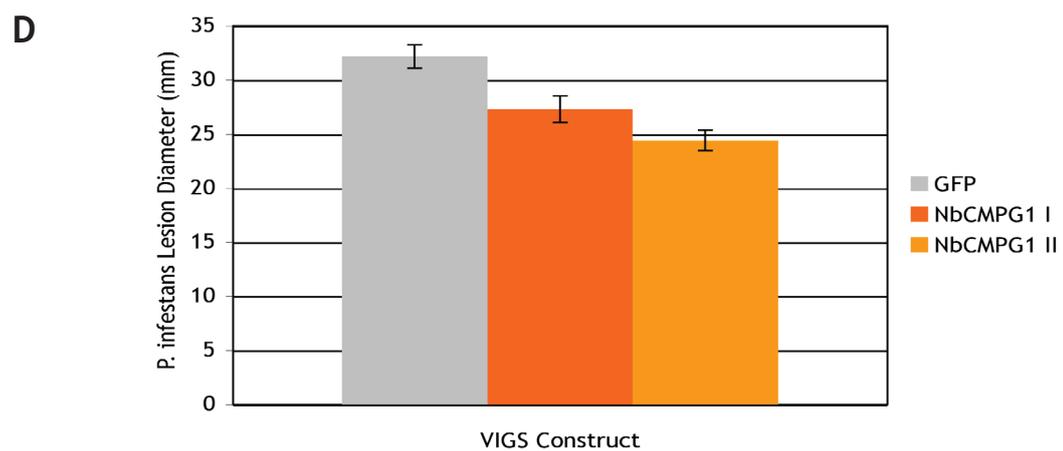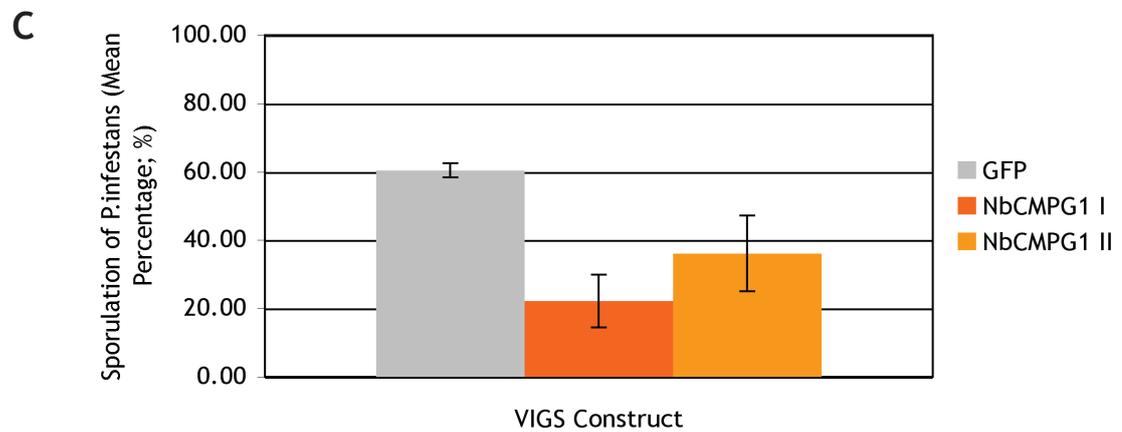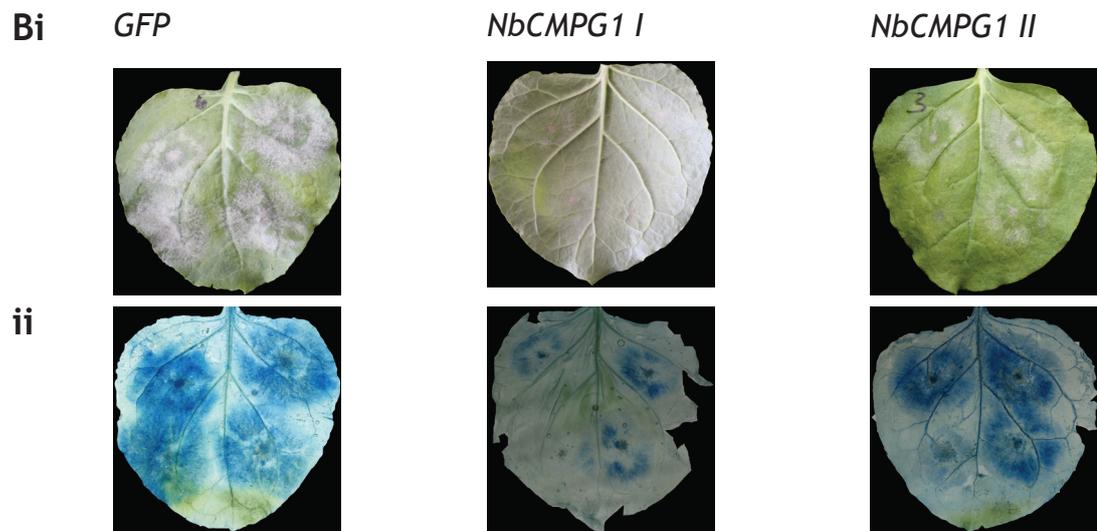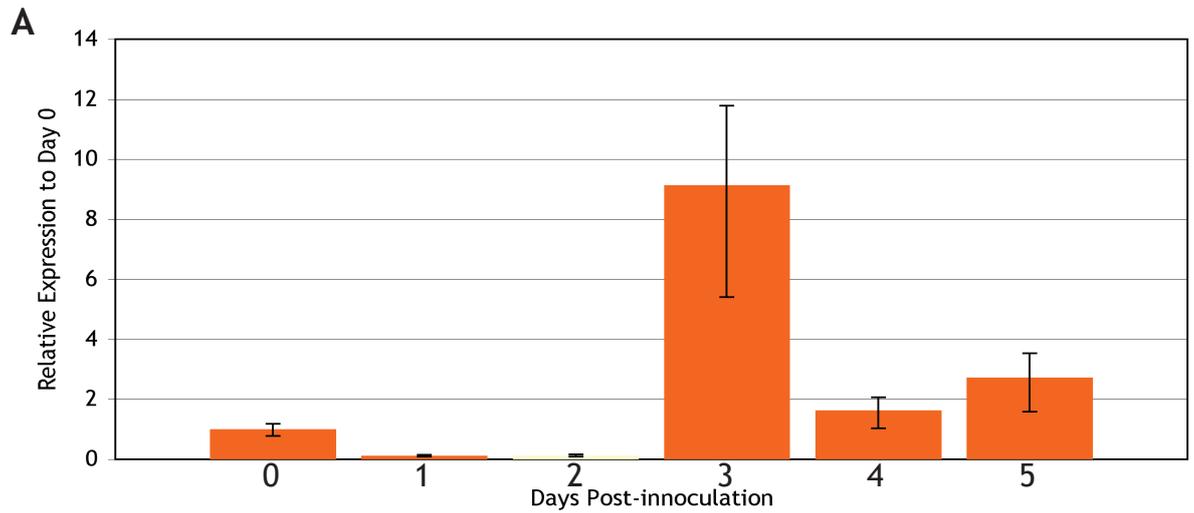
images taken for one of the experimental replicates and represent what was seen over 3 replicates. The images show there is more *P. infestans* sporulation on the TRV::*GFP* control plants compared to the TRV::*NbCMPG1 I* and TRV::*NbCMPG1 II* silenced plants. The graph in **Figure 4.9C** shows mean percentage of infection sites showing typical, normal levels of *P. infestans* sporulation. The TRV::*GFP* control showed 60.42% of infection sites produced clear, visible sporulation, whereas TRV::*NbCMPG1 I* and *TRV::NbCMPG1 II* silenced plants showed only 22.22% and 36.11% sporulating sites, respectively. Error bars showed there was no significant difference between the *NbCMPG1* silenced plants but they were significantly different to the *GFP* control.

To confirm if there was a difference in lesion size the diameters (mm) of lesions on the NbCMPG1 silenced plants were measured (**Figure 4.9D**). There was a statistically significant reduction in the lesion diameter on the *NbCMPG1* silenced plants compared to the *GFP* controls. The *GFP* control has a mean lesion diameter of 32.18mm whereas the *NbCMPG1 I* and *NbCMPG1 II* silenced plants have a reduced mean diameter of 27.32mm and 24.41mm respectively. Error bars produced no overlap between both the *NbCMPG1* silenced lines and the *GFP* controls showing the results were consistent and reliable between the control plants and the *NbCMPG1* silenced plants. These data show, surprisingly, that *P. infestans* (isolate 88069) requires CMPG1 to produce normal sporulating lesions in the necrotrophic stage of infection. CMPG1 is therefore required for the *P. infestans*'s (88069) infection cycle. *P. infestans* 88069 is an *PiAvr3a^{EM}* homozygote. Experiments were attempted with the *P. infestans* Ca65 isolate, which is a *PiAvr3a^{KI}* homozygote. However, the Ca65 isolate proved to be a poor pathogen and no conclusive or reliable data were obtained (data not shown).

4.2.12 In *N. benthamiana NbCMPG1* Silenced Plants there is More PiAvr3a^{KI} Induced HR When Co-expressed with R3a

The *NbCMPG1* VIGSed *R3a* transgenic *N. benthamiana* plants were infiltrated with *Agrobacterium* delivered *PiAvr3a^{KI}* in the pGRAB vector and the amount of HR recorded (2.8 *In planta* Protein Expression & 2.9 VIGS). The Mean Percentage R3a HR (%) for each VIGSed construct is shown in the bar graph in **Figure 4.10**. From the bar graph it can be seen that the *GFP* control had a Mean Percentage R3a HR of 68.03%. The *NbCMPG1 I* and *NbCMPG1 II* VIGSed plants had a mean percentage of 93.30% and 100.00% respectively. The error bars for the different VIGSed constructs show no over lap (NbCMPG1II did not have an error bar as all the values for all the replicate experiments gave a value of 100.00%). This shows that there is increased HR between the *GFP* control and the *NbCMPG1* silenced plants. There was no overlap between the two *NbCMPG1* constructs and this could be due to a difference in silencing efficiency. However, both constructs showed

Figure 4.10 Bar graph of the effect of pGRAB::PiAvr3a^{KI} induced HR.
VIGS pYL156::*NbCMPG1 I* and pYL156::*NbCMPG1 II* constructs compared to
a pYL156::*GFP* control on *N. benthamiana* (Co-infiltrated with *R3a*) and R3a
transgenic *N. benthamiana*. Error bars for the HRs for each VIGS construct are
shown and the graph represents the mean of 3 replicate experiments. Error bars
(+/-) were calculated using Standard Deviation divided by the square route of
the population (n).
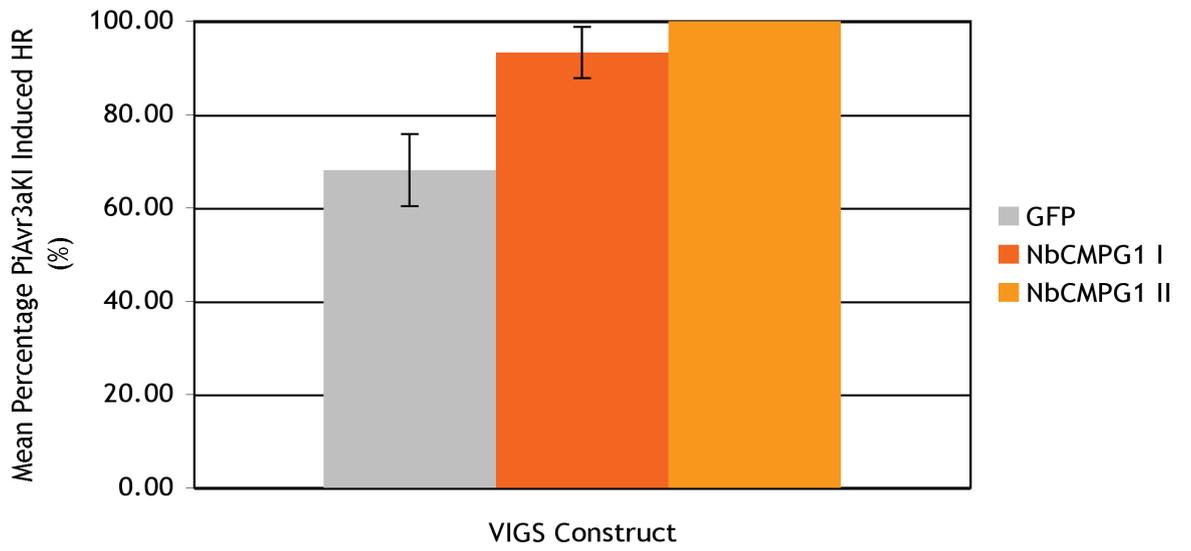
the same trend (increased HR) when compared to the *GFP* control and therefore both are silencing effectively.

This result shows that CMPG1 is not required for R3a-mediated HR. CMPG1 is not a "*guardee*" (See the Guard Hypothesis, Introduction) because R3a-mediated HR still occurs on the VIGSed lines.

4.3 Discussion

As referred to in the Introduction (Chapter 1) a number of plant genes have been found to be involved in plant defence. In this thesis a relationship between the plant defence protein, StCMPG1 and the pathogen effector protein, PiAvr3a, has been identified. The aim of the work in this chapter was to understand the functional role behind this interaction and to establish if CMPG1 plays a general role in defence to multiple pathogens. The conclusions drawn from 4.2 are described below.

4.3.1 PiAvr3a Generally Suppresses CMPG1-mediated CD

The avirulence genes *Avr4* and *Avr9* code for fungal elicitors that originate from the biotrophic fungus *C. fulvum*. The host for this pathogen is tomato and only tomatoes that express the *Cf-4* or *Cf-9* genes will have resistance against *C. fulvum* expressing *Avr4* or *Avr9*, respectively. This fungal-host interaction is a model system used in plant science to investigate pathogen-host interactions.

Cf genes code for extra-cytoplasmic proteins with LRR motifs and are membrane-anchored glycoproteins. Cf proteins are known as Receptor-like proteins (RLP) and are predicted to function at the host's PM (Stergiopolis and de Wit, 2009). In *Cf* transgenic plants the Avr protein induces oxidative bursts, electrolyte leakage, ethylene, SA and PR protein production as well as PCD (Joosten *et al.*, 1997 & Honee *et al.*, 1998)

González-Lamothe *et al.* (2006) previously showed that *N. benthamiana* silenced for *NbCMPG1* had reduced HR after Avr9/Cf-9 elicitation and the over expression of *NtCMPG1* induced a stronger HR in transgenic *Cf-9 N. tabacum* plants after Avr9 infiltration. They also showed that NtCMPG1 is involved in the ICD response and that tomato silenced for *CMPG1* showed a decrease in resistance to *C. fulvum* (González-Lamothe *et al.*, 2006).

Results in **Figure 4.4** confirmed that there is reduced Avr9/Cf-9 elicited HR in *N. benthamiana* plants silenced for *NbCMPG1*. The experiment was extended to Avr4/Cf-4 and revealed that CMPG1 was also required for this HR. *Cf-4* and *Cf-9* have structural similarities (Rowland *et al.*, 2005). They have identical, cytoplasmic C-terminal domains and have been found to share signalling components. For example *ACIF1* (*Avr9/Cf-9-INDUCED F-BOX1*; *NbACRE189*), which codes for an F-box E3 ligase and therefore involved in ubiquitination. It is required for both HRs. The data in this chapter show that CMPG1 is another signalling component which is common to these two Cfs.

Interestingly in **Figure 4.5** there was a decrease in the HR elicited in *Cf-9* transgenic *N. tabacum* by Avr9 in the presence of both PiAvr3as. It can be hypothesised that PiAvr3a is interacting with CMPG1 and preventing the CD triggered by this gene-for-gene interaction. Supporting evidence for this hypothesis is that the PiAvr3a$^{KI/Y147del}$ mutant form does not suppress this HR (**Figure 4.5**). From the Y2H and sYFP data in Chapter 3 it was shown that the interaction between PiAvr3a and CMPG1 required this terminal aa.

4.3.2 CMPG1 is Involved in the Plant's HR Response to Bacterial Pathogen *E. amylovora*

E. amylovora is a gram-negative, necrotrophic bacterium that causes Fireblight. It infects apples, pears and other members of the *Rosaceae* family. It is a systemic disease and delivers effector proteins via a T3SS (Zhao *et al.*, 2005). *E. amylovora* is not a pathogen of *N. benthamiana* and *N. benthamiana* is a non-host for *E. amylovora*. *N. benthamiana* responds with a clear HR.

From the data, it can be concluded that *NbCMPG1* is up regulated during the *N. benthamiana* resistance response (**Figure 4.7**). **Figure 4.7a** time-course shows an early peak for *NbCMPG1* expression which is known to occur during pathogen stimuli. The graph also shows a later peak for *NbCMPG1* expression during which visible death symptoms are present (HR). This implies that HR required NbCMPG1 and is therefore NbCMPG1-dependent.

Figure 4.8 shows that PiAvr3a^{KI} and PiAvr3a^{EM} suppress the non-host HR seen on *N. benthamiana* during *E. amylovora* infection. The PiAvr3a$^{KI/Y147del}$ cannot and it is also the form that does not interact or stabilise CMPG1. From this it can be concluded that PiAvr3a can suppress CMPG1-mediated CD and can stabilise CMPG1.

CMPG1 is involved in the CD triggered by elicitors from a range of pathogens including oomycetes, fungi and bacteria. PiAvr3a^{KI} strongly, and PiAvr3a^{EM} weakly, suppress all of these. The PiAvr3a$^{KI/Y147del}$ does not and also does not stabilise CMPG1. In conclusion, CMPG1 is an important virulence target for the effector PiAvr3a probably in order to suppress the CD in the biotrophic phase of infection.

4.3.3 *P. Infestans*, whilst Presumably Targeting CMPG1 in the Biotrophic Phase, Requires CMPG1 for CD Triggered in the Necrotrophic Phase

A time-course (**Figure 4.9A**) of leaf samples taken daily, between 0 and 5 dpi of *P. infestans* showed a peak at 3 dpi for the expression of NbCMPG1. In addition, an early, rapid up-regulation of CMPG1 was observed 1 Hr after *P. Infestans* inoculation, consistent with previous rapid transcript accumulation seen previously in response to various pathogen elicitors (Bos *et al.*, 2010). The later up-regulation of *CMPG1*

seen here provides evidence that CMPG1 activity may contribute to PCD triggered during the necrotrophic phase of *P. infestans* infection. This is similar to the host cysteine protease cathepsin B, which is involved in PCD and is induced at a similar stage (3 dpi) of a compatible interaction between potato and *P. infestans* (Gilroy *et al.*, 2007). This implies a possible duel role for CMPG1 not only in the early stages of infection (biotrophy) but also in the later stages (necrotrophy) during *P. infestans* infection (Bos *et al.*, 2010).

VIGS of *NbCMPG1* had an effect on the sporulation of *P. infestans*. **Figure 4.9B-D** shows the sporulation of *P. infestans* on *N. benthamiana* leaves was reduced. However, the trypan staining in **Figure 4.9Bii** showed little difference in the amount of colonisation. This agrees with the hypothesis that CMPG1 potentially is co-opted by the pathogen during the necrotrophic phase, to contribute to PCD,

Chapter 5. PiAvr3a Acts as an Ub Conjugating Enzyme (E2) in the Presence of StCMPG1

5.1 Introduction

In Chapters 3&4 the actions of PiAvr3a on StCMPG1 during infection as well as their location in the cell was investigated and conclusions drawn. In summary; PiAvr3a^{KI} and PiAvr3a^{EM} stabilise CMPG1 and the PiAvr3a$^{KI/del147}$ mutant does not. PiAvr3a modifies or inhibits CMPG1 activity. A range of CD, requiring CMPG1, are suppressed by PiAvr3a^{KI} and PiAvr3a^{EM} and not the PiAvr3a$^{KI/del147}$ mutant. In addition, CMPG1 is degraded in the 26S proteasome and CMPG1 U-box mutants lack E3 ligase activity and are stabilised (Bos *et al.*, 2010). Based on the observations in Chapters 3&4 as well as other published data (Bos *et al.*, 2010, Birch *et al.*, 2009, Gonzàlez-Lamothe *et al.*, 2006 & Yang *et al.*, 2006), in Chapter 5 a biochemical approach was used to try to understand the interaction between PiAvr3a and CMPG1. This biochemical approach involved the use of recombinant protein and *in vitro* ubiquitination assays. This technique recreates the Ub cycle *in vitro* allowing the specific parts of the cycle to be changed and the Ub activity of that protein combination to be determined.

This approach was used because ubiquitination assays have been successful in the past to confirm the function of other proteins (including CMPG1; see below) in the ubiquitin cycle. Two sets of ubiquitination assays in particular provided evidence that this system could be useful for this project. Of direct relevence, work by Yang *et al* (2006) involved the use of ubiquitination assay to show that NtACRE276 and its *A. thaliana* homologue AtPub17 both had E3 ligase activity. AtPub17 is an E3 ligase that, like CMPG1, is involved in plant defence responses (Yang *et al.*, 2006). The second example, by Gonzàlez-Lamothe *et al.* (2006), used ubqitination assays to provide evidence that NtCMPG1 (NtACRE74) is an E3 ligase (Gonzàlez-Lamothe *et al.*, 2006). These examples provided supporting evidence that ubiquitination assays could be used to investigate if PiAvr3a was inactivating the E3 ligase activity of StCMPG1 *in vitro*. This in turn would present data as to why PiAvr3a was targeting StCMPG1 during host infection.

5.1.1 Aims and Objectives

To try and find a biochemical role for PiAvr3a in the cell in relation to CMPG1. There were two objectives for Chapter 5.

i. To provide biochemical information as to the function of PiAvr3a in the cell in relation to CMPG1. Originally, the hypothesis was that PiAvr3a would block StCMPG1 E3 ligase activity, preventing HR and allowing infection.

ii. After initial work was performed it was hoped to then develop the assay to establish the Ub lysine involved in the ubiquitination by CMPG1 in the presence of PiAvr3a. This would be achieved using Ub lysine mutants.

5.2 Results

5.2.1 Does PiAvr3a act as an E2 Conjugating Enzyme *in vitro*?

Preparation for the ubiquitination assay involved making constructs to synthesise each protein to be investigated. Sequences of StCMPG1, PiAvr3a^{KI}, PiAvr3a^{EM} and PiAvr3a$^{KIdel/Y147}$ (all obtained from the Y2H screen performed by Dr M Armstrong; SCRI Dundee, Scotland) were cloned into protein expression vectors (2.4 DNA Methods). Positive clones were identified using restriction digests and DNA sequencing. Positive clones for each construct were transformed into *E. coli* BL21 cells and the corresponding protein was expressed using IPTG protein induction. This protein was purified depending on the vector's epitope tag and protein's solubility. Finally, the protein was dialysed, with a final dialysis in ubiquitination buffer (2.13 Protein Expression and Purification using *E. Coli* [BL21]). Once all the proteins were prepared, they were stored and used as part of the ubiquitination assays (2.15 Plant Ubiquitination Assay). **Figure 5.1A-F** show the proteins expressed for the assays as well as diagrams of the constructs used. Of those constructs expressed and purified; AtPub17 (positive E3 ligase control), AtUbq113KR (mutant ubiquitin; K29, K48 & K63) and AtUbq11 (ubiquitin for the assay) were already available in the laboratory (Arnott Laboratory, The University of Glasgow, Scotland; Yang *et al.*, 2006).

Figure 5.2 is a western blot probed with anti:HA (the tag present on the ubiquitin; 2.12 Protein Methods) and it's corresponding ponceau. The western shows an ubiquitination assay (Ubiquitination assay 1; 2.15 Plant Ubiquitination Assay) including its negative control assay lane. The human E2 UbcH5b was used as the E2 in the assay as this had been previously shown to be functional with plant proteins (**Figure 5.3B**; Yang *et al.*, 2006 & Gonzàlez-Lamothe *et al.*, 2006). Lane 4 is the assay with the E2 represented using PiAvr3a^{EM} and AtPub17 as the E3. This shows little higher banding showing there are no ubiquitination chains forming and therefore the cycle is not occurring with those proteins. This supports the Y2H performed by Dr M Armstrong (SCRI, Dundee, Scotland), which showed there was no interaction between AtPub17 and PiAvr3a^{EM} or PiAvr3a^{KI} (results not shown). In lane 5 the E2 is PiAvr3a^{EM}, the E3 is StCMPG1, and it can be seen there is a stronger band about the 175 KDa mark. This implies some ubiquitination is occurring when this combination of proteins is used in the assay. Therefore, it was concluded that PiAvr3a^{EM} may act as an E2 *in vitro*. Lane 6 is the assay with the E2 represented using PiAvr3a^{KI} and AtPub17 as the E3. This shows some higher banding showing there are ubiquitination chains forming and therefore the cycle is occurring with those proteins despite the lack of interaction in Y2H. In lane 7 the E2 is PiAvr3a^{KI}, and the E3 is StCMPG1 and it can be seen there is a stronger banding in around the 175 KDa mark. This implies

Figure 5.1 Protein Purification of Recombinant Protein Post Expression and Pre-dialysis. Arrows indicate the protein band that corresponds to the construct in question.

Ai. Schematic representation of the pET30::HAAtUbq11WT construct. The relative positions of the T7 promoter, LacI, 6xHIS tag, 3XHA tag, AtUbq11WT and T7 terminator are shown.

Aii. Coomassie SDS-PAGE gel of the HIS Bind purification. The protein elutions 1&2 are shown. Sizes are indicated in Kilo Daltons (KDa).

Bi. Schematic representation of the pDEST17::PiAvr3a^{EM} construct. The relative positions of the T7 promoter, RBS, ATG, 6xHIS tag, PiAvr3a^{EM} and T7 terminator are shown.

Bii. Western blot exposure (above) and corresponding ponceau stained PVDF membrane (below) after HIS primary antibody probing showing the purified elutions 1&2 (1&2) of pDEST17::PiAvr3a^{EM} at the 17 KDa region.

Ci. Schematic representation of the pDEST17::PiAvr3a^{KI} construct. The relative positions of the T7 promoter, RBS, ATG, 6xHIS tag, PiAvr3a^{KI} and T7 terminator are shown.

Cii. Western blot exposure (above) and corresponding ponceau stained PVDF membrane (below) after HIS primary antibody probing showing the purified elution 2 of pDEST17::PiAvr3a^{KI} at the 17 KDa region.

Di. StCMPG1 Wild type in the pDEST15 vector system. A Schematic representation of the pDEST15::StCMPG1 construct. The relative positions of the T7 promoter, RBS, ATG, 6xHIS tag, StCMPG1 and T7 terminator are shown.

ii. Western blot exposure (above) and corresponding ponceau stained PVDF membrane (below) after GST primary antibody probing post induction. "T3" is the induced protein at time (T) 3 Hrs post-IPTG induction.

Ei. Schematic representation of the pDEST15::AtPub17WT construct. The relative positions of the T7 promoter, GST tag, AtPub17 WT and T7 terminator are shown.

ii. Comassie stained SDS-PAGE gel (above left) and western blot exposure (above right) and corresponding ponceau stained PVDF membrane (below) after GST primary antibody probing showing the inclusion body purification fraction of pDEST15::AtPub17WT.

Fi. Schematic representation of the pET30::HAAtUbq113KR construct. The relative positions of the T7 promoter, LacI, 6xHIS tag, 3XHA tag, AtUbq113KR and T7 terminator are shown. The lysines mutated are K29, K48 and K63.

ii. Coomassie SDS-PAGE gel of the HIS Bind purification. The purified protein band is shown (arrow). Size is indicated in KDa.

Ai pET30

T7t | Lac | 6xHIS | 3xHA | AtUbq11 | T7t

ii

17KDa

11KDa

1 2

Bi pDEST17

T7t | RBS | ATG | 6xHIS | PiAvr3a^{EM} | T7t

ii

17KDa

17KDa

1 2

Ci pDEST17

T7t | RBS | ATG | 6xHIS | PiAvr3a^{KI} | T7t

ii

20KDa

20KDa

2

Di

ii

Ei

ii

Fi

ii
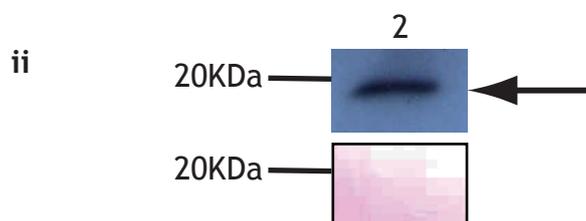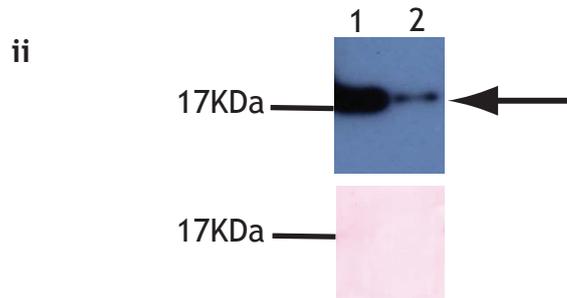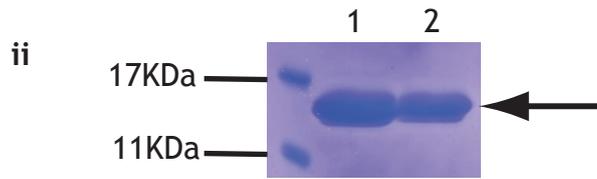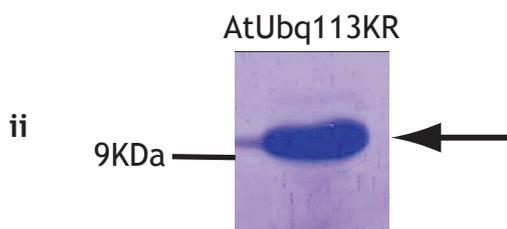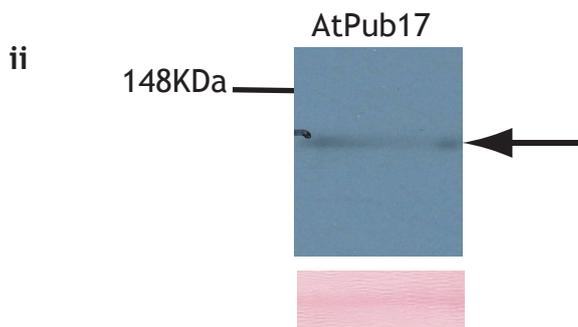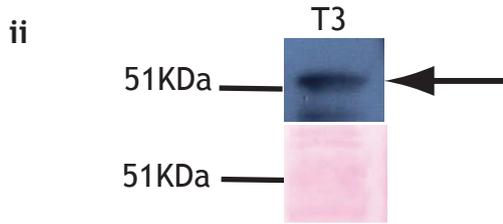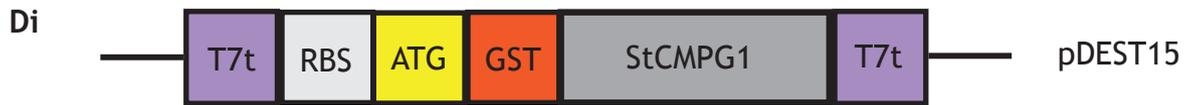
Figure 5.2 Ubiquitination Assay 1.

A. Table displaying the variable component proteins in the ubiquitination assay. The left hand column lists the proteins by name that varied between samples. The numbered columns (1-7) correspond to the sample lanes in part B. The + and – in the table show the presence or absence (respectively) of that particular protein in the assay sample. Approximate protein sizes are also listed (KDa) and *E. coli* proteins may have been present due to the protein purification process.

B. Western blot exposure of a ubiquitination assay (above) after primary antibody probing with anti:HA. Below is the corresponding ponceau stained PVDF membrane. Protein marker sizes are shown between 32.5 KDa to 175 KDa.

A

Component	Approx. Protein Size (KDa)	1 (-E1)	2 (-E2)	3 (-E3)	4 (EM/ AtPub17)	5 (EM/ StCMPG1b)	6 (KI/ AtPub17)	7 (KI/ StCMPG1b)
E1	118	+	+	-	+	+	+	+
UbcH5b	27	+	-	+	-	-	-	-
PiAvr3a^{KI}	20	-	-	-	-	-	+	+
PiAvr3a^{EM}	20	-	-	-	+	+	-	-
AtPub17	80	-	+	+	+	-	+	-
StCMPG1b	55	-	-	-	-	+	-	+
AtUbq11WT	10	+	+	+	+	+	+	+

B
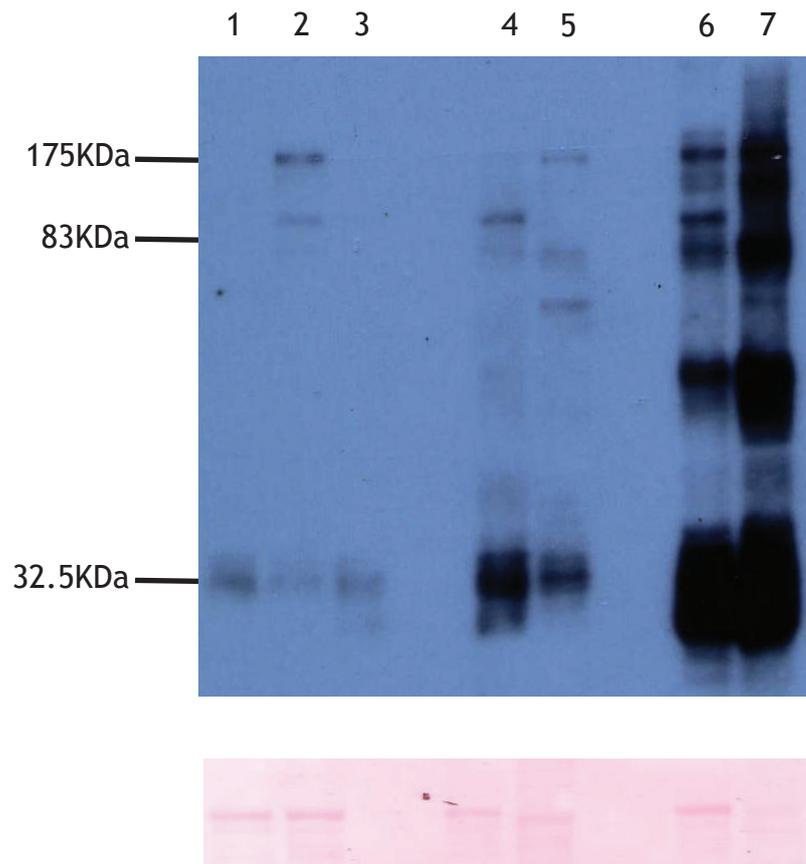
some ubiquitination is occurring when this combination of proteins is used in the assay. Therefore, it was concluded that PiAvr3a^{KI} also may act as an E2 *in vitro*. There is more banding and the banding is stronger than that seen in the PiAvr3a^{EM} equivalent lanes and this led to the conclusion that PiAvr3a^{KI} ubiquitinates more effectively than the PiAvr3a^{EM}, and that PiAvr3a may act as an E2 and and is more active (specific) with CMPG1 than AtPub17.

5.2.2 Does PiAvr3a Require the Ub Lysines Thought to be Involved in Disease Defence and Protein Degradation as part of the Ubiquitination of CMPG1?

Figure 5.3 (Ubiquitination assay 2; 2.15 Plant Ubiquitination Assay) shows an assay performed with the AtUbq11WT or AtUbq113KR (lysines 29, 48 & 63 to mutated to arginines) Ub. Lanes 1 & 2 are controls using the purchased UbcH5b (Enzo® Life Sciences) as the E2 and AtPub17 as the E3 with either WT or 3KR AtUbq11. It can be seen that ubiqiutination occurs more strongly with the WT Ub compared to the 3KR Ub mutant. This corresponds with previous work that shows that the three lysines mutated are the predominant Ks involved in this ubiquitination. Lane 3 is a negative control which has no E2 present and as predicted shows no higher banding associated with ubiquitination. Lanes 4 and 5 show the ubiquitination when PiAvr3a^{KI} is used as the E2 and the effect the mutant Ub has on that ubiquitination (Lane 5). It can be seen that there is some ubiqiutination with the WT Ub but considerably less with the 3KR mutant Ub. This provides preliminary evidence that the PiAvr3a^{KI} is not only acting as an E2, as previously shown, but that it is also ubiquitinating using one or more of the 3 mutated lysines. Lanes 6 and 7 show the ubiquitination when PiAvr3a^{EM} is used as the E2 and the effect the mutant Ub has on that ubiquitination (Lane 7). It can be seen that there is some ubiquitination with the WT Ub but considerably less/none with the 3KR mutant Ub. This provides preliminary evidence that the PiAvr3a^{EM} is also not only acting as an E2, as previously shown, but that it is also ubiquitinating using one or more of the 3 mutated lysines. This ubiquitination was less than that seen for PiAvr3a^{KI} and supports previous data from Chapter 3 & Chapter 4 that PiAvr3a^{KI} performs more strongly compared to PiAvr3a^{EM}. The implications of this result will be discussed below (**5.3**).

After Ubiquitination assays 1 & 2 were performed the next line of investigation was to try and find out which of the three lysines in the 3KR mutant Ub were being utilised by PiAvr3a. The additional proteins used for this assay are shown in **Figure 5.4B-D**. These parts of the figure show the three single mutant Ub made using QuikChange® and the original WT Ub (AtUbq11WT in the pET30 vector). Once successful clones were checked using restriction digest and DNA sequenced, these proteins were expressed and purified using the same method used to acquire the WT Ub. The first, initial assay is shown in **Figure 5.5**.

Figure 5.3 Ubiquitination Assay 2.

A. Table displaying the variable component proteins in the ubiquitination assay. The left hand column lists the proteins by name that varied between samples. The numbered columns (1-7) correspond to the sample lanes in **5.3B**. The + and – in the table show the presence or absence (respectively) of that particular protein in the assay sample.

B. Western blot exposure of a ubiquitination assay (above) after primary antibody probing with anti:HA. Below is the corresponding ponceau stained PVDF membrane. Protein marker sizes are shown between 32.5 KDa to 175 KDa and *E. coli* proteins may have been present due to the protein purification process.

A

Component	Approx. Protein Size (KDa)	1 (WT)	2 (3KR)	3 (-E2)	4 (KI/ WT)	5 (KI/ 3KR)	6 (EM/ WT)	7 (EM/ 3KR)
E1	118	+	+	+	+	+	+	+
UbcH5b	27	+	+	-	-	-	-	-
PiAvr3a^{EM}	20	-	-	-	-	-	+	+
PiAvr3a^{KI}	20	-	-	-	+	+	-	-
AtPub17	80	+	+	-	-	-	-	-
StCMPG1	55	-	-	+	+	+	+	+
AtUbq11WT	10	+	-	+	+	-	+	-
AtUbq113KR	10	-	+	-	-	+	-	+

B
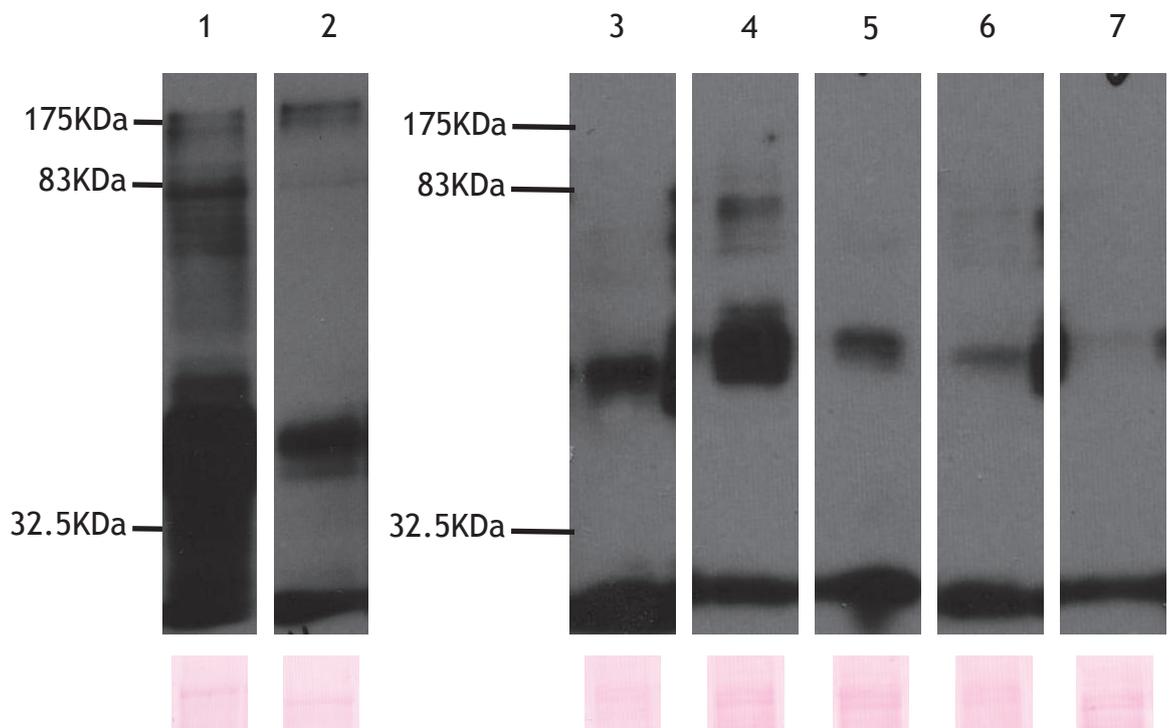
5.2.3 Are Ub-lysines 48 and 63 Required for Ubiquitination by PiAvr3a?

Figure 5.5Bi shows an assay where the Ub is the varying factor (2.15 Plant Ubiquitination Assay). Lane 1 is a positive control using PiAvr3a^{EM} as the E2, StCMPG1 as the E3 and AtUbq11WT as the Ub. Laddering can be seen in the lane showing the level of Ub occurring in the standard reaction. Lane 2 has AtUbq11K29R as the Ub and shows ubiquitination. This result shows that ubiquitination is still occurring when the K29 has been mutated and not functioning and therefore is not used by PiAvr3a^{EM} for ubiquitination. Lane 3 has AtUbq11K48R as the Ub and shows no ubiquitination. This result shows that K48 is used by PiAvr3a^{EM} for ubiquitination. Lane 4 has AtUbq11K63R as the Ub and also shows no ubiquitination. This result shows that K63 is used by PiAvr3a^{EM} for ubiquitination. From **Figure 5.5Ai&Bi** it can be concluded that PiAvr3a^{EM} is using both lysine 48 and 63 for ubiquitination.

In **Figure 5.5Bii**, Lane 1 is a positive control using PiAvr3a^{KI} as the E2, StCMPG1 as the E3 and AtUbq11WT as the Ub. Laddering can be seen in the lane showing the level of Ub occurring in the standard reaction. Lane 2 has AtUbq11K29R as the Ub and shows ubiquitination. This result shows that ubiquitination is still occurring when the K29 has been mutated and not functioning and therefore is not used by PiAvr3a^{KI} for ubiquitination. Lane 3 has AtUbq11K48R as the Ub and shows no ubiquitination. This result shows that K48 is used by PiAvr3a^{KI} for ubiquitination. Lane 4 has AtUbq11K63R as the Ub and also shows no ubiquitination. This result shows that K63 is used by PiAvr3a^{KI} for ubiquitination. From **Figure 5.5Aii&Bii** it can be concluded that PiAvr3a^{KI} is also using both lysine 48 and 63 for ubiquitination. The possible implication of this result will be discussed in **5.3**.

Interestingly the PiAvr3a^{EM} had stronger ubiquitination compared to the PiAvr3a^{KI} in this figure (**5.5**). It is uncertain as to why this occurred and as this particular experiment was only performed once it is not conclusive.

Figure 5.4 Protein Induction and Purification of Recombinant Protein Post-induction and Pre-dialysis.

Arrows indicate the protein band corresponding to the construct in question. Sizes are shown in kilodaltons (KDa).

Ai. Schematic representation of the pET30::AtUbq11K29R construct. The relative positions of the T7 promoter, lacI, 6xHIS tag, 3xHA, AtUbq11K29R and T7 terminator are shown.

Aii. Coomassie stained SDS-PAGE gel showing the purified pET30::AtUbq11K29R protein purified elutions 1-3 at the 10 KDa region.

Bi. Schematic representation of the pET30::AtUbq11K48R construct. The relative positions of the T7 promoter, lacI, 6xHIS tag, 3xHA, AtUbq11K48R and T7 terminator are shown.

Bii. Coomassie stained SDS-PAGE gel showing the purified pET30::AtUbq11K48R protein purified elutions 1-3 at the 10 KDa region.

Ci. Schematic representation of the pET30::AtUbq11K63R construct. The relative positions of the T7 promoter, lacI, 6xHIS tag, 3xHA, AtUbq11K63R and T7 terminator are shown.

Cii. Coomassie stained SDS-PAGE gel showing the purified pET30::AtUbq11K63R protein purified elutions 1-3 at the 10 KDa region.

Ai — T7t | Lac | 6xHIS | 3xHA | AtUbq11 K29R | T7t — pET30

ii — 1 2 3 — 9KDa

Bi — T7t | Lac | 6xHIS | 3xHA | AtUbq11 K48R | T7t — pET30

ii — 1 2 3 — 9KDa

Ci — T7t | Lac | 6xHIS | 3xHA | AtUbq11 K63R | T7t — pET30

ii — 1 2 3 — 9KDa
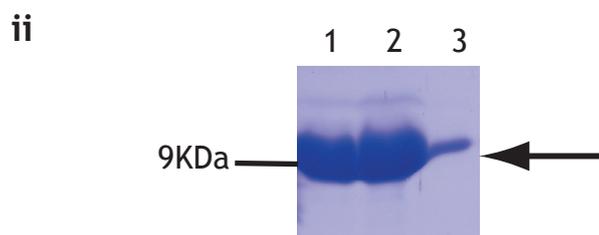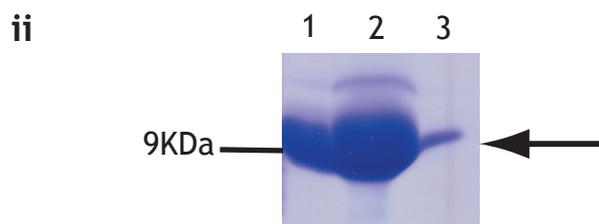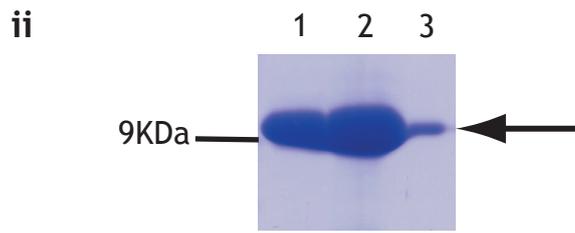
Figure 5.5 Ubiquitination Assay 3.

Ai. A table displaying the variable component proteins in the PiAvr3a^{EM} ubiquitination assay **5.6Bi**. The left hand column lists the proteins by name that varied between samples. The numbered columns (1-4) correspond to the sample lanes in 5.6Bi. The + and – in the table show the presence or absence (respectively) of that particular protein in the assay sample.

Aii. A table displaying the variable component proteins in the PiAvr3a^{KI} ubiquitination assay **5.6Bi**. The left hand column lists the proteins by name that varied between samples. The numbered columns (1-4) correspond to the sample lanes in **5.6Bi**. The + and – in the table shows the presence or absence (respectively) of that particular protein in the assay sample.

Bi. Western blot exposure of PiAvr3a^{EM} ubiquitination assay (above) after primary antibody probing with anti:HA. Below is the corresponding ponceau stained PVDF membrane. Protein marker sizes are shown between 32.5 KDa to 175 KDa and *E. coli* proteins may have been present due to the protein purification process.

Bii. Western blot exposure of PiAvr3a^{KI} ubiquitination assay (above) after primary antibody probing with anti:HA. Below is the corresponding ponceau stained PVDF membrane. Protein marker sizes are shown between 32.5 KDa to 175 KDa and *E. coli* proteins may have been present due to the protein purification process.

Ai

Component	1	2	3	4
E1	+	+	+	+
PiAvr3a^{EM}	+	+	+	+
StCMPG1	+	+	+	+
AtUbq11WT	+	-	-	-
AtUbq11K29R	-	+	-	-
AtUbq11K48R	-	-	+	-
AtUbq11K63R	-	-	-	+

Aii

Component	1	2	3	4
E1	+	+	+	+
PiAvr3a^{KI}	+	+	+	+
StCMPG1	+	+	+	+
AtUbq11WT	+	-	-	-
AtUbq11K29R	-	+	-	-
AtUbq11K48R	-	-	+	-
AtUbq11K63R	-	-	-	+

Bi
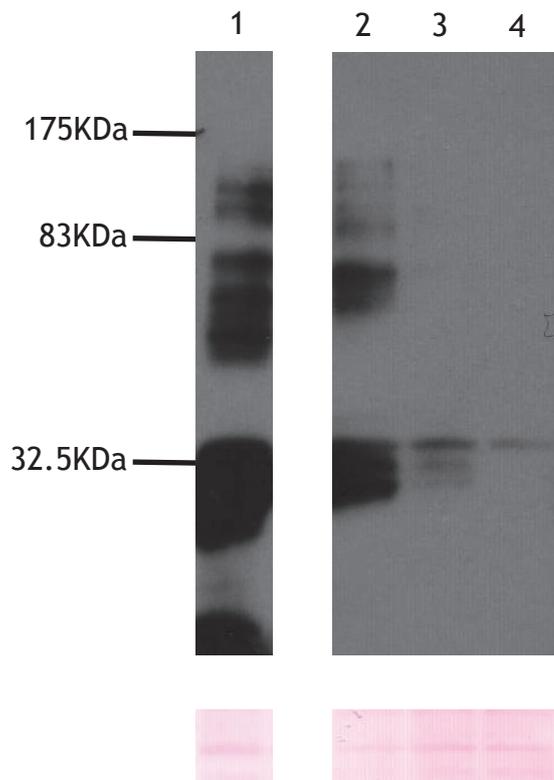
ii
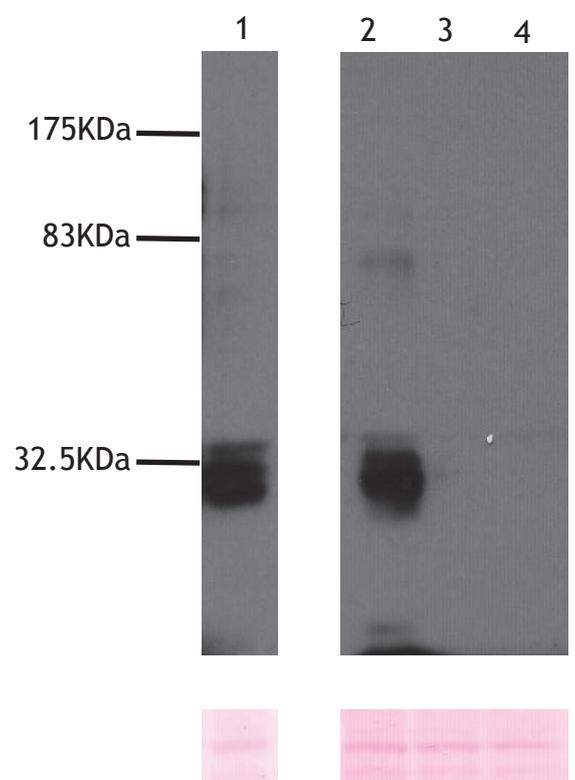
5.3 Discussion

Plant science research often requires focusing on a particular pathway in the plant to establish its function and purpose and initial observations can be achieved by using *in vitro* techniques. This enables the researcher to control the components of that pathway more effectively than if the work was carried out *in planta*. Ubiquitination assays are one such method and have proved successful in the past in establishing enzyme function (González-Lamothe et al., 2006; Yang *et al.*, 2006). This chapter aimed to use this technique to establish the effect of PiAvr3a on the plant ubiquitination cycle as part of its infection processes and interaction with the E3 ligase CMPG1. This chapter produced promising and suprising preliminary data. The conclusions drawn from this chapter are described below.

5.3.1 *In vitro* Ubiquitination Assays Conclude that PiAvr3a is Potentially an E2?

it was hypothesised that PiAvr3a would inhibit CMPG1 E3 ligase activity, possibly in the U-Box domain, preventing interaction after stabilisation. Supprisingly, in the *in vitro* assays this was not the case. This implies that PiAvr3a could be acting as an E2 in the plant and therefore changing the function of CMPG1 to aid pathogen infection. PiAvr3a had better ubiquitination with StCMPG1 compared to AtPub17.

During this part of the project, some problems with protein induction made continuing the preliminary work done in this chapter difficult to continue in the time available. After the initial assays were performed using StCMPG1 and PiAvr3a in the pDEST system more protein was required to continue the work. However, the constructs would no longer express protein. It may have been due to a frame shift mutation in the vector itself (Belfield *et al.*, 2007) or some other factor.   Experimental changes and even re-cloning into the pDEST vectors were unsuccessful and it was decided to clone into the pET system instead, as it had proved successful with the Ub. The proteins expressed and were purified; however when the assays were performed they were no longer successful. Despite many experimental changes, by the end of the project no more assays had produced significant data. The project would have benefited from using the PiAvr3a$^{KI/delY147}$ mutant to see if the 147 tyrosine was required for ubiquitination. Its gene was cloned and the protein expressed and purified (**Figure 5.4A**) in the pET system, however with the other elements of the assay, such as controls not working, unfortunately no data came from this.

PiAvr3a was not considered a candidate E2 because it has no cysteine, the point

at which the Ub is transferred. It was surprising that it nevertheless had this activity *in vitro*. Also, from the ubiquitination assay, the Y2H and the sYFP experiments it would appear that the interaction between CMPG1 and PiAvr3a is direct. It also seems that PiAvr3a^KI has greater ubiquitination compared to PiAvr3a^EM and therefore, it can be concluded, greater interaction consistent with previous data that PiAvr3a^KI interacts more strongly than PiAvr3a^EM.

In conclusion, promising and supprising data revealed that PiAv3a may act as an E2 conjugating enzyme. Further work is needed to confirm this. Moreover, it appeared to act via both lysines 48 and 63, perhaps suggesting that it forms a mixed chain on CMPG1 substrates. We need to identify the endogenous E2 working with CMPG1 in the plant itself to see how this ubiquitination works. However, it is possible PiAvr3a competes for binding to CMPG1 with the endogenous E2 to switch the Ub chain morphology, and thus the fate of CMPG1 substrates.

Chapter 6. Final Discussion

Investigating the individual proteins involved in plant defence and the pathways these proteins are part of is important to gain an understanding of infection and disease resistance process. In the future, it is hoped that this knowledge will help develop solutions to prevent crop infection, and increase crop yield. More specifically, CMPG1 was first found to be important in plant responses to infection by Kirsch *et al.* (2001) in parsley. It has further been found to have homology to NbACRE47 and AtPUB20 and AtPUB21 implying it is common to many plant species. CMPG1 is an U-Box E3 Ubiquitin ligase and involved in a number of different defence responses (INF1, Cf-4, Cf-9 & Pto/AvrPto; González-Lamothe *et al.*, 2006 and Gilroy *et al.*, 2011; Chapter 4).

PiAvr3a is an RxLR cytoplasmic effector protein. Its virulence function was shown by its ability to suppress ICD by Bos *et al.* (2006). This *P. infestans* protein and the plant protein CMPG1 were found to interact in Y2H studies performed by Dr M Armstrong (Bos *et al.*, 2010) and it is from this Y2H that the work performed in this study stemmed.

This project used *in planta* studies to investigate the CMPG1-PiAvr3a interaction. This involved the use of: co-infiltration, transient expression, western blots, sYFP, confocal microscopy and a fluorometer to provide evidence of the interaction. Next, the biological reason for why this interaction occurred was studied using VIGS and HR/CD suppression assays. Finally, the biochemical nature of this interaction was investigated using ubiquitination assays and purified proteins *in vitro*. All in all this thesis has provided data which has increased the overall understanding of the function of CMPG1 and PiAvr3a during infection. The following discussion relates the thesis findings, extending prior knowledge already published, and speculates possible future work to add to this understanding.

6.1 StCMPG1 is Stabilised by PiAvr3a and Accumulates in the Host Nucleus.
StCMPG1 protein can only be detected when co-expressed with PiAvr3a. Nevertheless, its expression in the absence of PiAvr3a can be detected at the RNA level. This led to the conclusion that StCMPG1 is degraded when PiAvr3a is not present. However, when PiAvr3a is present, StCMPG1 is stabilised. As StCMPG1 has been shown to degrade itself, *via* the 26S proteasome, its stabilisation indicates that PiAvr3a prevents its normal degradative function (Bos *et al.*, 2010).

Another example of a protein which self-ubiquitinates is HsMDM2, a Ub E3 ligase that promotes p53 ubiquitination and degradation. HsMDM2 self-ubiquitination can be interrupted by other proteins. This reduces the self-ubiquitination and promotes other forms of ubiquitination. By reducing self-ubiquitination, other forms of ubiquitination can be increased and *vice versa* (Song *et al.*, 2008). It is possible that this is the case here. StCMPG1s' ability to self-ubiquitinate is decreased in the presence of PiAvr3a resulting in its accumulation in the cell and promoting its presence and therefore ability to ubiquitinate another substrate in the nucleus or cytoplasm and/or move to the nucleus (Trujillo & Shirasu, 2010). However, this is speculation as the E2 with which StCMPG1 achieves ubiquitination, self or otherwise, is unknown, as are the target substrates of this E3 ligase. These would be useful to ascertain why this particular ubiquitination occurs and exactly why PiAvr3a would adapt this host cell process.

Why does StCMPG1 accumulate in the nucleus upon stabilisation? The critical observation is that CMPG1 is required for CD in response to a variety of elicitors. PiAvr3a suppresses all of these. Therefore, PiAvr3a suppresses CMPG1-mediated CD in the biotrophic phase of infection. This is the stage at which PiAvr3a is present. Why does it accumulate in the nucleus? This is unknown, however it is reminiscent of the fate of NPR1. NPR1 is required for SA responses and is turned over in the nucleus, and this is for its regulation and to control its activity (Spoel *et al.*, 2009).

The data collected also gave the indication that PiAvr3a^{KI} increased StCMPG1 stability when compared to PiAvr3a^{EM} and that both these forms were substantially better at stabilising StCMPG1 compared to the mutated PiAvr3a^{KI}, PiAvr3a$^{KI/Y147del}$. The absence of stabilisation by the PiAvr3a$^{KI/Y147del}$ shows the requirement of aa Y147 for the stabilisation to occur. Why StCMPG1 stabilisation varies between the two natural alleles is not known. Both PiAvr3a^{EM} and PiAvr3a^{KI} are required for virulence (Bos *et al.*, 2010). It is possible, from CD suppression assays, that PiAvr3a^{EM} is active sufficiently to prevent CD during *P. infestans* infection but has been altered to evade R3a recognition.

6.2 CMPG1-mediated CD is Associated with the Recognition of Pathogen Molecules at the Host PM.

The work achieved in Chapter 4 was extended by Dr E Gilroy after I had left the laboratory. The data collected showed that AvrPto/Pto HR and CD triggered by the oomycete PAMP CBEL are also CMPG1-dependent and suppressed by PiAvr3a. Cf-4/Avr4, Cf-9/Avr9, Pto/AvrPto, CBEL and INF1 (Gilroy *et al.*, 2011) are all associated with recognition at the PM. In contrast, R3a is not CMPG1-dependent

(Bos *et al.*, 2010). Dr E Gilroy has also investigated CDs mediated by other NBS-LRR resistance proteins (R2 and Rx), all of which are cytoplasmic. None are CMPG1-dependent and none are suppressed by Avr3a. Therefore, CMPG1-dependent CD is apparently associated with recognition of pathogen molecules at the host cell surface (**Figure 6.1**). PiAvr3a, in targeting CMPG1, appears to have a role in preventing signalling/signal transduction following the perception of diverse molecules at the surface of the host cell. Presumably, we can conclude that at least a component of the *E. amylovora* non-host HR is triggered by a pathogen molecule at the host PM.

In summary, the CD events dependent on CMPG1 to date include: Avr9/Cf-9, Avr4/Cf-4, pto/AvrPto, INF1, CBEL and *E. amylovora* (Chapter 4, Bos *et al.*, 2010, González-Lamothe *et al.*, 2006 & Gilroy *et al.*, 2011). It is likely that CMPG1 is a virulence target for PiAvr3a in order to suppress CD during the biotrophic phase. *P. infestans* required CMPG1 for the necrotrophic phase. However, R3a-dependent HR does not require CMPG1.

6.3 PiAvr3a is a Potential E2 Conjugating Enzyme and requires Ub Lysine 48 and 63 for Ubiquitination.

Results showed that, *in vitro*, PiAvr3a acts as an E2 conjugating enzyme. It was seen that the linkage produced required both of the tested Ub lysines K48 and K63. The knowledge about ubiquitin linkage and its effect on the destination and fate of the protein substrate is not fully resolved. K48 is the linkage associated with the degradation of protein substrates by the 26S proteasome. K63 is thought to be involved in modifying the activity of protein substrates and therefore changing cellular processes. There are a number of different link combinations that can be derived from K48 and K63. These include mono-ubiquitination as well as poly-ubiquitination. There is also evidence from research done in yeast and humans that ubiquitin chains can also form from more than one linkage type. For example: K48-K63-K48-K63 as well as forked chains (Kim *et al.*, 2007). It is believed that each different chain produces a different conclusion for the tagged substrate. It is possible that five different results can occur for CMPG1 depending on the situation. CMPG1 could be tagged with:

i. Mono-K48

ii. Mono-K63

iii. Poly-K48

iv. Poly-K63

v+. Combinations of the two (K48 & K63) including forked ub.

Figure 6.1 Model of the Involvement of CMPG1 in CD Triggered by Recognition of Pathogen Elicitors at the Cell Surface (membrane recognition) or Within the Host Cell Cytoplasm.

The oomycete PAMPs CBEL and INF1 are detected by unknown receptors at the host PM. INF1-triggered CD is known to be BAK1-dependent (Heese *et al.*, 2007). Avr9 and Avr4 from *C. fulvum* are apoplastic effectors detected by corresponding Cf R proteins, again predicted to reside in the PM. The AvrPto effector is recognised by Pto (in complex with the NBS-LRR protein PRF; not shown) at the PM. All of these interactions result in CMPG1-dependent CD, which can be suppressed by PiAvr3a, either by direct inhibition of CMPG1 activity, or through altering its activity to prevent its positive regulation of CD (indicated by a forked suppression line). The elicitor from *E. amylovora* that triggers CMPG1-dependent CD is unknown, but we predict it to be either extracellular and detected by a receptor at the host surface, or delivered inside the host cell by the T3SS and, like AvrPto, detected at the inside surface of the PM. Detection of the cytoplasmic effectors PiAvr3a and PiAvr2 from *P. infestans*, and the PVX coat protein (PVXCP) by corresponding NBS-LRR R proteins is CMPG1-independent and not suppressed by PiAvr3a. (Adapted from Gilroy *et al.*, 2011)

Intracellular Effectors
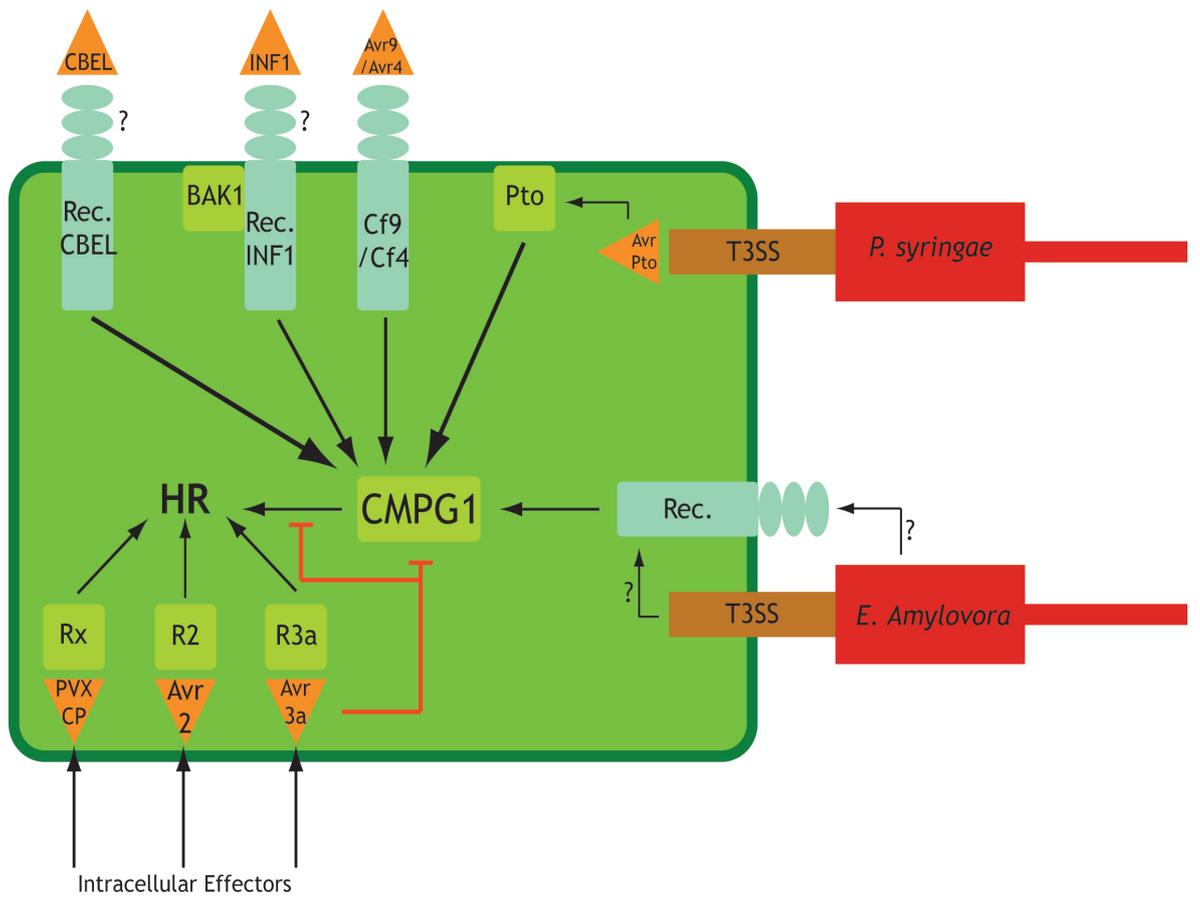
From the confocal microscope images, it appears CMPG1 goes to the nucleus but is not rapidly degraded in the presence of PiAvr3a. Therefore it can be concluded that possibly CMPG1 is changing cell signalling depending on the chain tagging it and that a major site of activity for CMPG1 is the nucleus.

6.4 Conclusions

This project's findings are summarised in the following bullet points:

•   StCMPG1 is stabilised *in planta* by the presence of PiAvr3a^{EM} and PiAvr3a^{KI} showing that StCMPG1 is possibly being targeted by PiAvr3a.

•   StCMPG1 undergoes some protein processing in the presence of PiAvr3a.

•   StCMPG1b accumulates in the nucleus and cytoplasm when stabilised by PiAvr3a providing a possible reason as to why CMPG1 is stabilised; changing cellular processes from within the nucleus.

•   PiAvr3a^{KI} is more effective compared to PiAvr3a^{EM} at CMPG1 interaction, stabilisation and HR (PCD) suppression.

•   PiAvr3a$^{KI/Y147del}$ mutant demonstrates the importance of the Y147 aa throughout the work as this mutant protein does not interact with CMPG1, not stabilise it and not suppress CMPG1-dependent HR.

•   PiAvr3a CD suppression and recognition by R3a are CMPG1-independent activities. CMPG1 is not involved in this response, and does not require PiAvr3as' Y147aa.

•   PiAvr3a generally suppresses CMPG1-mediated CD. This provides a possible CD assay technique to confirm or deny the involvement of CMPG1 in a particular HR.

•   CMPG1 is involved in the plants' HR response to *E. amylovora*.

•   *P. infestans* requires CMPG1 for CD triggered in the necrotrophic phase as well as the biotrophic phase.

•   PiAvr3a acts as an E2 *in vitro*.

•   Initial work shows PiAvr3a requires K48 and K63 to achieve ubiquitination *in vitro*.

However, there are still many aspects of the role of CMPG1 in pathogen responses within the cell to be investigated.

6.5 Improvements

Some key improvements to the experimental procedure could have be made with hindsight. The use of cell death assays gave consistant and publication quality data (Gilroy et al., 2011) however another technique could have been used involving the use of trypan blue staining and computer software to record the amount of leaf staining (HR). This numerical reading could have been used to

see if there was a difference in HR.

Secondly, colony count studies could have been performed for *P. infestans* and *E. amylovora* (Chapter 4) to observe any changes in colony growth on the VIGSed *N. benthamiana.*

6.6 Future Work

The aim of future work is to continue expanding the knowledge regarding CMPG1, PiAvr3a and associated proteins and possible interactions. One of the main questions still left unanswered is: What is the endogenous plant E2 that is ubiquitinating CMPG1 when PiAvr3a is not present? Not all the E2s in the plant have been discovered and, of the 30 or so that have, not all have been fully investigated. This work could start with a Y2H screen involving the CMPG1 U-Box to identify possible candidates. When possible candidates have been identified they could be verified with ubiquitination assays as well as VIGS of the E2 candidates to see if they are involved in INF1 CD.

It is believed that CMPG1 self-ubiquitinates. However, CMPG1 is an E3 ligase and therefore may not only self-ubiquitinate. It would expand current understanding to find the substrates of ubiquitination where CMPG1 is the E3 ligase. What CMPG1 ubiquitinates will help place the role of CMPG1 in relation to defence pathways that it acts on. A Y2H involving the ARM repeat region could be used to begin to ascertain this.

Another important angle of investigation is to find the structure of PiAvr3a. The structure would help to understand the active site(s) and hopefully resolve how it is acting as an E2 enzyme. It would also help to determine how PiAvr3a is interacting with CMPG1. This could be achieved using X-ray crystallography and NMR.

In addition, larger CMPG1 bands were observed suggesting that this protein is modified. It would be interesting to know what these bands were. They could result from ubiquitination, phosphorylation or possibly SUMOylation. Unfortunately, Co-IPs were unsuccessful. In the future, if another technique or variation of the Co-IP was developed it could be used to identify these upper bands.

The ubiquitination assay is a useful tool to investigate enzyme activity *in vitro*. However, it could be improved. At the moment the E1 used is that from human. To make the assay more realistic to a plant's ubiquitination it would be better to use the plant E1. This is not commercially available and therefore developing a

reliable and consistent plant E1 protein production would be a huge help in the work done using these assays.

The other CMPG1-interactors from the original Y2H screen performed by Dr M Armstrong should also be investigated as they may help to increase the overall understanding of CMPG1s role in the plant. CMPG1 may have other functions and roles not related to CMPG1 dependent plant defence and this would be interesting to ascertain. This could be done using on line information on co-expressed genes/CMPG1 targets and using similar techniques as used in this project.

Appendices

A1 Primers Used in This Study.

Primer Name	Sequence (5'-3')	Used For
rt17	CGTCAAGGCCAGGATCCAAGATAAGGAGGG	QuikChange K27R Fwd
rt18	CCCTCCTTATCTTGGATCCTGGCCTTGACG	QuikChange K27R Rev
rt19	GATCTTCGCCGGAAGGCAACTTGAGG	QuikChange K48R Fwd
rt20	CCTCAAGTTGCCTTCCGGCGAAGATC	QuikChange K48R Rev
rt21	GGATTACAACATCCAGAGGGAGTCTACGC	QuikChange K63R Fwd
rt22	GCGTAGACTCCCTCTGGATGTTGTAATCC	QuikChange K63R Rev
rt39	GGTGGGAATCAAACATGTCC	RT-PCR CMPG1 in N. benthamiana expression. Fwd
rt40	AACGATGAAATCGACCCAAG	RT-PCR CMPG1 in N. benthamiana expression. Rev
rt41	ACCAAGGTCCTGGTGTATGG	RT-PCR PiAvr3a in N. benthamiana expression. Fwd
rt42	TGATTGTACTTTGCGCCTTG	RT-PCR PiAvr3a in N. benthamiana expression. Rev
Nb25S Fwd	CACGGACCAAGGAGTCTGACAT	qRT-PCR. Nb25S Control Fwd
Nb25S Rev	TCCCACCAATCAGCTTCCTTAC	qRT-PCR. Nb25S Control Rev
RTS1	GTGTGCCTGTTTTGGTGAAG	qRT-PCR. NbCMPG1 Fwd
RTS2	TTTTGAAATGCACCAACTTGA	qRT-PCR. NbCMPG1 Rev
RTS3	GCTTCAACAGGGGAAGTGAT	qRT-PCR. NbCMPG1 Fwd
RTS4	ACCACACCATGCAACGTAAC	qRT-PCR. NbCMPG1 Rev

A2 Publications:

Birch, P.R., Armstrong, M., Bos, J., Boevink, P., Gilroy, E.M., Taylor, R.M., Wawra, S., Pritchard, L., Conti, L., Ewan, R., Whisson, S.C., van West, P., Sadanandom, A., and Kamoun, S. (2009). Towards understanding the virulence functions of RXLR effectors of the oomycete plant pathogen *Phytophthora infestans*. *Journal of Experimental Botany* **60**, 1133-1140.

Bos, J.I.B., Armstrong, M.R., Gilroy, E.M., Boevink, P.C., Hein, I., Taylor, R.M., Zhendong, T., Engelhardt, S., Vetukuri, R.R., Harrowerd, B., Dixeliusg, C., Bryand, G., Sadanandom, A., Whisson, S.C., Kamoun, S., & Birch, P.R.J. (2010). *Phytophthora infestans* effector AVR3a is essential for virulence and manipulates plant immunity by stabilizing host E3 ligase CMPG1. *Proceedings of the National Academy of Sciences* **107**, 9909-9914.

Gilroy, E.M., Taylor, R.M., Hein. I., Boveink, P., Sadanandom, A. & Birch, P.R.J. (2011). CMPG1-dependent cell death follows perception of diverse pathogen elicitors at the host plasma membrane and is suppressed by *Phytophthora infestans* RXLR effector AVR3a. New Phytologist **190**(3):653-66.

References

Aguilar, R.C. and Wendland, B. (2003). Ubiquitin: not just for proteasomes anymore. *Current Opinion in Cell Biology* **15**, 184-190.

Alfano, J.R., and Collmer, A. (2004). Type III secretion system effector proteins: double agents in bacterial disease and plant defence. *Annual Review Phytopathology* **42**, 385-414.

Allen, R.L., Bittner-Eddy, P.D., Grenville-Briggs, L.J., Meitz, J.C., Rehmany, A.P., Rose, L.E. & Beynon, J.L. (2004). Host-parasite coevolutionary conflict between *Arabidopsis* and downy mildew. *Science* **306**, 1957-1960.

Armstrong, M.R., Whisson, S.C., Pritchard, L., Bos, J.I., Venter, E., Avrova, A.O., Rehmany, A.P., Bohme, U., Brooks, K., Cherevach, I., Hamlin, N., White, B., Fraser, A., Lord, A., Quail, M.A., Churcher, C., Hall, N., Berriman, M., Huang, S., Kamoun, S., Beynon, J.L., and Birch, P.R. (2005). An ancestral oomycete locus contains late blight avirulence gene Avr3a, encoding a protein that is recognized in the host cytoplasm. *Proceedings of the National Academy of Sciences* **102**, 7766-7771.

Batoko, H., Zheng, H., Hawes, C. & Moorea,I. (2000). A Rab1 GTPase Is Required for Transport between the Endoplasmic Reticulum and Golgi Apparatus and for Normal Golgi Movement in Plants. *The Plant Cell* **12**, 2201-2217.

Belfield, E.J., Hughes, R.K., Tsesmetzis, N., Naldrett, M.J. & Casey, R. (2007). The gateway pDEST17 expression vector encodes a -1 ribosomal frameshifting sequence. *Nucleic Acids Research*. **35**.

Belkhadir, Y., Subramaniam, R. & Dangl, J.L. (2004). Plant Disease Resistance Protein Signalling: NBS-LRR Proteins and Their Partners. *Current Opinion in Plant Biology* **7**, 391-399.

Birch, P.R., Armstrong, M., Bos, J., Boevink, P., Gilroy, E.M., Taylor, R.M., Wawra, S., Pritchard, L., Conti, L., Ewan, R., Whisson, S.C., van West, P., Sadanandom, A. & Kamoun, S. (2009). Towards understanding the virulence functions of RXLR effectors of the oomycete plant pathogen *Phytophthora infestans*. *The Journal of Experimental Botany* **60**, 1133-1140.

Birch, P.R. and Whisson., S. (2001). *Phytophthora infestans* enters the genomics era. *Molecular Plant Pathology* **2**, 257-263.

Block, A., Li, G., Fu, Z.Q. & Alfano, J.R. (2008). Phytopathogen type III effector weaponry

and their plant targets. *Current Opinion in Plant Biology* **1**, 396-403.

Boller, T. and He, S.Y. (2009). Innate Immunity in Plants: An Arms Race Between Pattern Recognition Receptors in Plants and Effectors in Microbial Pathogens. *Science* **324**, 742-744.

Bopopi, M.J., Vandeputte, O.M., Himanen, K., Mol, K., Vaessen, Q., Jaziri, M.E. & Baucher, M. (2010). Ectopic expression of PtaRHE1, encoding a poplar RING-H2 protein with E3 ligase activity, alters plant development and induces defence-related responses. *The Journal of Experimental Botany* **61**, 297-310.

Bos, J.I., Chaparro-Garcia, A., Quesada-Ocampo, L.M., Gardener, B.B., and Kamoun, S. (2009). Distinct Amino Acids of the *Phytophthora infestans* Effector AVR3a Condition Activation of R3a Hypersensitivity and Suppression of Cell Death. *Molecular Plant Microbe Interactions* **22**, 269-281.

Bos, J.I., Kanneganti, T.D., Young, C., Cakir, C., Huitema, E., Win, J., Armstrong, M.R., Birch, P.R., and Kamoun, S. (2006). The C-terminal half of *Phytophthora infestans* RXLR effector AVR3a is sufficient to trigger R3a-mediated hypersensitivity and suppress INF1-induced cell death in *Nicotiana benthamiana*. *The Plant Journal* **48**, 165-176.

Bos, J.I.B., Armstrong, M.R., Gilroy, E.M., Boevink, P.C., Hein, I., Taylor, R.M., Zhendong, T., Engelhardt, S., Vetukuri, R.R., Harrowerd, B., Dixeliusg, C., Bryand, G., Sadanandom, A., Whisson, S.C., Kamoun, S., & Birch, P.R.J. (2010). *Phytophthora infestans* effector AVR3a is essential for virulence and manipulates plant immunity by stabilizing host E3 ligase CMPG1. *Proceedings of the National Academy of Sciences* **107**, 9909-9914.

Brunner, F., Rosahl, S., Lee, J., Rudd, J.J., Geiler, C., Kauppinen, S., Rasmussen, G., Scheel, D. and Nürnberger, T. (2002). Pep-13, a plant defence-inducing pathogen-associated pattern from *Phytophthora* transglutaminases. . *The European Molecular Biology Organisation Journal* **21**, 6681-6688.

Burch-Smith, T.M., Anderson, J.C., Martin, G.B., & Dinesh-Kumar, S.P. (2004). Applications and advantages of virus-induced gene silencing for gene function studies in plants. *The Plant Journal* **39**, 734-746.

Burch-Smith, T.M., Schiff, M., Caplan, J.L., Tsao, J., Czymmek, K. & Dinesh-Kumar, S.P. (2007). A Novel Role for the TIR Domain in Association with Pathogen-Derived Elicitors. *PLOS Biology* 5(**3**) 501-514.

Callis, J. & Vierstra, R.D. (2000). Protein degradation in signalling. *Current Opinion in Plant Biology* **3**, 381-386.

Chinchilla, D., Zipfel, C., Robatzek, S., Kemmerling, B., Nurnberger, T., Jones, J.D., Felix, G. & Boller, T. (2007) A flagellin-induced complex of the receptor FLS2 and BAK1 initiates plant defence. *Nature* **448**, 497-500.

Chisholm, S.T., Coaker, G., Day, B. & Staskawicz, B.J. (2006). Host-Microbe Interactions: Shaping the Evolution of the Plant Immune Response. *Cell* **124**, 803-814.

Collmer, A., Badel, J.L., Charkowski, A.O., Deng, W.L., Fouts, D.E., Ramos, A.R., Rehm, A.H., Anderson, D.M., Schneewind, O., van Dijk, K., and Alfano, J.R. (2000). Pseudomonas syringae Hrp type III secretion system and effector proteins. *Proceedings of the National Academy of Sciences* **97**, 8770-8777.

Day, B., Dahlbeck, D. & Staskawicz, B.J. (2006). NDR1 Interaction with RIN4 Mediates the Differential Activation of Multiple Disease Resistance Pathways in *Arabidopsis*. *The Plant Cell* **18**, 2782-2791.

Delaure, S.L., Van Hemelrijck, W., De Bolle, M.F.C., Cammue, B.P.A. & De Coninck, B.M.A. (2008). Building up plant defences by breaking down proteins. *Plant Science* **174**, 375-385.

Deshales, R.J. (1999). SCF and cullin/RING H2-Based Ubiquitin Ligases. *Annual Review of Cell and Developmental Biology* 435-467.

Devoto, A., Muskett, P.R. & Shirasu, K. (2003). Role of Ubiquitination in the Regulation of Plant Defence against Pathogens. *Current Opinion in Plant Biology* **6**, 307-311.

Downes, B. and Vierstra, R.D. (2005). Post-translational regulation in plants employing a diverse set of polypeptide tags. The *Biochemical Society* 393-399.

Dreher, K. and Callis, J. (2007). Ubiquitin, Hormones and Biotic Stress in Plants. *Annals of Botany* 1-35.

Dumas, B., Bottin, A., Gaulin, E. and Esquerré-Tugayé, M.T. (2008). Cellulose-binding domains: cellulose associated-defensive sensing partners? *Trends Plant Science* **13**, 160-164.

Durrant, W.E., Rowland, O., Piedras, P., Hammond-Kosack, K.E. & Jones, J.D.G. (2000). cDNA-AFLP Reveals a Striking Overlap in Race-Specific Resistance and Wound Response Gene Expression Profiles. *The Plant Cell* **12**, 963-977.

Earley, K.W., Haag, J.R., Pontes, O., Opper, K., Juehne, T., Song, K. & Pikaard, C.S. (2006). Gateway-compatible vectors for plant functional genomics and proteomics. *The*

Plant Journal **45**, 616-629.

Fellbrich, G., Romanski, A., Varet, A., Blume, B., Brunner, F., Engelhardt, S., Felix, G., Kemmerling, B., Krzymowska, M. and Nürnberger, T. (2002). NPP1, a *Phytophthora*-associated trigger of plant defence in parsley and *Arabidopsis*. *The Plant Journal* **32**, 375-390.

Flor, H.H. (1942). Inheritance of pathogenicity in *Melampsora lini*. *Phytopathology* **32**, 653-669.

Gao, Z., Chung, E., Eitas, T.K. & Dangl, J.L. (2011). Plant intracellular innate immune receptor Resistance to *Pseudomonas syringae pv. maculicola* 1 (RPM1) is activated at, and functions on, the plasma membrane. *Proceedings of the National Academy of Sciences* 108(**18**), 7619–7624.

Garcıa, A.V., Blanvillain-Baufume, S., Huibers, R.P., Wiermer, M., Li, G., Gobbato, E., Rietz, S. & Parker, J.E. (2010). Balanced Nuclear and Cytoplasmic Activities of EDS1 Are Required for a Complete Plant Innate Immune Response. *PLOS* 6(**7**) 1-15.

Gaulin, E., Dramé, N., Lafitte, C., Torto-Alalibo, T., Martinez, Y., Ameline-Torregrosa, C., Khatib, M., Mazarguil, H., Villalba-Mateos, F., Kamoun, S.,Mazars, C., Dumas, B., Bottin, A., Esquerré-Tugayé, M.T. and Rickauer, M. (2006). Cellulose binding domains of a *Phytophthora* cell wall protein are novel pathogen-associated molecular patterns. *The Plant Cell* **18**, 1766-1777.

Gfeller, A., Liechti, R. & Farmer, E.E. (2010). *Arabidopsis* Jasmonate Signaling Pathway. *Science Signalling* 3(**109**).

Gilroy, E.M., Hein, I., van der Hoorn, R., Boevink, P.C., Venter, E., McLellan, H., Kaffarnik, F., Hrubikova, K., Shaw, J., Holeva, M., Lopez, E.C., Borras-Hidalgo, O., Pritchard, L., Loake, G.J., Lacomme, C., and Birch, P.R. (2007). Involvement of cathepsin B in the plant disease resistance hypersensitive response. *The Plant Journal* **52**, 1-13.

Gilroy, E.M., Taylor, R.M., Hein. I., Boveink, P., Sadanandom, A. & Birch, P.R.J. (2011). CMPG1-dependent cell death follows perception of diverse pathogen elicitors at the host plasma membrane and is suppressed by *Phytophthora infestans* RXLR effector AVR3a. New Phytologist **190(3)**, 653-66.

Glickman, M. and Ciechanover., A. (2002). The Ubiquitin-Proteosome Proteolytic Pathway: Destruction for the Sake of Construction. *Physiological Reviews* **82**, 373-416.

Gomez-Gomez, L. and Boller, T. (2000). FLS2: An LRR Receptor-like Kinase Involved in the Perception of the Bacterial Elicitor Flagellin in *Arabidopsis*. *Molecular Cell* **5**, 1003-1011.

González-Lamothe, R., Tsitsigiannis, D.I., Ludwig, A.A., Panicot, M., Shirasu, K. & Jones, J.D.G. (2006). The U-Box Protein CMPG1 Is Required for Efficient Activation of defence Mechanisms Triggered by Multiple Resistance Genes in Tobacco and Tomato. *The Plant Cell* **18**, 1067-1083.

Gou, M., Su, N., Zheng, J., Huai, J., Wu, G., Zhao, J., He, J., Tang, D., Yang, S. & Wang, G. (2009). An F-box gene, CPR30, functions as a negative regulator of the defense response in *Arabidopsis*. *The Plant Journal* **60**, 757–770.

Grant, S.R., Fisher, E.J., Chang, J.H., Mole, B.M., and Dangl, J.L. (2006). Subterfuge and manipulation: Type III effector proteins of phytopathogenic bacteria. *Annual Review of Microbiology* **60**, 425-449.

Grouffaud, S., van West, P., Avrova, A.O., Birch, P.R.J. & Whisson, S.C. . (2008). *Plasmodium falciparum* and *Hyaloperonospora parasitica* effector translocation motifs are functional in *Phytophthora infestans*. *Microbiology* **154**, 3743-3751.

Hammond-Kosack, K.E., Tang, S., Harrison, K. & Jones, J.D.G. (1998). The Tomato Cf-9 Disease Resistance Gene Functions in Tobacco and Potato to Confer Responsiveness to the Fungal Avirulence Gene Product Avr9. *The Plant Cell* **10**, 1251-1266.

Heese, A., Hann, D.R., Gimenez-Ibanez, S., Jones, A.M., He, K., Li J., Schroeder, J.I., Peck, S.C. and Rathjen, J.P. (2007). The receptor-like kinase SERK3/BAK1 is a central regulator of innate immunity in plants. *Proceedings of the National Academy of Sciences* **104**, 12217-12212 12222.

Hein, I., Gilroy, E.M., Armstrong, M.R., & Birch, P.R.J. (2009). The zig-zag-zig in oomycete-plant interactions. *Molecular Plant Pathology* **10**, 547-562.

Hicke, L. (2001). Protein Regulation By Monoubiquitin. *Nature* **2**, 195-201.

Honee, G., Buitink, J., Jabs T.,, De Kloe, J., Sijbolts, F., Apotheker, M., Weide, R., Sijen, T., Stuiver, M. & De Wit, P.J.G.M. (1998). Induction of Defence-Related Responses in Cf9 Tomato Cells by the AVR9 Elicitor Peptide of *Cladosporium fulvum* Is Developmentally Regulated. *Plant Physiology* **117**, 809-820.

Hueck, C.J. (1998). Type III protein secretion systems in bacterial pathogens of animals and plants. *Microbiology and Molecular Biology Reviews* **62**, 379-433.

Janjusevic, R., Abramovitch, R.B., Martin, G.B. & Stebbins, C.E. (2006). A bacterial inhibitor of host programmed cell death defences in an E3 ubiquitin ligase. *Science* 311.

Jones, J.D. and Dangle, J.L. (2006). The Plant Immune System. *Nature* **444**, 323-329.

Joosten, M.H.A.J., Vogelsang, R., Cozijnsen, T.J., Verberne, M.C. & De Wit, P.J.G.M. (1997). The Biotrophic Fungus *Cladosporium fulvum* Circumvents Cf-4 Mediated Resistance by Producing Unstable AVR4 Elicitors. *The Plant Cell* **9**, 367-379.

Judelson, H.S. (1997). The genetics and biology of *Phytophthora infestans*: modern approaches to a historical challenge. *Fungal Genetics and Biology* 22(**2**), 65-76.

Judelson, H.S., Tyler, B.M. & Michelmore, R.W. (1991). Transformation of the oomycete pathogen, *Phytophthora infestans*. *Molecular Plant-Microbe Interactions* **4**, 602-607.

Kaloshian, I. (2004). Gene-for-gene Disease Resistance: Bridging Insect Pest and Pathogen Defence. The *Journal of Chemical Ecology* **30**, 2419-2438.

Kamoun, S. (2006). A catalogue of the effector secretome of plant pathogenic oomycetes. *Annual Review Phytopathology.* **44**, 41-60.

Kim, H.S. and Delaney, T.P. (2002). *Arabidopsis* SON1 Is an F-Box Protein That Regulates a Novel Induced Defence Response Independent of Both Salicylic Acid and Systemic Acquired Resistance. *The Plant Cell* **14**, 1469-1482.

Kim, H.T., Kim, K.P., Lledias, F., Kisselev, A.F., Scaglione, K.M.,, and Skowyra, D., Gygi, S.P. & Goldberg, A.L. (2007). Certain Pairs of Ubiquitin-conjugating Enzymes (E2s) and Ubiquitin-Protein Ligases (E3s) Synthesize Nondegradable Forked Ubiquitin Chains Containing All Possible Isopeptide Linkages. The *Journal of Biological Chemistry* **282**, 17375-17386.

Kirsch, C., Logemann, E., Lippok, B., Schmelzer, E. & Hahlbrock, K. (2001). A highly specific pathogen-responsive promoter element from the immediate-early activated CMPG1 gene in *Petroselinum crispum*. *The Plant Journal* **26**, 217-227.

Kornitzer, D. and Ciechanover, A. (2000). Modes of Regulation of Ubiquitin-Mediated Protein Degradation. *The Journal of Cellular Physiology* **182**, 1-11.

Krüger, J., Thomas, C.M., Golstein, C., Dixon, M.S., Smoker, M., Tang, S., Mulder, L & Jones J.D. (2002). A tomato cysteine protease required for Cf-2-dependent disease resistance and suppression of autonecrosis. *Science* **296**, 744-747.

Latijnhouwers, M., Hawes, C., Carvalho, C., Oparka, K., Gillingham, A.K. & Boevink, P. (2005). An *Arabidopsis* GRIP domain protein locates to the trans-Golgi and binds the small GTPase ARL1. *The Plant J*ournal **44**, 459-470.

Liu, Z., Bos, J.I.B., Armstrong, M., Whisson, S.C., da Cunha, L., Torto, T., Win, J., Avrova, A.O., Wright, F., Birch, P.R.J. and Kamoun, S. (2005). Patterns of diversifying selection in the phytotoxin-like scr74 gene family of *Phytophthora infestans*. *Molecular Biology and Evolution* **22**, 659-672.

Lu, R., Martin-Hernandez, A.M., Peart, J.R., Malcuit, I. & Baulcombe, D.C. (2003). Virus-induced gene silencing in plants. *Nature Methods* **30**, 296-303.

Mackey, D., Holt, B.F. & Wiig, A. (2002). RIN4 Interacts with *Pseudomonas syringae* Type III Effector Molecules and is Required for RPM1-Mediated Resistance in *Arabidopsis*. *Cell* **108**, 743-754.

Medzhitov, R.J. and Janeway, C.A. Jr (1997). innate immunity: impact on the adaptive immun response. *Current Opinion in Immunology* 9, 4-9.

Nandi, D., Tahiliani, P., Kumar, A. & Chandu, D. (2006). The Ubiquitin-proteasome System. *Indian Academy of Sciences* **31**, 137-155.

Ni, X., Tian, Z., Liu, J., Song, B. & Xie, C. (2009). Cloning and molecular characterization of the potato RING finger protein gene StRFP1 and its function in potato broad-spectrum resistance against *Phytophthora infestans*. *The Journal of Plant Physiology*. 167(**6**), 488-96.

Nimchuk, Z., Eulgem, T., Holt, B.F. & Dangl, J.L. (2003). Recognition and Response in the Plant Immune System. *Annual Review of Genetics* **37**, 579-609.

Nurnberger, T., Nennstiel, D., Jabs, T., Sacks, W.R., Hahlbrock, K., and and Scheel, D. (1994). High Affinity Binding of a Fungal Oligopeptide Elicitor to Parsley Plasma Membranes Triggers Multiple Defence Responses. *Cell* **78**, 449-480.

Oh, S., Young, C., Lee, M., Oliva, R., Bozkurt, T.O., Cano, L.M., Win, J., Bos, J.I.B., Liu, H., van Damme, M., Morgan, W., Choi, D., Van der Vossen, E.A.G., Vleehouwers, V.G.A.A. & Kamoun, S. (2009). In Planta Expression Screens of *Phytophthora infestans* RXLR Effectors Reveal Diverse Phenotypes, Including Activation of the *Solanum bulbocastanum* Disease Resistance Protein Rpi-blb2. *The Plant Cell* **21**, 2928-2947.

Orsomando, G., Lornzi, M., Raffaelli, N., Dalla Rizza,M., Mezzetti, B. and Ruggieri, S.

(2001). Phytotoxic protein PcF: purification, characterisation and cDNA sequencing of a novel hydroxyproline-containing factor secreted by the strawberry pathogen *Phytophthora cactorum*. *The Journal of Biological Chemistry* **276**, 21575-21584.

Peart, J.R., Cook, G., Feys, B.J., Parker, J.E. & Baulcombe D.C. (2002). An EDS1 orthologue is required for N-mediated resistance against tobacco mosaic virus. *The Plant Journal* **29**, 569-579.

Pickart, C.M. (2001a). Mechanisms Underlying Ubiquitination. *Annual Review of Biochemistry* **70**, 503-533.

Pickart, C.M. (2001b). Ubiquitin Enters the New Millennium. *Molecular cell* **8**, 499-504.

Pickart, C.M. and Fushman, D. (2004). Polyubiquitin Chains: Polymeric Protein Signals. *Current Opinion in Chemical Biology* 8(**6**), 610-616.

Qutob, D., Tedman-Jones, J. & Gijzen, M. (2006). Effector-triggered immunity by the plant pathogen *Phytophthora*. *TRENDS in Microbiology* **14**(11), 470-473.

Qutob, D., Kemmerling, B., Brunner, F., Küfner, I., Engelhardt, S., Gust, A.A., Luberacki, B., Seitz, H.U., Stahl, D., Rauhut, T., Glawischnig, E., Schween, G., Lacombe, B., Watanabe, N., Lam, E., Schlichting, R., Scheel, D., Nau, K., Dodt, G., Hubert, D., Gijzen, M. and Nürnberger, T. (2006). Phytotoxicity and innate immune responses induced by Nep1-like proteins. *The Plant Cell* **18**, 3721-3744.

Rehmany, A.P., Gordon, A., Rose, L.E., Allen, R.L., Armstrong, M.R., Whisson, S.C., Kamoun, S., Tyler, B.M., Birch, P.R., and Beynon, J.L. (2005). Differential recognition of highly divergent downy mildew avirulence gene alleles by RPP1 resistance genes from two *Arabidopsis* lines. *The Plant Cell* **17**, 1839-1850.

Rooney, H.C., Van't Klooster, J.W., van der Hoorn, R.A., Joosten, M.H., Jones, J.D. & de Wit, P.J. (2005). *Cladosporium* Avr2 inhibits tomato Rcr3 protease required for Cf-2-dependent disease resistance. *Science* **308(5729)**, 1783-6.

Roos-Mattjus, P. and Sistonen, L. (2004). The ubiquitin-proteasome pathway. *Annals of Medicine* **36**, 285-295.

Rosebrock, T.R., Zend, L., Brady, J.J., Abramovitch, R.B., Xiao, F. & Martin, G.B. (2007). A Bacterial E3 ligase targets a host protein kinase to disrupt plant immunity. *Nature* **448**, 370-374.

Rowland, O., Ludwig, A.A., Merrick, C.J., Baillieul, F., Tracy, F.E., Durrant, W.E., Fritz-Laylin, L., Nekrasov, V., Sjolander, k., Yoshioka, H. & Jones, J.G.D. (2005). Functional Analysis of Avr9/Cf-9 Rapidly Elicited Genes Identifies a Protein Kinase, ACIK1, That Is Essential for Full Cf-9–Dependent Disease Resistance in Tomato. *The Plant Cell* **17**, 295-310.

Schumann, G.L. & D'Arcy, C.J. (2000). Late blight of potato and tomato. *The Plant Health Instructor.* DOI: 10.1094/PHI-I-2000-0724-01.

Schwechheimer, C. (2004). The COP9 signalsome (CSN): an evolutionary conserved proteolysis regulator in eukaryotic development. *Biochimica et Biophysica Acta* **1695**, 45-54.

Schwessinger, B. and Zipfel, C. (2008). News from the frontline: recent insights into PAMP-triggered immunity in plants. *Current Opinion in Plant Biology* **11**, 389-395.

Shan, W., Cao, M., Leung, D., & Tyler, B.M. (2004). The Avr1b locus of *Phytophthora sojae* encodes an elicitor and a regulator required for avirulence on soybean plants carrying resistance gene Rps1b. *Molecular Plant Microbe Interactions* **17**, 394-403.

Smith, A.M., Coupland, G., Dolan, L., Harberd, N., Jones, J., Martin, C., Sablowski, R. & Amey, A. (2009). *Plant Biology* ISBN 978-0-8153-4025-6

Song, M.S., Song, S.J., Kim, S.Y., Oh, H.Y. & Lim, D-S. (2008). The tumour suppressor RASSF1A promotes MDM2 self-ubiquitination by disrupting the MDM2–DAXX–HAUSP complex. *The European Molecular Biology Organisation Journal* **27**, 1863-1874.

Spoel, S.H., Mou, Z., Tada, Y., Spivey, N.W., Genschik, P. & Dong, Z. (2009). Proteasome-Mediated Turnover of the Transcription Coactivator NPR1 Plays Dual Roles in Regulating Plant Immunity. *Cell* **137**, 860-872.

Stergiopoulos, I. and de Wit, P.J. (2009). Fungal Effector Proteins. *Annual Review of Phytopathology* **47**, 233-263.

Sun, L. and Chen, Z.J. (2004). The novel functions of ubiquitination in signalling. *Current Opinion in Cell Biology* **16**, 119-126.

Takken, F.L.W. and Joosten, M.H.A.J. (2000). plant resistance Genes: Their Structure, Function and Evolution. *The European Journal of Plant Pathology* **106**, 699-713.

Thomas, C.M., Dixon, M.S., Parniske, M., Golstein, C. & Jones, J.D. (1998). Genetic and molecular analysis of tomato Cf genes for resistance to *Cladosporium fulvum*. *Philosophical Transactions of the Royal Society B: Biological Sciences* **29**, 1413-1424.

Toth, I.K., Sullivan, L., Brierley, J., Avrova, A.O., Hyman, L.J., Holeva, M., Broodfoot, M., Perombelon, C.M. and McNiol, J. (2003). Relationship between potato seed tuber contamination by *Erwinia carotovora subsp. atroseptica*, blackleg development and progeny tuber contamination. *Plant Pathology* **52**, 119-126.

Trujillo, M., Ichmura, K., Casais, C. & Shirasu, K. (2008). Negative Regulation of PAMP-Triggered Immunity by an E3 Ubiquitin Ligase Triplet in *Arabidopsis*. *Current Biology* **18**, 1-6.

Trujillo, M. and Shirasu., K. (2010). Ubiquitination in plant immunity. *Current Opinion in Plant Biology* **13**, 402-408.

Turner, J.G., Ellis, C. & Devoto, A. (2002). The Jasmonate Signal Pathway. *The Plant Cell*. **14** Suppl:S153-64. Review

van der Biezen, E.A. and Jones, J.D.G. (1998). Plant disease-resistance proteins and the gene-for-gene concept. *FrontLines* **23**, 454-456.

van der Burg, H.A., Tsitsigiannis, D.I., Rowland, O., Lo, J., Rallapalli, G., MacLean, D., Takken, F.L.W. & Jones, J.D.G. (2008). The F-Box Protein ACRE189/ACIF1 Regulates Cell Death and Defence Responses Activated during Pathogen Recognition in Tobacco and Tomato. *The Plant Cell* **20**, 697-719.

van der Hoorn, R.A.L. and Kamoun, S. (2008). From Guard to Decoy: A New Model for Perception of Plant Pathogen Effectors. *The Plant Cell* **20**, 2009-2017.

Van Esse, P.H., van't Klooster, J.W., Bolton, M.D., Yadeta, K.A., van Baarlen, P., Boeren, S., Vervoort, J., de Wit, P.J.G.M. & Thommaab, B.P.H.J. (2008). The *Cladosporium fulvum* Virulence Protein Avr2 Inhibits Host Proteases Required for Basal Defence. *The Plant Cell* **20**, 1948-1963.

van Poppel, P.M.J.A., Guo, J., van de Vondervoort, P.J.I., Jung, M.W.M., Birch, P.R.J., Whisson, S.C. & Gover, F. (2008). The *Phytophthora infestans* avirulence gene Avr4 encodes an RXLR-dEER effector. *Molecular Plant Microbe Interactions* **21**, 1460-1470.

Vierstra, R. (2003). The Ubiquitin/26S Proteasome Pathway, the Complex last Chapter in the Life of Many Plant Proteins. *Trends in Plant Science* **8**, 135-142.

Vleehouwers, V.G., Rietman, H., Krenek, P., Champouret, N., Young, C., Oh, S.K., Wang, M., Bouwmeester, K., Vosman, B., Visser, R.G., Jacobsen, E., Govers, F., Kamoun, S. & Van der Vossen, E.A. (2008). Effector genomics accelerates discovery and functional